INTERACTIONS BETWEEN A NATIVE SEDGE, *CAREX NUDATA*, AND PHYSICAL RIVER PROCESSES: A MODEL OF COUPLED BIOGEOMORPHIC DEVELOPMENT

by

MATTHEW N. GOSLIN

A DISSERTATION

Presented to the Department of Geography
and the Division of Graduate Studies of the University of Oregon
in partial fulfillment of the requirements
for the degree of
Doctor of Philosophy

September 2021

DISSERTATION APPROVAL PAGE

Student: Matthew N. Goslin

Title: Interactions between a native sedge, *Carex nudata*, and physical river processes: a model of coupled biogeomorphic development

This dissertation has been accepted and approved in partial fulfillment of the requirements for the Doctor of Philosophy degree in the Department of Geography by:

Patricia McDowell	Chairperson
W. Andrew Marcus	Core Member
Daniel Gavin Scott	Core Member
Bridgham	Institutional Representative

and

Andrew Karduna	Interim Vice Provost for Graduate Studies

Original approval signatures are on file with the University of Oregon Division of Graduate Studies.

Degree awarded September 2021

DISSERTATION ABSTRACT

Matthew N. Goslin

Doctor of Philosophy

Department of Geography

September 2021

Title: Interactions between a native sedge, *Carex nudata*, and physical river processes: a model of coupled biogeomorphic development

I explored the effects of the riparian sedge, *Carex nudata*, on geomorphic processes in the Middle Fork John Day River, Oregon (MFJDR) as well as the environmental drivers of *C. nudata*'s distribution, building an integrative conceptual model of stream evolution in rivers with *C. nudata*.

I investigated the environmental drivers of *C. nudata* distribution and tested the hypothesis that distribution is driven by stream power by conducting field sampling across 31 sites in the John Day and Santiam basins of Oregon. *C. nudata* abundance was inversely related with canopy cover and displayed a positive threshold response relative to stream power, mostly absent in streams with low stream power.

Within the MFJDR, I used repeated topographic surveys and historic aerial imagery to investigate changes in channel morphology associated with *C. nudata*. Repeated surveys showed continuing bank erosion and small-scale changes such as scour in front of *C. nudata* fringes. Historic aerial imagery revealed that *C. nudata* islands most often originate from *C. nudata* fringes becoming detached from retreating banks rather than from initial establishment in midchannel positions.

The continuing erosion of banks with *C. nudata* fringes raised the question of whether banks with *C. nudata* fringes are eroding at rates similar to banks without *C.*

nudata. I addressed this question by establishing erosion pin arrays at 7 sites with *C. nudata* fringes and 7 without, measuring pins seasonally for 2 years. Erosion rates did not differ between sites with and without *C. nudata*. Furthermore, winter erosion was equal or greater than erosion during the spring snowmelt-driven peak flows pointing to the importance of winter processes such as freeze-thaw soil weakening that are likely independent of *C. nudata* patterns.

I propose a conceptual model in which alternative pathways of channel development are possible after the establishment of *C. nudata*: 1) bank stabilization; 2) formation of a compound channel as banks retreat; 3) the formation of islands within the channel as banks retreat and scour occurs behind a *C. nudata* fringe. The potential for alternative pathways can lead to a diversity of channel forms, facilitating complexity, a key goal of river restoration.

This dissertation includes unpublished co-authored material.

CURRICULUM VITAE

NAME OF AUTHOR: Matthew N. Goslin

GRADUATE AND UNDERGRADUATE SCHOOLS ATTENDED:

University of Oregon, Eugene, OR
Oregon State University, Corvallis, OR
Pacific Lutheran University, Tacoma, WA

DEGREES AWARDED:

Doctor of Philosophy, Geography, 2021, University of Oregon
Master of Science, Forest Science, 1997, Oregon State University
Bachelor of Science, Biology, 1989, Pacific Lutheran University

AREAS OF SPECIAL INTEREST:

Fluvial Geomorphology

Biogeography

PROFESSIONAL EXPERIENCE:

Conservation Geographer and GIS Analyst, Ecotrust, 2004-2010

GIS Analyst, NOAA Fisheries, 2002-2004

GRANTS, AWARDS, AND HONORS:

Doctoral Dissertation Research Improvement Award, NSF, 2014

Student Research Award, Geological Society of America, 2016, 2014

Reds Wolman Award, American Association of Geographers, 2013

Student Research Award, Northwest Science Association, 2013

ACKNOWLEDGMENTS

I would like to express appreciation to my adviser, Pat McDowell, and my committee members, Andrew Marcus, Dan Gavin and Scott Bridgham. Pat McDowell has been an extraordinary mentor, adviser and partner in research from whom I have learned a great deal, and whose company I have enjoyed across many days in the field. Andrew Marcus was a wonderful mentor and encourager when I first began this program and an advocate throughout this process. Scott Bridgham and Dan Gavin both provided extensive advice as I formulated my ideas and methods for the ecology-focused chapter (2) and provided thorough, helpful reviews of my work. Many other faculty were generous in their assistance, particularly Desiree Tullos at Oregon State University (OSU) who helped me brainstorm ideas and methods near the beginning of this research, Mark Fonstad at UO who helped hone analytical approaches at later stages, and Jake Bendix (Syracuse University) whose work inspired many of my ideas. Special mention must go to Vicente Monleon-Moscardo, U.S. Forest Service, my faithful friend ever since we did our M.S. degrees together at OSU, who provided critical statistical consulting throughout this project, brainstormed ideas and listened to all of my stories. Josh Roering (UO), Bruce McCune (OSU), Michael Hughes (OIT) and Pat Bartlein (UO) also offered advice or assistance at different points. Peg Boulay (UO), director of the Environmental Leadership Program, was a great gateway to several fantastic field assistants.

I am particularly grateful to all of the field assistants who helped me and with whom I enjoyed many memorable adventures in the field. Particular recognition goes to James Major, Sarah Hanchett and Emily Erickson who took on leadership roles and assisted over the course of multiple seasons and tasks. Jake Prickett, Corey Guerrant,

Geoffrey Marcus, Leela Hickman, Zoe Wellschlager, Alex Held-Martinez, Nick Pai, Kadie Hayward, Drew Thompson, Chris So and J. D. Lancaster all provided invaluable assistance.

I am indebted to the Confederated Tribes of the Warm Springs for allowing me to work on their lands, the beautiful Oxbow and Forrest Conservation Areas. It has been a privilege to watch the great care given to restoring these lands. In their work for the Tribes, Brian Cochrane and Emily Davis provided valued support.

One of the great privileges of my research has been to be part of a larger community of land managers, restoration workers and scientists from whom I could learn and with whom I could share my discoveries as they unfolded, the Middle Fork John Day River Intensively Monitored Watershed (IMW) program. Our annual face-to-face meetings were a highlight each year as well as random encounters in the field with so many who were enthusiastic about this place we love. Special mention goes to John Selker (OSU), Ken Fetcho (Oregon Watershed Enhancement Board) and Mark Croghan (U.S.B.R), IMW participants who provided insights, good conversation and encouragement.

Les Zaitz and Scotta Callister, owners of the Boulder Creek Ranch Cabin, and dedicated Oregon newspaper professionals, provided a wonderful place to stay and friendship during cold weather field trips.

I was supported by many friendships at UO during this process. I was especially privileged to enjoy great office-mates in Columbia 246 who always seemed to sense when we all needed laughter and when we needed quiet: Kuan-chi Wang, Jean Faye, Weicheng Wang, Adriana Uscanga-Castillo, Holly Moulton and Jewell Bohlinger. It was

a pleasure to work with and exchange ideas with the many members of the River Rats graduate student group: Aaron Zettler-Mann, Polly Lind, James Dietrich, Helen Beeson, Daniel Baldwin, Swagata Goswami, Christina Shintani, Christina Appleby, Jenna Duffin, Sarah Praskiewicz, Jane Atha, Suzanne Walther, Denise Tu, Amanda Reinholtz, Jenn Kusler, Dion Webster, Nicole Merrill and Dakota Whitman amd Eric Levenson. Apart from these work groups, UO graduate students Yi Yu, Meche Lu, Shuo Xu and Jesus Napancca were particularly good friends and supporters, partners in hiking and dinner parties throughout my time here.

I am especially thankful to my parents, Lew and Kay Goslin, who have supported me throughout my career and especially during this PhD work, providing support and assistance in many ways. My sister, Rebecca, and her family, Kevin, Carson, Trevor and Lauren, who provided me with much and listened to my many stories. All now know that "sedges have edges." I have dedicated this dissertation to my father who, in particular, was an avid supporter of my academic pursuits, accompanied me on field trips when I was younger (doing my M.S.), helped build equipment for my field work – painting erosion pins and building a style to get over a fence -- and in these later years has been eager to simply discuss my work and listen to each of my new discoveries. His friendship, ready assistance, patience and easy smile have buoyed me throughout my life.

I received funding for this work from the Northwest Science Association, Native Plant Society of Oregon, American Association of Geographers (Geomorphology Specialty Group), Geological Society of America, the California Native Plant Society, and the UO Geography Department. This research was supported by National Science Foundation DDRI award 1434326.

dedicated to my father, Lewis Goslin, friend and supporter

TABLE OF CONTENTS

LIST OF FIGURES

LIST OF TABLES

I. INTRODUCTION

Conceptual Background

Biogeomorphology is an emergent discipline that explicitly recognizes and explores the linkages between ecological and geomorphological processes (Corenblit et al. 2007, Bendix and Stella 2013). Within ecology, environmental gradients and physical processes such as disturbance have long been recognized as critical drivers of species distribution and community dynamics. Jones et al. (1994) introduced the concept of ecosystem engineers, biological organisms with the capacity to modify the environment in ways that may enhance their success. Likewise, fluvial geomorphology focused almost exclusively on the physical processes in rivers until the latter part of the 20th when the role of biological organisms in altering physical processes and facilitating the evolution of stream channels became increasingly recognized (Hughes 1997). Emerging research has unveiled geomorphological functions played by a wide range of organisms from the well-known to the surprising: beavers, salmon, caddis flies, mollusks and a diversity of plants (Gutiérrez et al. 2003, Hassan et al. 2008, Johnson et al. 2009, Hassan et al. 2011, DeVries 2012, Liffen et al. 2013, Hood and Larson 2015). The interaction between vegetation and physical river processes is particularly salient given the ubiquity of vegetation across most river systems and the stabilizing, boundary-forming role vegetation often plays in river systems.

In river systems, riparian plant species distribution may be driven by environmental factors such as elevation above the water table, and communities may be structured by flood disturbance (Shafroth et al. 2000, Stromberg 2001). Nevertheless, plants are increasingly recognized not simply as passive features responding to gradients, flow and disturbance, but also as active agents capable of altering the physical template of the river. Vegetation may stabilize banks, often leading to channel narrowing (Anderson et al. 2004, Rodrigues et al. 2007). Beyond bank stabilization, plants may present resistance to flow, altering velocities and direction which in turn leads to altered patterns of sedimentation and erosion (Rodrigues et al. 2006). Flume studies using simple arrangements of plants or artificial surrogates have demonstrated changes in sedimentation relative to experimental plants and the redirection of erosive forces (Bennett et al. 2002, Ishikawa et al. 2003). In both flume and natural experiments, the

expansion of vegetation has been found to shift braided channels toward sinuous, single thread channels (Gran and Paola 2001, Birken and Cooper 2006, Hicks et al. 2007, Tal and Paola 2007). In natural rivers, different plant species offer differing degrees and forms of resistance, leading to complex patterns of sedimentation and erosion that challenge simple generalizations (Rodrigues et al. 2006).

As the capacity of plants to alter physical river processes has gained increasing attention, a critique has emerged that studies of plant-river interactions are typically unidirectional, ignoring the feedbacks between plant species establishment and the evolving river channel. Addressing this gap, Corenblit et al. (2007) proposed the concept of biogeomorphic succession in which reciprocal interactions between vegetation and physical processes drive the linked development of both the plant community and fluvial landforms. This seminal article represents both the cumulative work of several of its authors who have taken such an integrative approach as well as a call for further research that explicitly recognizes such linkages in stream evolution. For example, in the Tagliamento River in Italy, *Populus* or *Salix* sp. drive island formation via alternative pathways characterized by varying rates of development and persistence dependent on the initial mode of tree or shrub establishment (Edwards et al. 1999, Gurnell et al. 2001). Gurnell and Petts (2006) further demonstrate that the pattern of plant persistence in these braided channels can be explained by the key hydrologic variables of stream power and moisture availability. The Tagliamento studies offer a conceptual model that ties together the reciprocal effects of the fluvial environment on plant establishment patterns and the effects of plant establishment patterns on fluvial landform development.

In another high energy river, the Tech River in France, Corenblit et al. (2009) demonstrated differential patterns of aggradation and erosion associated with differing plant communities along an elevation gradient at distances away from the base flow channel. Corenblit et al. (2009) postulated that communities of shrubs and pioneer tree seedlings instigate positive feedbacks that stabilize landforms and promote succession. In low energy river systems in England, Gurnell et al. (2006) found that the interaction between stream power and the sediment-trapping aquatic macrophyte, *Sparganium erectum*, drove the development of alternative channel forms.

While these studies and others have demonstrated reciprocal interactions between plants and rivers as well as the capacity for plants to function as ecosystem engineers, the range of cases represented remains limited. Certain plant guilds (trees and shrubs such as *Salix* and *Populus* sp., aquatic macrophytes) and certain river types (high energy braided rivers, low energy rivers with fine sediments) have been studied extensively while other river types and species have received little attention (Gurnell et al. 2012).

Carex nudata and the Middle Fork John Day River

This dissertation builds upon the conceptual framework of reciprocal plant-river interactions and biogeomorphic succession envisioned by Corenblit et al. (2007) and the gaps in this area of inquiry identified by Gurnell et al. (2012) and Vaughan et al. (2009). I explore both directions of the relationship between the riparian sedge, *Carex nudata*, and the fluvial environment in which it occurs. *C. nudata* represents a plant form that does not belong to guilds previously studied, and it occurs within medium-energy rivers, a type that has been understudied in the context of biogeomorphic succession.

The research presented here has emerged out of ongoing research and restoration work in the Middle Fork of the John Day River (MFJDR) in eastern Oregon where *C. nudata,* a native species, has expanded dramatically following the removal of cattle grazing from river banks in the late 1990s. Historically, the MFJDR was heavily degraded by cattle grazing, tree removal and gold dredge mining. However, the river is currently the focus of enormous investments in active restoration because of its high potential for recovering threatened salmon populations (NFJDWC 2021). In the midst of this resource-intensive restoration, the unaided explosion of *C. nudata* following passive restoration has been one of the most surprising developments. The sedge is now the dominant stream-side plant species and a prominent feature of the riverscape, growing along the edges of gravel bars, at the base of cut banks and in the middle of the river as islands.

C. nudata derives its common name, torrent sedge, from its ability to maintain mid-channel footholds in steep, fast rivers due to its remarkably strong, dense root system. While *C. nudata* is particularly prominent in the MFJDR, it occurs in varying densities in rivers throughout the Pacific Northwest and California. Previous research on *C. nudata* in the Eel River in northern California focused on its ecological function as a

possible keystone species, capturing sediment and creating stabilized substrate within which other species could potentially establish, enhancing diversity and altering competitive relationships within the streamside plant community (Levine 1999, 2000a, Levine 2000b). Anecdotal evidence in the MFJDR has suggested that *C. nudata* may be altering channel morphology and planform in the form of growing islands and resulting side channels (McDowell 2011). A tussock-forming sedge, it forms a solid obstruction with its mass of dense roots and captured sediment such that it might aptly be described as an "organic boulder" that can grow and reproduce (pers. comm. McDowell). Furthermore, the patchy distribution of *C. nudata* within river basins and reaches suggests hydrological and geomorphological controls on its initial distribution.

In light of emerging inquiry around plant-river interactions, *C. nudata* may serve as a model of bidirectional relationships between vegetation and physical river processes (Corenblit et al. 2007). This dissertation examines both sides of this relationship, how hydrological and geomorphic factors may drive *C. nudata* distribution and how *C. nudata* may alter hydrologic and geomorphic patterns. The MFJDR offers a natural laboratory to explore how the expansion of a particular species may be driving channel evolution, and how that species' initial establishment pattern, potentially patterned by the initial geomorphic template, may lead to alternative pathways of channel development. Examining both sides of this relationship, I will build a conceptual model of development for rivers in which *C. nudata* becomes a key stream side plant species.

Research Structure and Objectives

The research presented in this dissertation aims at three overall objectives

A. Determine the environmental factors that drive *C. nudata* distribution within basins
B. Determine how *C. nudata* alters river planform and channel morphology at the reach scale.
C. Build a conceptual model of coupled developmental pathways of *C. nudata* establishment and channel evolution in rivers where *C. nudata* is prominent.

Objective A is addressed in Chapter 2, Objective B is addressed in Chapters 3 and 4 and Objective C is woven in and built upon through each of these chapters. Multiple questions are nested within Objectives A and B.

Objective A: C. nudata Distribution

Chapter 2 Questions

The first article chapter, Chapter 2, is aimed at testing the hypothesis that stream power drives *C. nudata* patterns within basins. *C. nudata* exhibits traits associated with disturbance-adapted species, propagating only by widely dispersed, water-transported seeds, not by rhizomes, and establishing at the edge of the low-flow channel during summer, a position that would experience the highest shear stress in subsequent peak flows. A preliminary, coarse-scale, range-wide species distribution model developed using Maxent, a presence-only model that can be used with herbarium records, suggested that hydrological variables were the most important explanators of *C. nudata* distribution. This preliminary study suggested the hypothesis that mean stream power - the energy of the river across its width and an effective metric of a river's disturbance capacity – may be driving the pattern of *C. nudata* within basins. We tested this hypothesis via fine-scale sampling of *C. nudata*, hydraulic metrics, and other environmental variables at 30 sites distributed from headwaters-to-mouth in two study basins, the John Day and Santiam basins, that represent two distinct climates within which *C. nudata* occurs.

1) Does stream power drive *C. nudata* distribution within basins?
2) Do other environmental variables explain *C. nudata* distribution in addition to or instead of stream power?
3) What systematic upstream-to-downstream patterns within basins result from the relationship between *C. nudata* and the environmental drivers of its distribution?
4) If there are systematic patterns of *C. nudata* distribution within basins, what predictions can be made about where *C. nudata* may be geomorphologically effective within basins?

Objective B: *C. nudata* Geomorphological Effects

Chapter 3 Questions

The second article chapter, Chapter 3, uses repeated topographic surveys and historic aerial imagery to describe change, looking both backward and forward, in reaches with5 *C. nudata*. In a review of ecohydrogeomorphic research, Vaughan *et al.*

(2009) noted a propensity for static descriptions of pattern and space-for-time substitutions in this field of research and emphasize a need for experimental studies and repeated surveys to assess trajectories of change. The study design in this chapter is a response to this critique. Using five survey sites representative of reaches with *C. nudata* in the MFJDR, we begin with a question that is essentially a static description addressed with our first topographic survey.

1) What morphological features distinguish channels with *C. nudata?*

Following repeated topographic surveys of these same five sites two years later, we assess questions of change.

2) What patterns of erosion and deposition are associated with *C. nudata*?

Using a sequence of historic aerial imagery beginning in 1989, prior to the removal of cattle grazing, we assess questions of historic change by reconstructing the temporal and spatial pattern of *C. nudata* cohort establishment and planform evolution at our five sites during this period of expansion.

3) How has planform – channel boundaries, bank tops and islands – evolved relative to patterns of *C. nudata* establishment?

The reconstruction of historic change at these sites revealed that one of the most prominent features of the MFJDR, *C. nudata* islands, could originate via a pathway we had not anticipated. That is, we had assumed that all *C. nudata* islands originated via mid-channel establishment, perhaps on midchannel gravel bars. However, we discovered that the *C. nudata* islands at one of our sites did not originate from midchannel establishment but rather from establishment as a fringe at the base of a cut bank which became an island as the bank retreated and the *C. nudata* fringe became detached from the bank. Given the ubiquity of *C. nudata* islands in the MFJDR and the resulting development of multi-threaded channels, this led to a critical question:

4) What is the primary pathway of *C. nudata* island genesis and the relative importance of different pathways of island genesis?

We addressed this final question by reconstructing the evolution of all islands over a 10 km stretch of river using the same sequence of historic aerial imagery used in reconstructing the history of our study sites.

The results of Chapter 3 in conjunction with our understanding of *C. nudata* distribution in Chapter 2 allow us to begin building an integrative conceptual model of alternative developmental pathways in reaches with *C. nudata*.

Chapter 4 Questions

One of the key revelations of the study presented in Chapter 3 was that banks are continuing to retreat behind the *C. nudata* fringes at their base, and that this continued retreat may be critical to the development of the distinctive channel morphologies associated with *C. nudata*. This finding was somewhat unexpected given that vegetation has often been found to slow erosion and stabilize banks. However, the ecology and morphology of *C. nudata* are distinct relative to plant guilds typically included in studies of vegetation and bank erosion. Previous paradigms about vegetation and bank erosion may not be applicable. Therefore, a critical question raised by these findings is addressed in Chapter 4.

1) Do banks with *C. nudata* fringes erode and retreat at rates slower, faster or no different than banks without *C. nudata* fringes?

We addressed this question by establishing erosion pin arrays at 7 sites with *C. nudata* fringes (including our original 5 full survey sites) and 7 sites without *C. nudata*, measuring erosion pins over three seasonal periods across two years. We also conducted annual bank top topographic surveys of these same sites over a span of five years.

While this study was initially motivated by the question of comparative bank retreats between reaches with and without *C. nudata*, the measuring of erosion pins across three different seasons over two years was intended to isolate by season distinct erosion processes associated with these different seasons and evaluate the relative importance of these processes. We recognized that little is known about which bank erosion processes are important in the MFJDR. Because bank retreat is such a critical process in the evolution of channels and planform, understanding which bank erosion processes are important in the MFJDR is critical to understanding stream evolution in this system and the role of *C. nudata* in this evolution. Thus, the following question also drove this study:

2) What is the relative importance of each season and the erosion processes associated with each season in the overall erosion of banks in the MFJDR?

And finally, given that bank face erosion is a quasi-continuous process whereas bank retreat may be a stochastic process via mass failures facilitated by ongoing erosion, we addressed a final, secondary question:

3) What is the relationship between bank face erosion rates and bank top retreat rates?

The results from Chapter 4 deepen our understanding of bank erosion processes, the role of different vegetation types in modifying bank erosion processes and our conceptual model of channel evolution in systems with *C. nudata*.

Chapters 3 and 4 are co-authored with Patricia McDowell.

Management Implications

We have framed the research presented here as motivated by research gaps in the arena of plant-river interactions and the potential of *C. nudata* to serve as a model species for exploring coupled biogeomorphic development in river systems. Nevertheless, this research is also motivated by the potential for the application of lessons learned from this research to river restoration and management.

Throughout the West Coast, enormous resources are being poured into river restoration projects and these efforts are driven, in particular, by the listing of salmon species under the U.S. Endangered Species Act. Prioritized for its high potential for recovering salmon populations, the MFJDR has been a locus for active restoration projects including: extensive planting of trees, placement of engineered log jams and re-engineering of dredged channels toward a meandering form. The research in this dissertation has grown out of the 10-year Intensively Monitored Watershed (IMW) program in the MFJDR intended to assess the effectiveness of these many active restoration projects. Within this context, *C. nudata* is perceived positively by land managers and restoration practitioners as a native species that may be naturally facilitating the habitat diversity critical for healthy salmon populations (Beechie and Bolton 1999). Nevertheless, our understanding of *C. nudata*'s effect on channel development has been entirely anecdotal. The research presented in this dissertation is intended to provide an evidence-based, detailed understanding of how effectively *C. nudata* may be facilitating channel evolution in a direction consistent with restoration goals such as enhancing complexity and habitat diversity (Beechie et al. 2008, Roni et al.

2008), changes that have resulted entirely from the passive restoration of removing cattle grazing from river banks.

In addition to *C. nudata*'s natural expansion following passive restoration, *C. nudata* is now being transplanted into active restoration projects including newly engineered channels. However, the transplanting of *C. nudata* is often practiced without consideration of what factors are conducive to its persistence or how exactly it may influence channel development. The findings from Chapter 2 can inform where seeding or transplanting of *C. nudata* would be most likely to succeed. The findings from Chapters 3 and 4 can inform where plantings and transplanting would likely be most effective in facilitating the evolution of desired channel forms and restoration goals

A key hypothesis of my investigation of *C. nudata* species patterns is that distribution may be driven by the hydrological regime. The alteration of hydrological regimes by dams can have adverse impacts on riparian plant species (Fenner et al. 1985, Nilsson and Svedmark 2002). Across the region, there are programs to reform dam operations and experiment with environmental flows that mimic natural flow regimes (Richter et al. 2006). However, there is a large gap in knowledge about the hydrological niches of riparian plants outside of well-studied *Populus* species (Gregory et al. 2007a, b). Understanding the hydrological drivers of *C. nudata* distribution could also be a key contribution to the process of environment flow planning, especially given the significant role *C. nudata* can play in river ecosystems.

The conceptual model developed here could be especially useful in predicting trajectories of change in other gravel bed rivers with dense *C. nudata* populations. For instance, *C. nudata* is particularly abundant in northern California, including the Trinity River, a river where flows have been severely reduced and altered in timing by dams. The Trinity River Restoration Program is now engaged in a significant adaptive management experiment to restore more natural flow regimes (TRRP 2013). How will channel morphology interact with *C. nudata* populations in response to environmental flows? Our model may provide a starting point for addressing such questions.

II. CAN HYDROLOGICAL DRIVERS EXPLAIN THE SPECIES DISTRIBUTION OF THE RIPARIAN SEDGE, CAREX NUDATA, WITHIN RIVER BASINS?

Introduction

Species distribution models of terrestrial plants typically rely on explanatory variables describing climate and underlying terrain such as soils, geology and topography (Guisan and Zimmermann 2000, Franklin 2010). The distribution of riparian and aquatic species, however, may also be driven by hydrological variables that vary longitudinally (upstream to downstream) through a watershed and which integrate both watershed-level climate and geology as well as local reach-level topography. The extent to which longitudinally-varying hydrological variables drive riparian species patterns versus those of climate or local terrain is a critical question for river ecology (Engelhardt et al. 2012). Many studies of the distribution of aquatic and riparian species have focused on local variables such as the transverse changes in water availability or potential flood inundation across a stream's active channel and valley (Osterkamp and Hupp 1984, Auble et al. 1994, Shafroth et al. 1998, Dixon et al. 2002, Auble et al. 2005, Robertson 2006, Mosner et al. 2011). A few studies have explained the distribution of species or community types not only with local variables but also with longitudinally-varying hydrological variables such as discharge, stream power, patterns in flow variation and velocity (Bendix 1994, 1999, O'Hare et al. 2011, Engelhardt et al. 2012).

Riparian and aquatic plant species can have significant effects on the geomorphic evolution of streams (Gurnell and Petts 2006, Kamada 2008, Gurnell et al. 2010, Corenblit et al. 2014, O'Hare et al. 2016). Investigations of plant species patterns within river basins have focused overwhelmingly on two groups of plants that have also been the focus of research on geomorphic effects: woody species such as *Populus* and *Salix* spp. that typically occur in medium to high energy streams (Turner et al. 2004, Friedman et al. 2006, Stromberg et al. 2010, Bejarano et al. 2013) and aquatic macrophtyes that typically occur in lower energy streams (Riis and Biggs 2001, Riis et al. 2008, Gurnell et al. 2010, O'Hare et al. 2011). Less attention has been given to the distribution of riparian herbaceous species such as sedges. Given the significant geomorphic role of many of these species, especially in stabilizing stream-edge substrate or banks (Platts and Nelson

1989, Micheli and Kirchner 2002a), there is a particular need for a greater understanding of the distribution of such herbaceous riparian species.

This study investigates the distribution of the herbaceous species, *Carex nudata*, commonly known as "torrent sedge." The distribution of *C. nudata* suggests a pattern that defies explanation by climate variables, suggesting that its distribution may be driven primarily by hydrological patterns, therefore serving as a model species for exploring the relationships between hydrological river variables and riparian taxa. *C. nudata* occurs from central California (coastal mountains to Sierra Nevada) through Oregon into southern Washington state, U.S.A (Fig. 2.1). In Oregon, *C. nudata* occurs both in coastal basins with high rainfall and a maritime temperature regime and in the basins of eastern Oregon marked by dry continental climates. At a finer resolution, within-basin distribution of *C. nudata* is patchy: it is absent from large portions but locally abundant in other areas. This distinctive within-basin patterning suggests a hydrological or perhaps geological/geomorphic driver of these patterns.

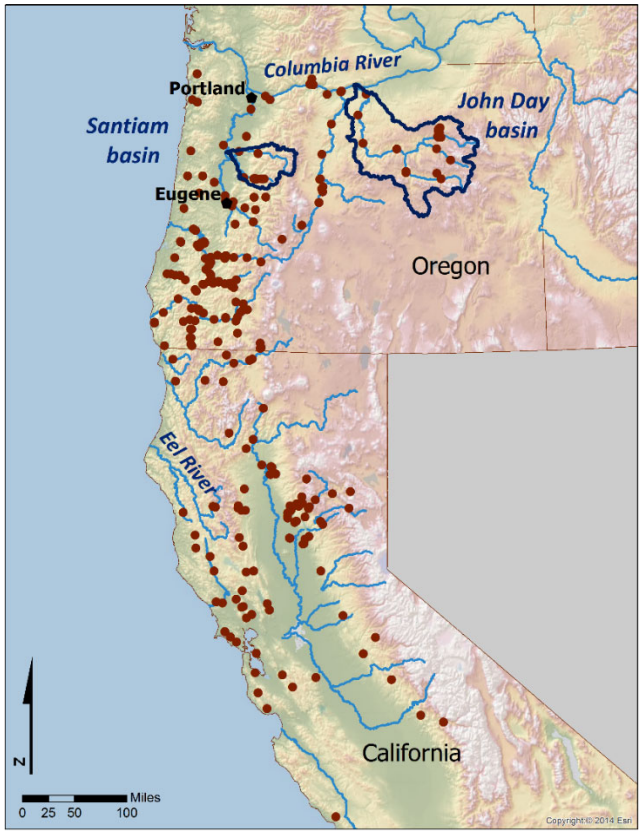

Figure 2.1. Range-wide distribution of *C. nudata* represented by herbarium records (brown circles) and location of Santiam and John Day study basins.

C. nudata captured the attention of researchers and land managers in the Middle Fork John Day River (MFJDR) of eastern Oregon where it expanded rapidly in the 1990s after being released from cattle grazing pressure following the establishment of private conservation areas and grazing reforms on U.S. Forest Service lands. As *C. nudata* has expanded, it has driven changes in channel morphology. *C. nudata* propagates primarily by river-dispersed seed in mid-summer, establishing along the edges of the low flow channel. It forms distinct tussocks and is not rhizomatous (Wilson et al. 2008). The diameter of a mature tussock may be >0.5 m at its base and >1 m at its leaf crown (Fig. 2.2). With its extremely dense, strong root network, *C. nudata* is capable of resisting high energy flows. Grouped together, tussocks may form a linear patch at the base of cut banks or along the edge of gravel bars. Coalescing tussocks can evolve into islands. The diverse features built by *C. nudata* appear to be driving the evolution of the MFJDR from a simple single thread river toward a complex multi-threaded river of islands and side channels. Given that its geomorphic effects appear to be consistent with restoration goals, *C. nudata* is now commonly transplanted into restoration projects within the MFJDR and is among a suite of plants used in restoration projects in southern Oregon and northern California (Steinfeld 2001, Evans et al. 2003). The expansion of *C. nudata* and the consequent evolution of channel morphology in the MFJDR sparked the ecological question of what drives the distribution of *C. nudata* at both local and basin-wide scales, and whether its geomorphic role is unique to the MFJDR or apparent in other systems.

Figure 2.2. *C. nudata* tussocks in the MFJDR. For reference, the river bank left of photo is approximately .8 m in height. The *C. nudata* island consists of two mature tussocks.

C. nudata has been studied in few locations with the exception of the South Fork of the Eel River, California, where *C. nudata* was found to play a keystone ecological role (Levine 1999, 2000a, 2001, 2003). In gravel bed rivers such as the South Fork Eel or the MFJDR, *C. nudata* tussocks trap sediment as they grow, building stable patches of substrate amid otherwise unstable, unvegetated habitat. Levine (1999, 2000a, 2001) describes *C. nudata* tussocks as focal points of plant colonization within this system and demonstrated indirect facilitation of other species through the provision of stable habitat and reductions in herbivory via sheltering from *C. nudata* leaves.

Both the reproductive strategy and habitat in which *C. nudata* is found suggest that it is a disturbance-adapted species, both capable of colonizing newly opened habitat at stream edges and capable of resisting disturbance. *C. nudata* is positioned at the point along the active channel cross section where the interaction between biological and physical forces is most intense (Gurnell et al. 2016). In rivers with *C. nudata*, aquatic macrophytes do not co-occur in significant densities, indicating that stream energy is too high for colonization of the perennially inundated portion of the channel.

Given *C. nudata*'s apparent disturbance-adapted traits, I hypothesized that stream power, a proxy for fluvial disturbance, drives *C. nudata* distribution. Preliminary observations across longitudinal river profiles suggested that *C. nudata* occurred within upstream and downstream limits within basins. Fluvial geomorphological theory posits that stream power should vary systematically through basins with a peak at intermediate positions within basins (Knighton 1999). I hypothesized that there must be a lower limit for stream power below which there is insufficient disturbance to favor a disturbance-adapted species such as *C. nudata*, and there must also be an upper limit for stream power above which even *C. nudata* cannot withstand the force of the river (Fig. 2.3).

I addressed the following questions:

1) Does stream power explain *C. nudata* distribution within basins?
2) Do other environmental variables explain *C. nudata* distribution in addition to or instead of stream power?
3) What systematic patterns within basins result from the relationship between *C. nudata* and the environmental drivers of its distribution?

4) If there are systematic patterns of *C. nudata* distribution within basins, what predictions can be made about where *C. nudata* may be geomorphologically effective within basins?

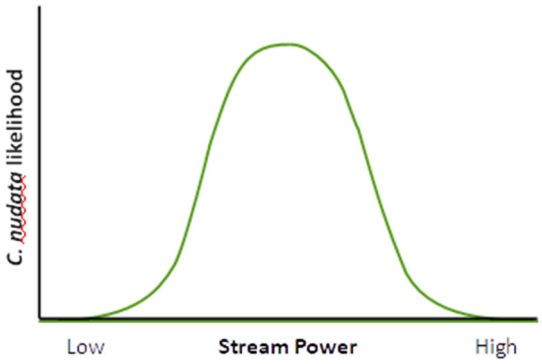

Figure 2.3. Hypothesized relationship between *C. nudata* likelihood and stream power.

Stream Power: Theory and Applications

Stream power represents the energy exerted by flowing water against the surfaces across which it flows (Bendix 1999). This is the energy that can potentially damage or destroy existing vegetation and mobilize sediment, creating newly exposed and colonizable surfaces. Stream power can be described by *total stream power*, the total energy of flowing water at a cross section of a river, or by *mean stream power*, the average energy of the flowing water across a river cross section (Rhoads 1987, Fonstad 2003). Total stream power, Ω (W/m), is a function of river discharge, Q (m^3/s), and river energy slope, S, and a constant, the specific weight of water, γ, (9800 N/m^3).

$$\Omega = \gamma Q S \tag{1}$$

Mean stream power, ω, (W/m^2) is simply

$$\omega = \Omega / w \tag{2}$$

where w represents width. Mean stream power represents energy per unit area of the stream bed and accounts for the fact that this total energy at a cross section is distributed across the width of the river. Therefore, given the same total stream power, a narrower stream will experience greater mean stream power than a wider stream across which that energy is more broadly distributed. Mean stream power, ω, is closely related to shear

stress at common peak flows such as the 2-year flood (Q_2) and can be an effective metric of stream competence, the size of sediment a stream is capable of mobilizing (Costa 1983, Lawler 1992, Lawler 1995). Stream power patterns may drive the pattern of sediment erosion and deposition zones (Graf 1983, Magilligan 1992, Lecce 2013).

Given that, within basins from headwaters to outlet, there are systematic changes in slope (decreases), discharge (increases) and width (increases), it has been shown that theoretically, both total and mean stream power should increase from headwater reaches to a peak at intermediate positions and then decrease downstream to their lowest values near a river's outlet (Knighton 1999). In practice, complex topographies imposed by geology can lead to highly variable local slopes resulting in substantial variation in stream power throughout a basin (Bendix 1997, Fonstad 2003).

A limited number of studies have explored the relationship between stream power and the distribution of plant species or communities within basins. In two mountainous southern California watersheds, Bendix (1999) sampled woody species across river cross sections and was able to predict species occurrence along two axes representing unit stream power (determined at specific points along a cross section) and elevation above the stream channel. Bendix (1994) was also able to differentiate woody plant communities among sites within these two watersheds using detrended correspondence and axes that reflected gradients in mean stream power and fire disturbance interval. In Nevada across 18 upland watersheds, Engelhardt et al. (2012) included a surrogate for total stream power (drainage area/watershed relief) among an array of variables tested for their ability to explain the distribution of vegetation classes and found a positive relationship between the stream power index and the occurrence of the riparian shrub type (primarily *Salix* and *Betula* spp.). In the braided Tagliamento River in Italy, Gurnell and Petts (2006) found evidence to support a conceptual model of vegetated island development defined by gradients in stream power and water availability.

The hydrological niche of aquatic macrophyte species has been explained primarily in terms of stream velocity tolerance thresholds (Riis and Biggs 2003, Gurnell et al. 2006, Franklin et al. 2008, Vaughn and Davis 2015). Taking an alternative approach, O'Hare et al. (2011) differentiated aquatic macrophyte groups across 1650 river reaches in England using a principal components analysis in which one axis was driven

primarily by mean stream power. Consistent with the sensitivity of aquatic macrophytes to flood disturbance, groups were differentiated by stream power thresholds below which they occurred. Taken together, these studies demonstrate the potential for stream power to discriminate distribution patterns among both disturbance-sensitive aquatic macrophytes and disturbance-adapted woody species.

Tussock-forming sedges such as *C. nudata* have not been studied with respect to their relationship with longitudinally-varying hydrological variables. Furthermore, most of the studies described above have not attempted to build predictive models for individual species dependent upon hydrological variables, relying primarily on multivariate discriminant analyses or broad vegetation classes. I aim to build a predictive model that will test the hypothesis that the distribution of *C. nudata* can be explained by stream power variation in two basins representing distinct climate regimes.

Methods

To test hypotheses regarding environmental drivers of *C. nudata* distribution I took a two-step approach. In the first step, I used herbarium records of *C. nudata* occurrence across its entire range to build a range-wide predictive model of *C. nudata* employing a distribution model designed for presence only data, Maxent (Phillips et al. 2004, Peterson et al. 2007). Given the inference limitations associated with presence-only data (Royle et al. 2012, Hastie and Fithian 2013) and sampling biases inherit in herbarium records, some authors have recommended that such models be used primarily for hypothesis generation and sampling design (Merow et al. 2013), such that my use of Maxent was primarily for these two purposes. Full results are reported by Goslin (in prep-b), and results summarized here are only those relevant to the development of the hypotheses tested here. In the second step, the focus of this paper, I used the Maxent-derived predictive model to guide a random field sampling design, stratified by predicted *C. nudata* occurrence to ensure that field sampling included sufficient sites both with and without *C. nudata*. I conducted field sampling in two river basins that represented distinct climate regimes, the John Day basin in eastern Oregon and the Santiam basin in western Oregon, sampling a range of sites from headwaters to basin mouth along which stream power was expected to vary (Fig. 2.4). General procedures are described in this section.

See Appendix A: Supplementary Materials for further details on protocols, exceptions to general procedures and rationale for methodological choices.

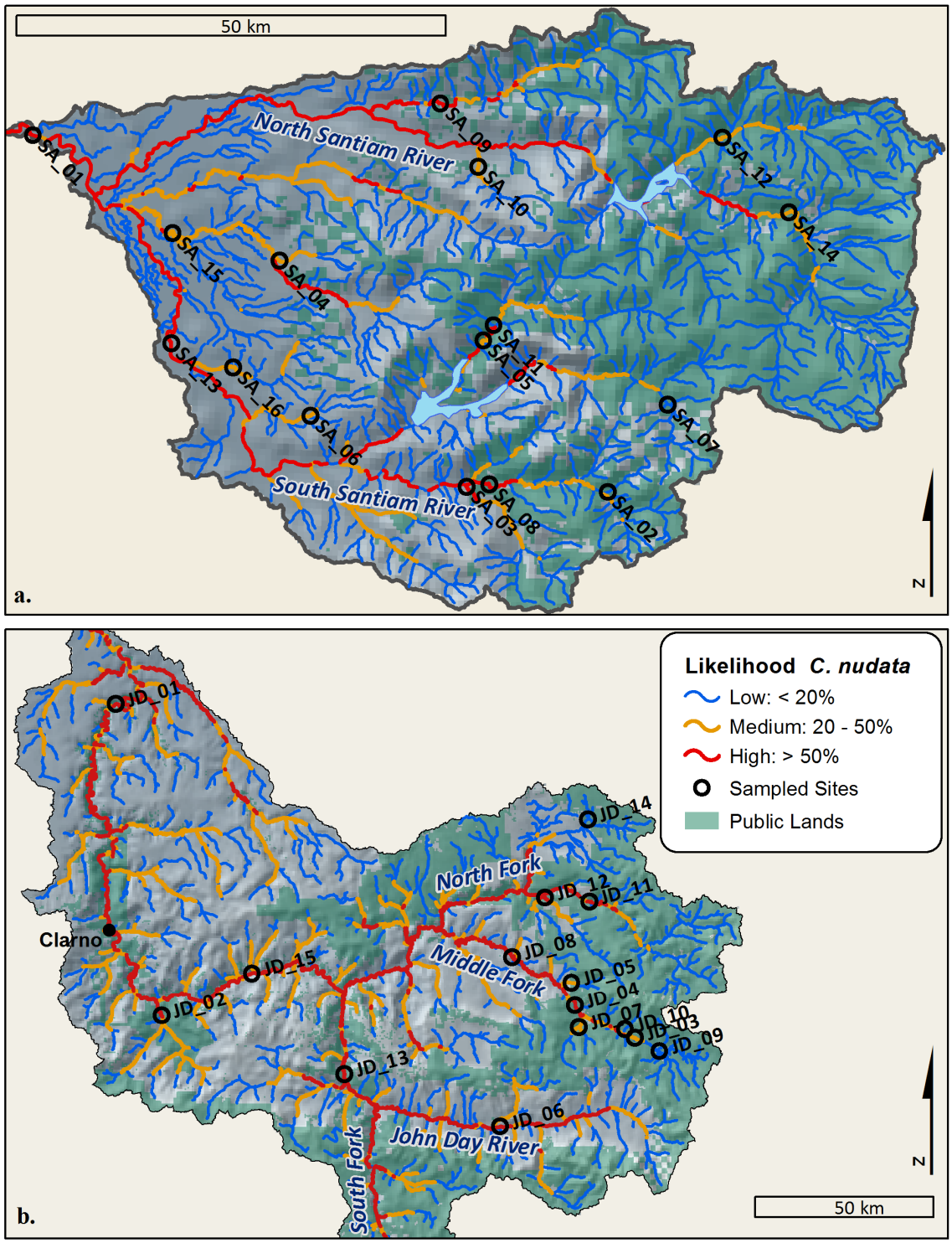

Figure 2.4. Survey sites in a) Santiam and b) John Day basins and Maxent likelihoods for *C. nudata*

Study basins

The John Day and Santiam River basins in Oregon are distinguished from each other by climate regime, geology and topography (Table 2.1; Figs. 2.1, 2.4).

Table 2.1. Basin characteristics.

	Santiam	John Day
Basin Area (km^2)	4,690	20,500
Mean Annual Precipitation (cm)	199	46
Mean Annual Discharge (m^3/s)	218	58.2
Min - Max Elevation (m)	49 – 3,200	81 – 2,760
Lower basin weather station, Elevation	Lebanon (100 m)	Arlington (84 m)
Jan min-max temp (°C)	1.2 – 8.9	-1.3 – 4.7
Days w min temp < 0 °C	32	75
Jul min-max temp (°C)	12.8 – 28.9	16.8 – 31.9
Annual precipitation (cm)	118	23
Mid basin weather station, Elevation	Cascadia (293 m)	Dayville (689 m)
Jan min-max temp (°C)	.3 – 7.5	-2.8 – 7.4
Days w min temp < 0 °C	70	116
Jul min-max temp (°C)	9.4 – 25.8	11.7 – 33.4
Annual precipitation (cm)	164	34

The Santiam consists of two major tributaries, the North and South Santiam. The North Santiam originates in the High Cascade Mountains and flows 161 km before meeting the South Santiam which originates in the lower elevation Western Cascade Mountains and flows 113 km before merging with the North Santiam and flowing as the lower Santiam 15 km further into the Willamette River (USGS 2013). The basin includes the Cascade Mountains (78%) and Willamette Valley (22%) ecoregions (EPA 2010, Omernik and Griffith 2014).

High elevation geology in the Santiam basin (North Santiam headwaters) comprises young, relatively permeable High Cascade volcanic rocks and glacial deposits. Most of the basin is the older, less permeable volcanic material of the Western Cascades. Lower reaches are underlaid by Quaternary alluvium associated with the wide Willamette River floodplain (Risley et al. 2012).

The climate is characterized by long cool, wet winters and warm, dry summers. Within the basin, rain falls at low elevations from fall through spring and at mid elevations in fall and spring. Snow accumulates at mid-to-high elevations in winter. As a result, the hydrological regime includes both rain-driven peak flows in fall, rain-on-snow flow events in winter and snow-melt driven peak flows in spring.

The John Day River, the third longest free-flowing river in the continental U.S., is a subbasin within the Columbia River basin. The basin consists of four tributaries, the North, Middle and South Forks, as well as the upper mainstem. The North and Middle Forks both originate in the northeast Blue Mountains, the Middle Fork flowing 121 km into the North Fork which flows 138 km to its junction with the Middle Fork and then another 50 km to its meeting with the mainstem. The mainstem John Day starts in the southeast corner of the basin in the Strawberry Mountains, flows 116 km to its junction with the South Fork, another 44 km to its junction with the North Fork and then 298 km to the Columbia River.

The basin includes two ecoregions: Blue Mountains (80%) and the Columbia Plateau (20%). Here forward, the "upper mainstem" will be defined as the 116 km of the river to its junction with the South Fork, the "middle mainstem" as the 164 km of river from this junction to Clarno near the transition to Columbia Plateau ecoregion, and the "lower John Day" as the 172 km of river from this transition point to the confluence with the Columbia River. The Columbia Plateau ecoregion was formed by Columbia flood basalts (Miocene), overlain by loess, leaving plateaus and rolling hills that have been carved into canyons by the lower John Day and its tributaries (OWRD 1986). The Blue Mountains region is an assemblage of older volcanic, metamorphic and sedimentary rock accreted, uplifted and faulted, forming a complex array of rugged hills, plateaus, canyons, alluvial basins and glaciated mountains. Both the middle and upper mainstem and each of the major tributaries include long unconstrained reaches across floodplains that alternate with constrained reaches, a marked contrast with the Santiam basin where unconstrained floodplains are found almost exclusively in the lower basin.

The John Day basin is characterized by cold winters and warm to hot summers with climates ranging from semi-arid to sub-humid (grasslands) across most of the basin, while climates at higher elevations (North, Middle and South Forks) support open *Pinus*

ponderosa forests. Seventy percent of the precipitation falls between November and March, primarily as snow in the upper portions of the basin such that hydrology is driven by snowmelt with spring peak flows, and late summer flows are sustained by groundwater (OWRD 1986).

Sampling Design Precursor: Range-wide Maxent Model

As a first step, I built a range-wide model of *C. nudata* distribution using location information from herbarium records for input into Maxent (Fig. 2.1), a widely-used species distribution model (SDM) for presence-only data (Phillips et al. 2004, Peterson et al. 2007). In addition to climate and terrain variables commonly used in plant SDMs, I used hydrological variables from the National Hydrographic Dataset (NHD) Plus (mean annual discharge, stream slope, cross-sectional area and velocity), and total stream power was derived from these variables (McKay et al. 2012, USGS 2016). However, mean stream power cannot be readily derived given that stream width estimates are not included in the NHD Plus. The model was restricted to the linear features of the NHD Plus, and *C. nudata* occurrence was modeled at the scale of a river reach, defined as the segment between two tributaries in the NHDPlus (mean length: 2 km).

The Maxent model with the strongest explanatory power included mean annual discharge, stream velocity and maximum annual temperature as the top three explanatory variables, and the hydrological variables dwarfed all other variables in explanatory power. Stream velocity, total stream power and maximum annual temperature offered an alternative model with slightly less explanatory power. The Maxent model results and my observations of *C. nudata* traits led to the hypothesis that mean stream powe r drove *C. nudata* distribution. The Maxent SDM also served as the guide for a systematic, unbiased sampling effort that would yield species presence and absence data and a fuller suite of explanatory variables derived at a finer scale than available from the NHD Plus data.

Sampling Design: Basin-wide Field Surveys

I surveyed 15 sites in the John Day basin and 16 in the Santiam basin (Fig. 2.4). I used a stratified random design in which potential survey reaches were stratified by Maxent-predicted likelihood of *C. nudata* occurrence such that the final sample would have an even distribution of sites with low, medium and high likelihood of occurrence.

Within these strata, survey reaches were chosen randomly as constrained by access and other issues. I restricted potential survey reaches to those that did not appear to have significant anthropogenic impacts, e.g. excluding sites with significant cattle grazing and those bordered by road embankments. To facilitate access, I constrained potential survey reaches to those in proximity to trails or roads and, initially, to those located on public land or Tribal conservation areas. While public lands are extensive in both basins, it became apparent that this constraint restricted representation of low discharge, low slope reaches (= very low stream power) common in the lower Santiam. To address this issue, I expanded the potential set of survey reaches to include two sites on private lands in the Santiam. The final set of sampled sites included a broad range of climatic and hydrological conditions representative of each basin.

Field Survey Design

Each surveyed site was 100 m in length and intended to be representative of the reach. Sites were surveyed in the summers of 2013 and 2014 from mid-July through mid-September, consistent with annual period of low flows and ideal for sampling *C. nudata*.

At each site, I laid out on each side of the river (bank) a 100-m tape along the water's edge (WE) following the planform of the stream (Fig. 2.5). For each bank, *C. nudata* abundance (percent occurrence) was estimated via a line intercept sample in which any *C. nudata* plants up to 2.5 m distance away from the WE were projected laterally on to the 100-m transect. In addition to bank-transect estimates of *C. nudata* abundance, I also sampled *C. nudata* presence/absence at points. At the 10, 50 and 90-m points along the 100-m survey transects, I recorded presence/absence by whether any part of a *C. nudata* plant occurred within a 1m radius. At sample points where *C. nudata* was present, I also evaluated the vigor of the nearest *C. nudata*, scoring vigor on a scale of 1-5 primarily based upon the size and density of the tussock.

To calculate mean stream power, three key variables are needed: slope, discharge and channel width. In my field surveys, I collected data necessary for estimating slope and width. At each site, I surveyed three cross sections located at 10, 50 and 90 m along the 100 m *C. nudata* survey transect (Fig. 2.5). I used a "rapid survey" approach using a laser range finder aimed at a fixed target on a stadia rod. I surveyed cross sections from bank-to-bank with at least one measurement above what I estimated to be the maximum

possible bankfull height of the river. Surveying entire cross sections rather than simply making field-based estimates of bankfull widths made possible the use of post-field hydraulic analyses for more accurate width estimates associated with the Q_2 flow, the peak flow that occurs at a frequency of every two years. Given that the field measurements of slope were intended to represent the energy slope of the river at Q_2 flow (rather than the low flow slope), I measured vertical changes in elevation from riffle top to riffle top, using the upstream and downstream riffles closest to (at the edge or outside) the 100 m survey site. I measured horizontal distance along what I estimated to be the centerline of the river channel at bankfull flow.

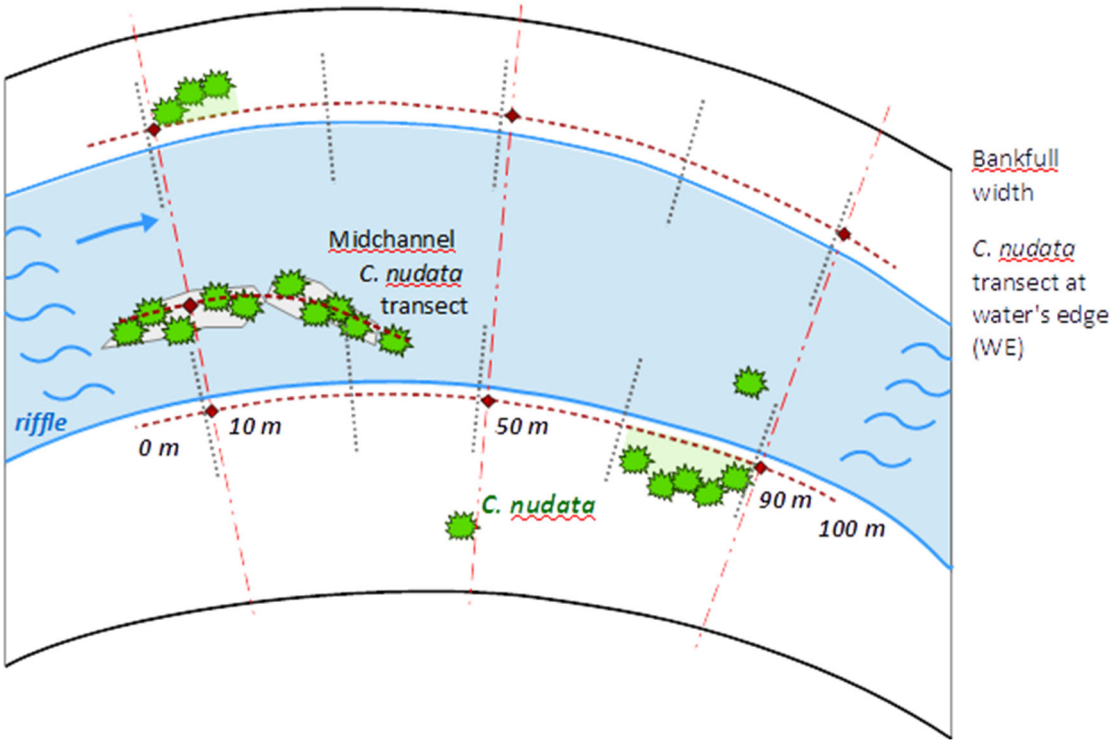

Figure 2.5. Field survey design. Dashed dark red lines represent *C. nudata* 100 m sampling transects. *C. nudata* presence/absence, canopy cover, substrate and vegetation plots sampled at the 10, 50, 90 m points on each bank. Dotted grey lines represent gravel count transects. Gravel count transects would also be placed on mid-channel bar but are not shown. Dashed-and-dotted red lines represent topographic cross-section surveys. Longitudinal and cross-sectional distances not scaled relative to each other.

In addition to measurements needed for the calculation of stream power, I sampled canopy cover and substrate at various scales. I used a spherical densiometer to estimate percent canopy cover at the 10, 50 and 90-m points along the 100-m transects on

each bank by averaging four measurements in cardinal directions at each point (Fiala et al. 2006). I also estimated the aspect of the river at each point. Densiometer measurements were also averaged to yield a bank-level canopy cover estimate. I used an aspect-weighted average in which the south-facing reading was given more weight (*1.5) and the north-facing reading less weight (*0.5).

To characterize substrate at the bank level, I conducted a variation on Wolman (1954) gravel counts with at least 50 particles counted for each bank. Particles were sampled at 0.5 m intervals along transects extending 2.5 m from WE into the river and 2.5 m from WE away from the river (Fig. 2.5). These perpendicular-to-the-river sampling transects were centered at the 10, 30, 50, 70, and 90 m points along the 100-m *C. nudata* transect. The gravel count design was intended to characterize the substrate potentially available for *C. nudata* colonization rather than the river bed as a whole.

At the points where *C. nudata* presence/absence had been determined (10, 50, 90 m), I used 1 m^2 substrate plots to make visual estimates of the percent cover of substrate classes: silt/clay, sand, gravels, cobbles, boulders, bedrock, bank material and vegetation (5% resolution). I placed plots along the WE with plots extending away from the water. However, in cases where >50% of the plot consisted of vegetation that prevented estimation of substrate, I instead used two 1-m^2 plots in various arrangements around the WE to ensure that close to 1 m^2 of substrate was sampled. Similar to the that used by O'Hare et al. (2011) and Bejarano et al. (2013), I calculated a bed caliber index (**BedCal**) in which the percentage of each substrate class is weighted by its value in the Wentworth phi scale (where ϕ is the $\log_2$ transformation of size in mm):

$$\mathbf{BedCal} = 10 * \mathrm{BR} + 9 * \mathrm{BO} + 6.5 * \mathrm{CO} + 4.5 * \mathrm{GR} - 1.5 * \mathrm{SA} - 6 * \mathrm{SiCl} \quad (3)$$

where BR (bedrock), BO (boulder), CO (cobble), GR (gravel), SA (sand), and SiCl (Silt & Clay) represent percentages by size class.

At these same points (10, 50, 90 m), I also made visual estimates of vegetative competition and available colonizable substrate in 1 m^2 vegetation plots (5% resolution). Vegetation plots always had one edge along the WE and extended away from the water. I made visual estimates of percent cover of vegetation classes and broader substrate types: *C. nudata*, non-*C. nudata* herbaceous vegetation, woody vegetation, moss, bare active

channel (any particle size or bedrock), bank material, elevated vegetated floodplain. Vegetative cover was estimated extending to a height of 1 m above the surface and vegetation classes could be overlapping (total could be >100%). However, by definition, the bare channel and bank material classes could never include any overlapping vegetation.

At sites with *C. nudata*, it was common for *C. nudata* to occur not only along the edges of the river but also attached to boulders or established on bars in the middle of the river. In most cases, I ignored these *C. nudata* within the wetted channel because they occurred as isolated individuals surrounded by uncolonizable habitat (water). However, in the Santiam basin, midchannel bars -- continuous, linear features -- were often the area with the highest *C. nudata* abundance. If a bar met certain criteria of minimum length and width, I treated it as a distinct river "bank," following a comparable protocol for sampling *C. nudata*, canopy cover and substrate (Fig. 2.5 and see Supplementary Materials for details).

Post-field Data Development: Discharge, Width, Stream Power and Climate

To test the hypothesis that *C. nudata* distribution can be explained by stream power I used stream power associated with peak flows that have a recurrence interval of two years on average, Q_2. The effective, or bankfull, discharge of a river is that which occurs with sufficient frequency and magnitude for a river's shape to be adjusted to that discharge (Wolman and Miller 1960). Bankfull discharge in humid temperate rivers has been theorized to have a return interval between 1 and 2 years (Eaton 2013). For each of the sites, I determined Q_2 using statistical models for natural flows derived from USGS stream gage data (Cooper 2005, Cooper 2006) along with map querying webtools that incorporate these models: for western Oregon, StreamStats (USGS 2016) and for eastern Oregon, the Oregon Water Resources Department Peak Discharge Mapping Tool (OWRD 2015). The flow estimates provided by these webtools for ungaged locations are derived from two types of models: 1) those based upon flows at the nearest gage on the same river adjusted by the difference in catchment area; 2) those based upon multiple gages across a hydrological region and multiple explanatory variables. I used the nearest-gage models for the 18 sites having drainage areas within +/- 50% of that of the nearest gage and used multiple predictor models for the other 13 sites.

In addition to Q_2 flows, I obtained mean monthly flows and annual low flows (flow exceeded 95% of the year, P_{95}) using the StreamStats and OWRD webtools. All of the monthly and low flow models are regional, multiple variable models rather than nearest gage models (Risley et al. 2008). Monthly mean and low flows were used to derive variables characterizing annual flow variation and spring peak to summer flow recession rate.

River widths associated with the Q_2 flow were determined using the cross-sectional survey data and hydraulic analysis. The hydraulic analysis employed an iterative approach using the continuity equation and the Manning's equation (see Supplementary Material for details). The widths estimated for the three cross sections at each site were averaged to yield a site-level Q_2 width (w) used to derive mean stream power from total stream power.

Climate variables for sites were extracted from the PRISM data set based on 1980-2010 normals (PRISM 2015). A list of climate and all other variables tested is presented in Table 2.2.

Statistical Analysis

I tested the relationship between environmental drivers and *C. nudata* distribution at two scales represented by two response variables: *C. nudata* abundance (%) at the scale of the river bank (100 m transects for left and right banks of a site and if present, mid-channel bar transect) and *C. nudata* presence/absence at points. Explanatory variables were measured at three scales: site (stream power, flow variability and climate), bank (canopy cover and substrate size) and point (canopy cover, substrate size and competing vegetation/available substrate).

Initial data exploration highlighted several issues with the data: the bank-level response variable, *C. nudata* percent occurrence, was not normally distributed and included a large number of zeros (>50% of banks); the relationship between *C. nudata* and several key variables appeared to be sigmoidal rather than linear; several explanatory variables were measured at the site level (n = 31) whereas response variables and other explanatory variables were measured at the finer scales of banks (n = 67) and points (n =196), and some degree of covariance might be expected between explanatory variables at the site level and those at finer scales.

To address these issues, I employed generalized linear mixed effects models (GLMM) with a logit link, a binomial (bank level) or binary (point level) distribution and a random intercept using *Site* as the grouping variable. Given that my objective was to test specific hypotheses and build a predictive model, I was inclined to use a parametric statistical approach such as a GLMM. The logit link available in a generalized linear model is inherently sigmoidal, so I anticipated it might be robust in modeling sigmoidal relationships, and quadratic terms could be used to accommodate hump-shaped relationships. Mixed effects models address the issue of any covariance by groups (e.g. sites) within the data, appropriate for hierarchical data (Bolker et al. 2009, Zuur et al. 2009). For all statistical tests, I used the GLIMMIX procedure available with SAS 9.4 software (SAS Institute 2013). As discussed in the Supplementary Materials, I explored alternative statistical approaches (e.g. non-linear mixed effects models, hurdle models, GAMs) but concluded that alternative approaches did not address the underlying issues with the data more successfully than the GLMM.

Given that a key objective was to test the hypothesis that *C. nudata* distribution is driven by stream power as well as to test which other variables might explain distribution, I built models using a directed forward stepwise approach. I first tested all single variable models. If stream power was a significant predictor, I then tested additional variables. If not, I built on the best single variable model and tested whether stream power was significant when added. At each step, I tested whether stream power was significant when added to the best previous model, and if stream power was significant, whether additional variables were significant. I stopped when additional variables proved insignificant, and I also tested alternative models.

I evaluated models by comparing both the significance levels of included variables and the distribution of residuals (minimizing heteroscedasticity), placing much weight on the latter comparison. A limitation of the pseudo-likelihood parameter estimation method used by PROC GLIMMIX is that it does not yield a test statistic that allows ready model comparison; the validity of the AIC and BIC statistics produced by the pseudo-likelihood method has been questioned by statisticians (Bolker et al. 2009, SAS Institute 2013).

In addition to models explaining *C. nudata* abundance or presence/absence, I tested models explaining the vigor of *C. nudata* individuals at sample points. I also tested the relationship between stream power and percent colonizable surface and vegetated cover. Finally, I explored graphically the systematic (upstream-to-downstream) relationships among multiple key variables through both basins.

Results

C. nudata Abundance along River Banks

Single-variable models of *C. nudata* abundance vs. each explanatory variable revealed that canopy cover (**CC**) was the single most significant explanator of *C. nudata* abundance with *C. nudata* abundance increasing as canopy cover decreased (p=.005, Fig. 2.6, Table 2.2). Neither mean stream power (**SPm**) nor total stream (**SPt**) power was a significant explanator alone. Other than canopy cover, the only other significant single variables ($p < .05$) were those representing flow variation -- the log difference between Q_2 peak flow and lowest flow by month (**Q2_minMo**) and the log difference between mean annual discharge and lowest flow by month (**P50_minMo**) -- but none of these were significant in combination with any other variables. Substrate variable -- median particle size (D_{50}) and percent stable substrate (**Stbl**) -- were marginally significant in single variable models ($p < .1$) with *C. nudata* abundance positively associated with larger/more stable substrate

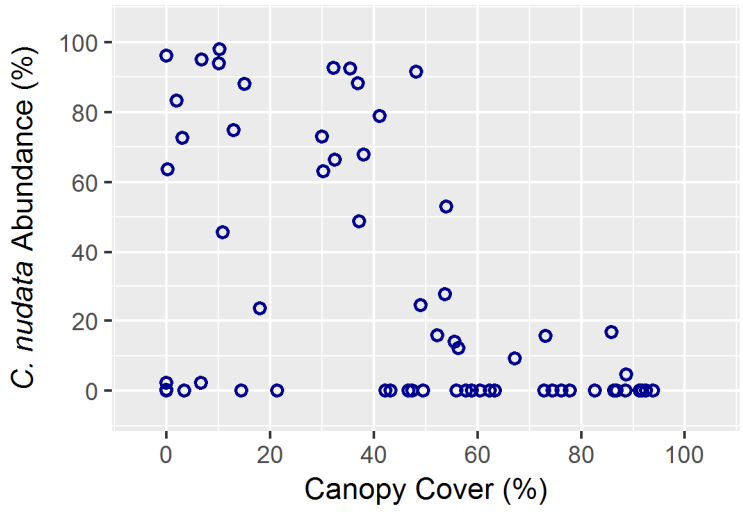

Figure 2.6. *C. nudata* abundance by bank vs. canopy cover.

Table 2.2. List of variables tested as explanators of *C. nudata* abundance by bank and significance (p values shown if < .1) in univariate model and then bivariate model with canopy cover (CC). Sign (+/-) represents sign of parameter in model.

Variables		Univariate Model (*p*)	Bivariate w CC (*p*)
CC	Canopy cover (%) weighted by aspect	.0053 (-)	
Aspect	Aspect, absolute	ns	ns
Q2	Q_2 - peak flow with 2 yr probability (m^3/s) – $\log_{10}$	ns	ns
SPt	Stream power, total (W/m) at Q_2 - $\log_{10}$ transform	ns	ns
SPm	Stream power, mean (W/m^2) at Q_2 - $\log_{10}$ transform	ns	.017 (+)
v	velocity at Q_2 (m/s)	ns	ns
wd	width to depth ratio at Q_2	ns	ns
D50	Median particle size, D_{50} - $\log_2$ transform	.077 (+)	.018 (+)
D84	Particle size at the 84^{th} percentile, D_{84} - $\log_2$ transform	ns	.016 (+)
Stbl	Percent stable substrate - cobbles, boulders, bedrock	.093 (+)	.0079 (+)
Fine	Percent fine substrate - silt/clay, sands	ns	ns
BkM	Percent bank material	ns	ns
BR	Percent bedrock	ns	ns
Tmn_MaxMo	Mean temperature, month w maximum annual temperature	ns	ns
Tmn_MinMo	Mean temperature, month w minimum annual temperature	ns	ns
gdd10	Growing degree days using base 10 °C	ns	.078 (-)
gdd05	Growing degree days using base 5 °C	ns	.095 (-)
P50_0407	Slope ($\log_{10}$ diff) of mean monthly flow (P_{50}), Apr-July	ns	ns
P50_0910	Slope ($\log_{10}$ diff) of mean monthly flow (P_{50}), Sept-Oct	ns	ns
Q2_minMo	Q_2 flow to mean flow of lowest flow month ($\log_{10}$ diff)	.046 (-)	ns
P50_minMo	Mean annual flow (P_{50}) to mean flow low month ($\log_{10}$ diff)	.042 (-)	ns

Mean stream power was indeed a significant explanator of *C. nudata* abundance when paired with canopy cover (Table 2.2). *C. nudata* abundance appeared to

demonstrate threshold-like behavior relative to stream power (Fig. 2.7). *C. nudata* was absent or minimally present at very low stream powers (< 50 W/m^2) and then increased steeply between 50-70 W/m^2. Above this threshold, *C. nudata* abundance appeared to be explained primarily by canopy cover. *C. nudata* persisted at very high stream powers (1000 W/m^2) with relatively high abundance where canopy cover was low (Fig. 2.7).

While a simple linear model with stream power and canopy cover was significant for each term, substituting an interaction term (**CC*SPm**) for canopy cover increased the significance of all parameters (Table 2.3) and better fit the threshold-like change in abundance across low to medium stream power values (Fig. 2.7a). Including both canopy cover and the interaction term made both insignificant. Nevertheless, the canopy cover with a quadratic model for stream power best fit the threshold behavior and yielded a better distribution of residuals with reduced heteroscedasticity (Table 2.3, Fig. 2.7b).

Basin identity (John Day vs. Santiam) was not significant when added to the model as a factor, indicating that the relationship between *C. nudata* and these explanatory variables was no different between basins.

The substrate size variables, D_{50}, D_{84} and % stable material (**Stbl**) were each found to be significant in a two-variable linear model with canopy cover (Table 2.2). None of the substrate variables were significant when added to the bivariate linear stream power and canopy cover model. This was not surprising given that each of these variables covaried with stream power. However, % stable material was marginally significant ($p <$ 0.1) when added to the quadratic stream power and canopy cover (Table 2.3).

No other variables proved significant when added to either the linear **CC + SPm** and **CC*SPm + SPm** models or the quadratic **CC + SPm** model.

C. nudata Presence/Absence at Points

Consistent with bank-level abundance relationships, *C. nudata* probability of occurrence at points could be explained with a model including mean stream power and point-level canopy cover. The fit of this model improved when canopy cover was replaced by an interaction between canopy cover and stream power (Table 2.4). Furthermore, the significance of the canopy cover and canopy cover interaction variables were a magnitude greater in the point-level models (p =. 0006, p =.0002) than the bank-level model (p = .002, p = .002).

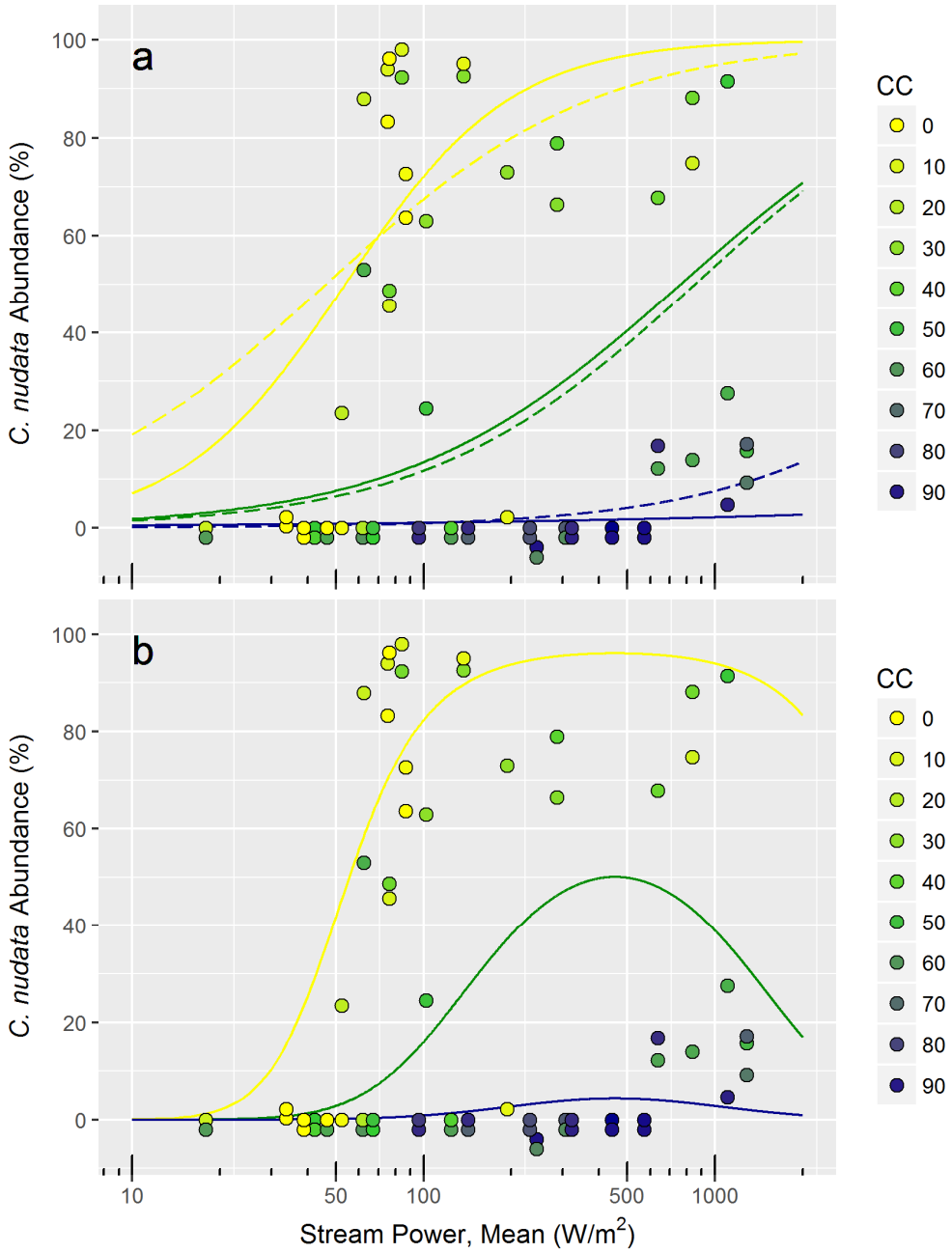

Figure 2.7. *C. nudata* abundance by bank vs. mean stream power and canopy cover (**CC**). In a) and b) data represented by points are the same. Lines represent predicted values from alternative models: a) the simple linear models or b) the quadratic model (**CC + SPm + SPm^2**), all using the logit link. In a) solid lines are the model with the interaction term **(SPm*CC + SPm)** and dashed lines are the model with no interaction (**CC + SPm**). Line color represents different input values for canopy cover: yellow for **CC** = 0%, green for **CC** = 48% (median), and blue for **CC** = 94% (maximum). *C. nudata* abundance values = 0 have been "jittered" for visibility, i.e. points below zero line all represent zero values.

Table 2.3. Alternative models for *C. nudata* abundance (%) by bank using canopy cover (CC), mean stream power (SPm) and percent stable material (Stbl) as explanatory variables.

Models: *C. nudata* % by bank =	β_0	β_1	β_2	β_3	β_4	
CC + **SPm**	-3.62*	-5.75**	2.17*			
CC∗SPm + **SPm**	-6.09**	-2.94**	3.52**			
CC + **SPm** + **SPm²**	-23.9*	-6.69**	20.4*	-3.84†		† β_3: p = .051
CC + **SPm** + **SPm²** + **Stbl**	-25.7*	-7.19**	20.2*	-4.11†	6.85†	† β_3: p = .053 β_4: p = .060

Notes: † $p < .1$, * $p < .05$, ** $p < .01$, *** $p < .001$

Table 2.4. Alternative models for C. nudata presence/absence (P/A) by points using point-level canopy cover (CC) and bed caliber (BedCal) from 1m^2 substrate plots and site-level mean stream power (SPm) as explanatory variables.

Models: *C. nudata* P/A by point =	β_0	β_1	β_2	β_3	
CC + **SPm**	-4.07†	-4.34***	2.19*		
CC∗SPm + **SPm**	-5.74*	-2.02***	3.06**		
CC*SPm + **SPm** + **BedCal**	-5.56*	-1.99***	2.21†	.291†	† β_2: p = .064 β_3: p = .057

Notes: † $p < .1$, * $p < .05$, ** $p < .01$, *** $p < .001$

Compared with bank-level models, fine scale measurement of substrate produced only small improvements in the explanatory power of substrate size when added to the bivariate point-level models. Substrate size from visual estimates (**BedCal**) was not significant when added to the **CC + SPm** model. When added to the **CC*SPm + SPm** interaction model, substrate size was marginally significant (p <.1; Table 2.4).

If stream power may be conceived as a proxy for disturbance, then available colonizable space may be the effect of that disturbance. Both variables measuring available colonizable space, bare channel (**Bare**) and surface not vegetated by species other than *C. nudata* (**NoVeg**), were positively and strongly related to mean stream power

(Table 2.5). The two variables differ in how they treat *C. nudata* occupied area within a plot; **Bare** could be considered a conservative estimate and **NoVeg** a liberal estimate of colonizable space. Given that both were significantly related to stream power, these metrics may be used to represent disturbance effect at a fine scale.

Table 2.5. Models of available colonizable space, NoVeg or Bare (from $1m^2$ vegetation plots), as response variables and mean stream power as explanator.

Models: Available space	β_0	β_1
NoVeg = SPm	-3.78**	2.32***
Bare = SPm	-4.65**	2.48****

Notes: ** $p < .01$, *** $p < .001$, **** $p < .001$

Using each of these point-level "available space" variables in a model with canopy cover, **NoVeg** was a significant explanator of *C. nudata* presence, but **Bare** was not (Table 2.6). Both variables proved to be significant explanators of *C. nudata* presence in models with canopy cover represented as an interaction with the available space variables. Substrate size at the point level (**BedCal**) was a significant explanator when added to the **NoVeg** + canopy cover interaction model (Table 2.6).

Table 2.6. Alternative models of *C. nudata* presence/absence (P/A) by points using point-level canopy cover (CC), available colonizable space variables (NoVeg, Bare) and bed caliber (BedCal) as explanatory variables.

Models: *C. nudata* P/A by point =	β_0	β_1	β_2	β_3	
CC + **NoVeg**	-2.48†	-3.35**	3.47*		
CC∗NoVeg + **NoVeg**	-3.57**	-3.70**	4.70**		
CC*Bare + **Bare**	-1.64*	-2.91*	1.96*		
CC + NoVeg + BedCal	-3.36*	-3.68**	2.52†	.302†	† β_2: $p = .075$; β_3: $p = .051$
CC*NoVeg + NoVeg + BedCal	-4.53**	-4.21**	3.82**	.314*	

Notes: † $p < .1$, * $p < .05$, ** $p < .01$, *** $p < .001$

Vigor of individual *C. nudata* plants was strongly and positively related to canopy cover (Table 2.7). Vigor had a significant but weak (low slope) negative relationship with mean stream power, but mean stream power was not significant when added to a model with canopy cover.

Table 2.7. Models of individual *C. nudata* vigor as a function of point-level canopy cover and mean stream power.

Models: Vigor, individual *C. nudata*	β_0	β_1	β_2
CC	4.27****	-1.90**	
SPm	4.10****	-.00095*	
CC + SPm	4.34****	-1.59*	-.0004 ns

Notes: ns = $p > .1$, † $p < .1$, * $p < .05$, ** $p < .01$, *** $p < .001$, **** $p < .0001$

Basin-wide Patterns of Explanatory Variables

Consistent with principles of downstream hydraulic geometry, both Q_2 flow and width increased and slopes decreased as drainage size increased in both basins (Figs. 8a,b,c). As expected in the drier John Day basin, flows and widths showed a much smaller rate of increase with increasing drainage area. While both basins showed a downward trend in slope relative to drainage area, some differences were apparent (Fig. 2.8c). High slopes could be found in both basins at small (< 50 km2) and intermediate drainage sizes (50-500 km2), but the lowest slopes at intermediate drainage sizes were found in the Santiam basin where smaller tributaries originating in lower foothills flowed across the broad Willamette basin floodplain. Across larger drainage sizes (>500 km^2), sites within the John Day maintained higher slopes than those of the Santiam.

In both basins, mean stream power started relatively high in the smallest sampled drainage areas, peaked and then declined with lower values at high drainage areas (>500 km^2, Fig. 2.8d). Both the highest values and the greatest variation in mean stream power were found across intermediate drainage areas (100-500 km^2). The John Day displayed a lower peak and less variation than the higher values and greater variation of the Santiam basin.

In both basins, canopy cover decreased as discharge increased downstream, consistent with stream widening (Fig. 2.9). However, for any given discharge, canopy

cover was much less in the John Day basin, a reflection of more open vegetation. Also, in the Santiam basin, the lowest canopy cover values at a given discharge were typically associated with the mid-channel bars, a feature of several sites.

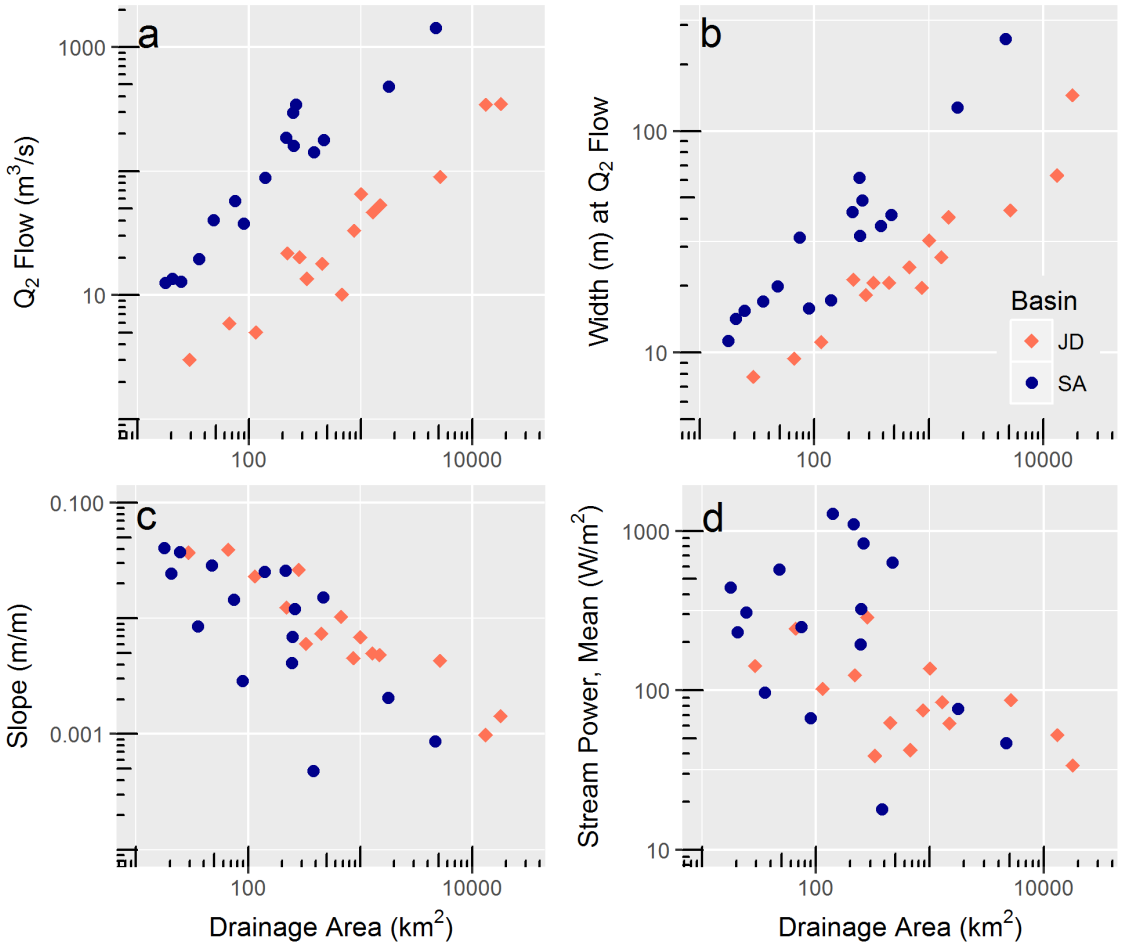

Figure 2.8. Basin-wide patterns of a) Q_2 peak flow, b) stream width, c) stream slope and d) mean stream power. All variables shown relative to increasing drainage area. Orange diamonds represent John Day (JD) basin, solid blue circles represent Santiam (SA) basin.

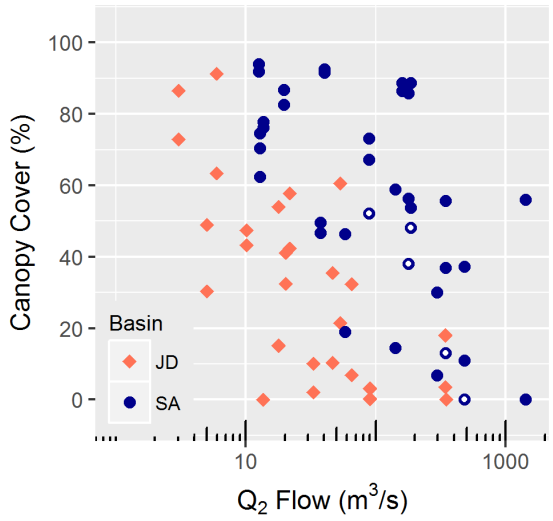

Figure 2.9. Canopy cover vs. Q_2 peak flow by basin. White dots in symbols are midchannel bars.

Discussion

C. nudata's Niche and Life History Strategy within the River Ecosystem

The results presented here, paired with observations of *C. nudata* phenology and traits, provide the basis for a conceptual model of *C. nudata*'s niche and life history strategy within the river ecosystem. In contrast with many riparian sedges, *C. nudata* is not rhizomatous such that its propagation is dependent primarily on water-borne seed dispersal, hydrochory, and germination occurs immediately after dispersal. Among hydrochorous species, three common strategies include: dispersal on the falling limb of the spring flood with immediate germination (e.g. *Salix* and *Populus* spp.), dispersal during summer low flows, and dispersal during the rising limb of fall flows (Merritt and Wohl 2002, Nilsson et al. 2010). Summer or fall dispersal is commonly followed by over-winter dormancy that make seeds the first available for colonization prior to the spring dispersers (Neff and Baldwin 2005, Nilsson et al. 2010). *Carex nudata* is thus challenged both by its lack of rhizomatous propagation and its late-to-the-game summer germination. *C. nudata* would not only be at a competitive disadvantage relative to any rhizomatous neighbors (if not distant from them), its root growth must also be fast enough to secure a foothold in a short time window before the end of the growing season and inundation by subsequent fall-to-spring peak flows.

In a prior investigation, Goslin (in prep-a) observed that *C. nudata* was associated with coarser substrates in reaches of the MJFJDR where a diversity of substrates was available. Goslin (in prep-a) conducted in-river seed planting experiments across four substrate classes to test the hypothesis that *C. nudata* established more successfully on coarser substrates. Contrary to expectations, *C. nudata* did not display significant differences in germination and survival across substrate classes during the first growing season. However, "fine deposits" plots were often invaded by sprouting rhizomes that overtopped *C. nudata* germinants. Relative to other substrate classes, these plots were closer to the leading edge of the vegetated "green line" dominated by rhizomatous sedges. In light of these results, the perception that *C. nudata* establishes preferentially on coarser substrates was revised toward a conception that this apparent preference is the outcome of a disturbance-adapted strategy in which *C. nudata* escapes competition by being capable of establishing where few other species are able.

The relationship between *C. nudata* distribution and stream power revealed by the basin-wide surveys presented here corroborates the conception of *C. nudata* as a disturbance-adapted species. Bank-level abundance demonstrated a positive relationship between *C. nudata* and mean stream power with a distinct threshold (50-70 W/m^2) below which *C. nudata* was rare and above which *C. nudata* abundance could potentially reach > 90% occurrence in a given reach. Above the minimum threshold, abundance was strongly related to light availability as represented by canopy cover.

Point-level probability of occurrence showed a similar, albeit slightly weaker, relationship with mean stream power and a tighter relationship with light availability estimated at this finer scale. Whereas mean stream power was estimated at the site level, available colonizable area, a possible effect of disturbance, was estimated at the point level using two different metrics (**Bare** and **NoVeg**). Both metrics of colonizable area proved to be strongly associated with site-level mean stream power. When included in a model with an interaction term with canopy cover (**Bare*CC + Bare, NoVeg*CC + NoVeg**), both of these fine scale estimates of disturbance effects were positively associated with probability of *C. nudata* occurrence. Together, these results point to the key role of disturbance in creating open, colonizable area for *C. nudata* free from competitive interference.

If fluvial disturbance sufficient to create competition-free colonizable space is a prerequisite for establishment, *C. nudata* must then overcome the challenge of establishing in habitat experiencing high shear stress during peak flows. Light availability may be the key limiting factor necessary for sufficient root growth and successful establishment. The strong relationship between bank-level abundance and canopy cover, the even tighter relationship between point-level probability of occurrence and canopy cover, and the strong relationship between individual plant vigor and canopy cover all indicate that *C. nudata* success is primarily light-limited.

The concept of the regeneration niche helps frame *C. nudata*'s habitat requirements and how these requirements compare with other well-researched riparian species. For *Salix* and *Populus* species that disperse and germinate immediately on the falling limb of the spring flood, Mahoney and Rood (1998) proposed a "regeneration box" in which establishment is limited by water availability tied to the receding water table and a recession rate that does not out-strip downward seedling root growth. Given that *C. nudata* seedlings disperse and germinate near the end of the spring-to-summer flow recession at elevations close to the lower limit of the receding water table, water availability and rapid downward root growth is likely less important than growing a sufficiently dense root mass by the end of the growing season to secure a foothold on a stable surface prior to fall-to-spring peak flows. My anecdotal observations suggest extremely high mortality of first year seedlings following fall-to-spring floods. The results here suggest that light availability may be the critical resource necessary for sufficient growth in the early years during which young *C. nudata* are vulnerable to large floods.

C. nudata Distribution Relative to Substrate

While these results point to light availability and stream energy as key dimensions of *C. nudata*'s niche, the role of substrate size is less clear. In addition to rapid, early root mass growth, it may be essential for *C. nudata* to establish on larger clasts that are simply less likely to be mobilized in high energy events. However, teasing out this relationship is problematic given that fluvial geomorphology theory would predict substrate size to be closely related to mean stream power for a stream in equilibrium (Brummer and Montgomery 2003). Nevertheless, not all stream reaches are in equilibrium, and historic

legacies may lead to larger than expected clasts (Rice and Church 1998). Furthermore, substrate heterogeneity within a reach may result in patches of larger clasts than the reach median.

Models for *C. nudata* that included substrate size (D_{50}, D_{84}**, Stbl, BedCal**) with canopy cover instead of stream power yielded significance values for substrate size comparable to those of stream power. However, as expected, substrate size covaried with stream power, and stream power is a driver of substrate size. Therefore, the critical question was whether substrate size explained additional variance after including stream power. Is *C. nudata* found on substrate sizes larger than those expected at a given stream power? No metrics of substrate size were significant when added to the simple linear models, but percent stable substrate was marginally significant (p=.06) when added to the quadratic model (Table 2.3). In general, percent stable substrate (bedrock, boulders and cobbles) was a better explanator across models than D_{50} and D_{84}. Metrics from particle size distributions (D_{50}, D_{84}) do not include bedrock given that it does not have measurable size, but bedrock was an important component in high energy streams and *C. nudata* was often found on bedrock with roots growing into cracks. While statistical evidence was not convincing, examination of model outliers and graphs of substrate size vs. stream power suggest that in sites with strong differences in substrate size among banks, *C. nudata* may be more abundant along the banks with larger substrate (Fig. 2.10). For example, the largest outlier across models was SA05_L, the left bank of Quartzville Creek (Fig. 2.11). Given the high site stream power and low bank canopy cover, *C. nudata* abundance was predicted to be high (90%) but less than 5% occurred. The left bank of this site was a gravel/cobble bar with lower-than-expected substrate sizes relative to stream power and likely mobile at peak flows. In contrast, the right bank was a clast-supported terrace, a historic legacy, consisting of large cobbles and boulders exposed as the river cut into the terrace, leading to larger-than-expected clasts along the water's edge and a continuous strip of *C. nudata*. At other sites in the Santiam, the mid-channel bars, the "banks" with the highest *C. nudata* abundance, often had the largest substrate sizes in addition to lower canopy cover (Fig. 2.10).

Given the heterogeneity of substrate within the bank units, I expected that substrate would be a more significant explanator in the finer-scale point-level models.

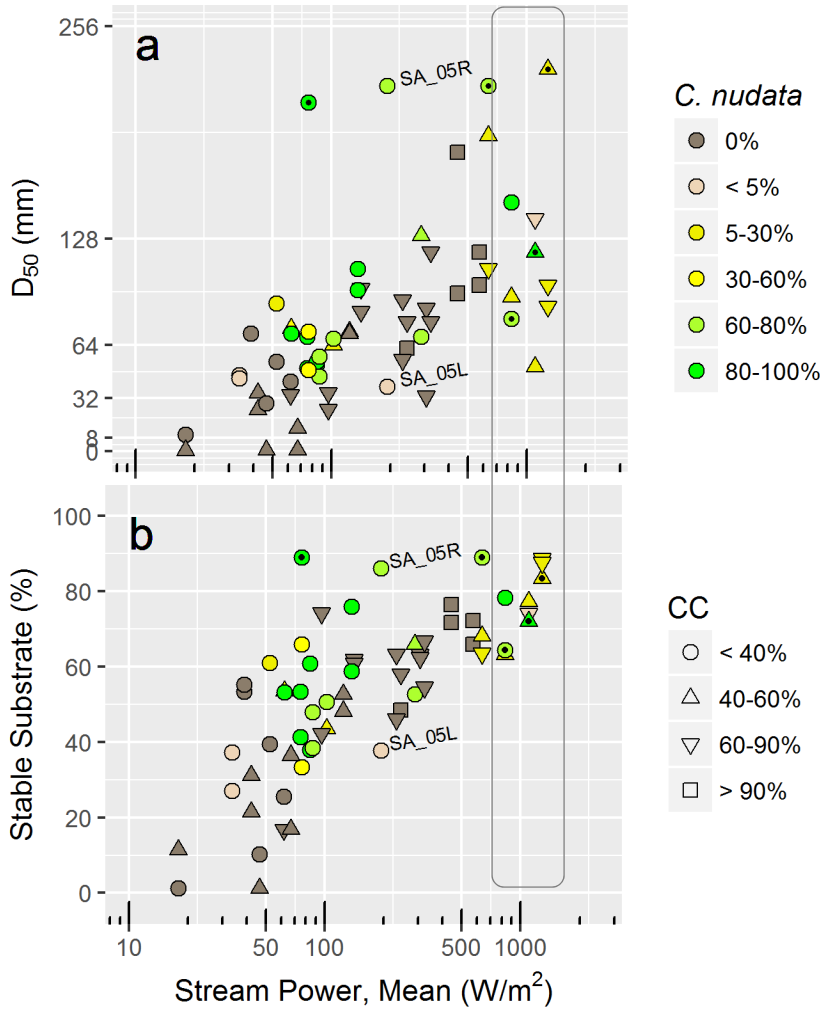

Figure 2.10. a) D_{50} and b) percent stable substrate (**Stbl**) vs. mean stream power with *C. nudata* abundance represented by colors and canopy cover (**CC**) by shapes. Black dots within symbols represent mid-channel bars. Vertical gray box encompasses sites with significant bedrock component.

However, bed caliber (1 m^2 plots) was not significant when added to the **CC** + **SPm** model. When added to the better-fitting interaction model (**CC*SPm + SPm**), bed caliber was marginally significant (p = .057). Although these results did not offer support for the hypothesis that substrate size at fine scales is a key component of *C. nudata*'s niche after accounting for stream power, I remain unconvinced that it is not important. The sampling design, visually estimated substrate plots, was efficient but had limitations. At points with *C. nudata*, plots by necessity captured substrate proximate to the *C. nudata* rather than the substrate on which *C. nudata* had established, substrate that would require excavation to sample. Furthermore, *C. nudata* after establishment can alter

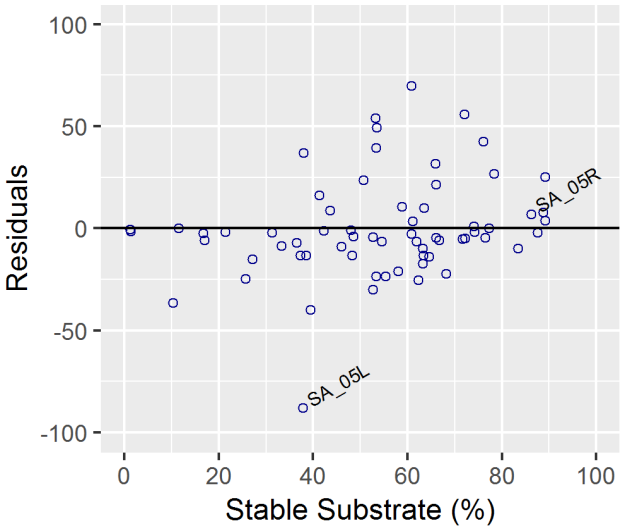

Figure 2.11. Residuals from the bank-level quadratic model (**CC** + **SPu** + **SPu²**) of *C. nudata* abundance (%) vs. percent stable substrate (**Stbl**).

substrate composition in its neighborhood by enhancing roughness and the deposition of fine sediment. Finally, the estimates of stream power were made at the site level. A full assessment of the balance between stream power, substrate size and particle mobility would require localized estimates of shear stress where *C. nudata* has established, a promising analysis but one beyond the scope of this paper.

C. nudata and High Stream Power

In my initial conception of the relationship between stream power and *C. nudata*, I hypothesized not only a lower stream power limit below which there was insufficient disturbance for *C. nudata* establishment, but also an upper limit at which stream power would be too high for survival. While the quadratic model does suggest a modest decline in *C. nudata* abundance at the highest stream powers sampled, the data does not support an upper threshold. The range of high stream powers over which *C. nudata* can establish is remarkable. These stream power values are at the high end of those documented for riparian vegetation (Bendix 1999). In the Santiam, it is possible that the sample design missed reaches with even higher stream power due to accessibility issues. None of the John Day sites approached the high stream power values at which a decline was predicted by the quadratic model. A salient feature of the quadratic model is that it also suggests that the decline in *C. nudata* abundance with very high stream power is more pronounced as light becomes limiting. Such a pattern fits the conception of *C. nudata*'s regeneration

niche: with less light and slower root growth, *C. nudata* is less likely to establish sufficient holding power to survive more extreme flood energy.

C. nudata Patterning within Basins

Given that *C. nudata*'s niche is shaped by two key variables, stream power and canopy cover, that are both driven by hydrology and vary systematically within basins, the distribution of *C. nudata* also displays systematic within-basin patterning (Fig. 2.12). A salient feature of the models fitting these data is that despite differences in climate, hydrology and geology among the study basins, the relationship between *C. nudata* and the two key variables was similar, that is, basin identity was not significant when included as a factor in the model, indicating a commonality in underlying processes. The differences in *C. nudata* distribution among the two basins reflects differences in within-basin variation of stream power and canopy cover driven by underlying geology, climate and topography.

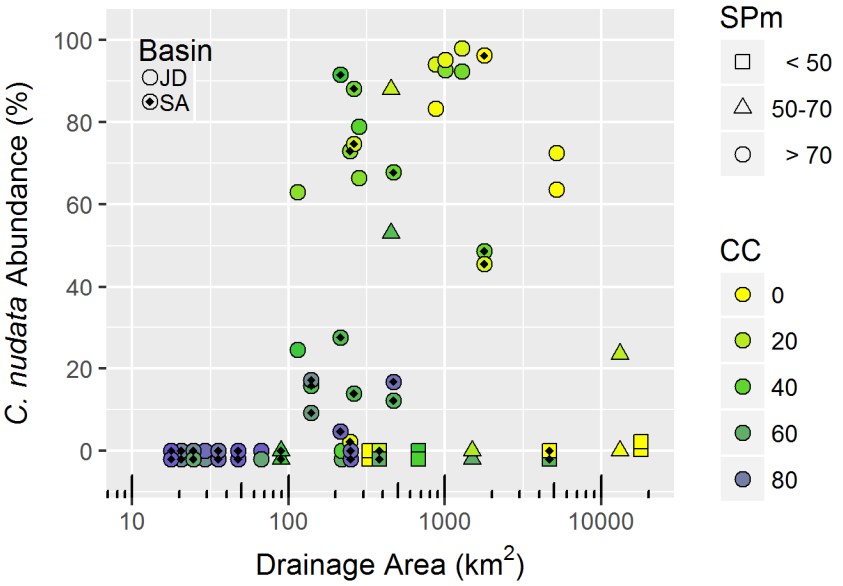

Figure 2.12. Within-basin patterning: *C. nudata* abundance vs. drainage area in the John Day (JD) and Santiam (SA) basins. Point shapes represent mean stream power (**SPm**, W/m^2) and colors represent percent canopy cover (**CC**). Black diamonds within symbols signify Santiam sites.

A conceptual model (Fig. 2.13) describes *C. nudata* patterning within basins. Canopy cover, itself, is driven by within-basin trends in hydrology interacting with local climate. Streams higher in a basin have smaller discharge and smaller widths, leading to

minimal light gaps above a stream. Given that steep slopes result in mean stream powers above the minimum threshold for successful *C. nudata* establishment, light is the limiting factor high in a basin. Moving downstream into mid-basin areas, mean stream power peaks and then declines, but continues to remain above the minimum threshold for *C. nudata* occurrence. Increasing discharge leads to wider streams and a larger light gap, such that *C. nudata* becomes more common. Moving further downstream, light may no longer be limiting, but flatter slopes and river widening result in mean stream powers below the threshold for *C. nudata* occurrence.

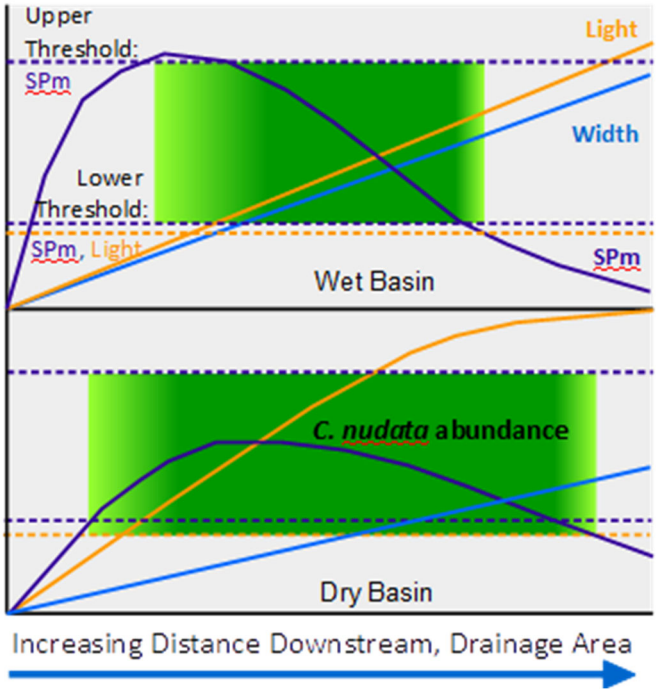

Figure 2.13. Conceptual model of basin-wide patterning in *C. nudata* abundance for a wet and dry basin. Increasing intensity of the green band between the lower and upper thresholds for SPm (mean stream power) represents increasing probability and abundance of *C. nudata*. The lower light threshold is treated as a fuzzy threshold given the gradual nature of the *C. nudata* vs canopy cover relationship in the data compared to the steeper SPm threshold. An upper SPm threshold is hypothetical given the limited support for such a threshold in the data.

The rate of canopy opening and subsequent *C. nudata* patterning may be modified by climate. The dense forests of the wetter Santiam basin prevent significant opening above a stream until mid-basin positions are reached and significant widening occurs. In drier basins such as the John Day, more open forests and riparian galleries allow greater

light availability at relatively high positions within the basin such that the upstream starting point for *C. nudata* may be higher.

Differences in basin geology and local topography may also modify this patterning via effects on stream power. In the relatively young volcanic geology of the western Cascades, streams at high-to-mid positions within the basin flow through constrained, relatively steep valleys resulting in high stream powers well above the minimum threshold for *C. nudata* establishment. In contrast, the older geology of the Blue Mountain ecoregion in the John Day has allowed streams to develop small, alluvial floodplains at relatively high positions in the basin. As a result, reaches with stream power below the minimum threshold for *C. nudata* establishment occurred at relatively high positions in the basin where both discharge and slope were low. For example, *C. nudata* was absent from the site JD_09, upper MFJDR, a gently sloping floodplain site where high light did not limit *C. nudata*, but low discharge and low-moderate slope resulted in low mean stream power (38.8 W/m^2). Another distinction between the two basins is the broad floodplain of the Willamette Valley across which the lower North and South Santiam and their foothill-originating tributaries flow. Canopy cover was relatively low in this agricultural landscape, but the tributaries flowing across this floodplain (SA_15, SA_16) displayed some of the lowest mean stream powers among sites.

C. nudata Basin Patterns and Biogeomorphology

With their dense, strong root systems, mature *C. nudata* stabilize patches of substrate and act like organic boulders (McDowell pers. comm), obstacles that can alter flow, erosion and deposition. In the MFJDR, *C. nudata* can induce geomorphological change because the species occurs at high frequencies, the size of *C. nudata* tussocks are significant relative to the size of the river, and sections of the river flow through alluvial floodplains with eroding, migrating banks. In the MFJDR, I have documented multiple, alternative trajectories of stream evolution: 1) bank stabilization following further vegetative colonization behind *C. nudata*, 2) the formation of compound channels as banks continue to erode behind *C. nudata* and 3) the formation of islands as stabilized *C. nudata* patches become “detached” from eroding banks. (Chapter 3). To what extent are these or different patterns of stream evolution apparent in basins where *C. nudata* occurs?

C. nudata occurs in high densities throughout the MFJDR and North Fork John Day River and in variable densities in the middle mainstem John Day. The John Day basin is particularly suitable habitat given that most of the river experiences mean stream powers above the minimum threshold for *C. nudata*, and canopy cover is rarely dense enough to limit light. Furthermore, discharge and associated widths increase slowly throughout the basin such that the size of *C. nudata* tussocks relative to river width remains significant throughout much of the upper and middle portions. Stream evolution trajectory 3 (island formation) appears to be prevalent primarily in the upper MFJDR (JD_03). However, I have observed both trajectory 1 (bank stabilization) and trajectory 2 (compound channel formation) in sites throughout the MFJDR (JD_03, JD_04, JD_08), the North Fork (JD_11) and the middle mainstem (JD_13). The requisite conditions for these effects appear to be a low flow channel of narrow-to-moderate width (5-10 m) dominated by dense *C. nudata* within an unconstrained alluvial reach allowing differential patterns of bank erosion.

Within the Santiam basin, *C. nudata* appears to play a less significant biogeomorphic role. Due to high canopy cover, *C. nudata* is absent in headwater streams. In mid-basin reaches with moderate light availability, *C. nudata* may be present but in low densities along the banks. Given the low densities of *C. nudata*, large stream widths and the prevalence of constrained and bedrock reaches, *C. nudata* likely has minimal effect on the evolution of most channel boundaries. However, *C. nudata* is present in high densities along mid-channel bars where light levels are high (SA_03, SA_08, SA_09, SA_13, SA_14). *C. nudata* may be facilitating the stabilization of these features, a positive feedback. I observed woody species such as *Salix* and *Alnus* spp. establishing within the sediment-trapping *C. nudata* tussocks on midchannel cobble/boulder bars which would otherwise be problematic to colonize, biogeomorphic succession facilitated by *C. nudata*. Finally, Quartzville Creek (SA_05) may be an exception to the generalization that *C. nudata* is having minimal impact on the channel boundaries. The right bank is not constrained by a hillslope but rather is a historic terrace composed of large clasts cut through by the river. This was the one site in the Santiam where *C. nudata* formed a relatively continuous fringe at the base of the bank, colonizing the large clasts

exposed by the bank's erosion, possibly stabilizing the bank toe and reducing further erosion.

Conclusions

The distribution of *Carex nudata* within basins of strikingly different climates could be explained in both basins by two variables, mean stream power and canopy cover, which are both driven by hydrological factors and vary systematically within basins. The relationship with mean stream power was consistent with a disturbance-adapted life history strategy requiring colonizable space for water-dispersed seeds and capable of resisting peak flows of high stream power. *C. nudata* has the capacity to act as an ecosystem engineer, altering channel morphology in certain reach types, and understanding its distribution is a first step in predicting where it may play a critical role in biogeomorphic successional processes. Other authors have suggested key ecosystem roles for the species (Levine 1999, 2000a). Understanding the hydrological drivers of its distribution may be critical as agencies engage in reformation of dam management through environmental flow programs (Richter et al. 2006, Merritt et al. 2010, Konrad et al. 2012). Alterations of the natural flow regime below dams may have negatively impacted *C. nudata* populations, and implementation of environmental flows that more closely mimic a natural flow regime may be critical to facilitating the conservation of these populations.

III. CHANNEL EVOLUTION ENGINEERED BY A NATIVE RIPARIAN SEDGE, CAREX NUDATA, FOLLOWING PASSIVE RESTORATION

This work will be submitted for publication with Patricia McDowell as a co-author, acknowledging her contribution to conceptual and methodological development.

Introduction

The Middle Fork John Day River and Carex nudata

In the Middle Fork John Day River (MFJDR) in northeastern Oregon, system-wide changes in riparian vegetation following passive restoration have opened the opportunity to investigate the coupled evolution of channel morphology and plant communities. In the 1990s vegetation was released from cattle grazing pressure following reformation of grazing practices by the U.S. Forest Service (USFS) and the removal of grazing from river banks within newly established conservation areas dedicated to salmon population recovery. Following these changes in management the native riparian sedge, *Carex nudata,* expanded rapidly across the riverscape and is now the dominant stream-side species in large portions of the basin. Anecdotal evidence has suggested that the expansion of *C. nudata* has been accompanied by changes in channel form, but the nature of these changes has not been clear and has implications both for restoration practice and our understanding of plant-river interactions. Land managers and restoration practitioners have perceived the expansion of *C. nudata* positively, but a key question is whether associated changes in river morphology are consistent with restoration goals.

Found in varying densities in rivers throughout Oregon and California, *C. nudata* derives its common name, torrent sedge, from its ability to grow in the middle of fast rivers due to its remarkably strong, dense root system (Levine 2000a). *C. nudata*'s life history traits are consistent with a disturbance-adapted strategy (Chapter 2). *C. nudata* is tussock-forming, not rhizomatous, and propagates primarily by seeds that are river-dispersed (Wilson et al. 2008). Seeds are dispersed and germinate immediately during summer low flows, placing newly established *C. nudata* at the edge of exposed substrate. *C. nudata* can be found established along the edges of gravel bars, as a fringe at the base of cut banks, and as low mid-channel islands exposed during low summer flow levels (Fig. 3.1). The diameter of a mature tussock may be >0.5 m at its base and >1 m at its

leaf crown. As a significant obstacle, *C. nudata* tussocks may alter patterns of flow, erosion and deposition.

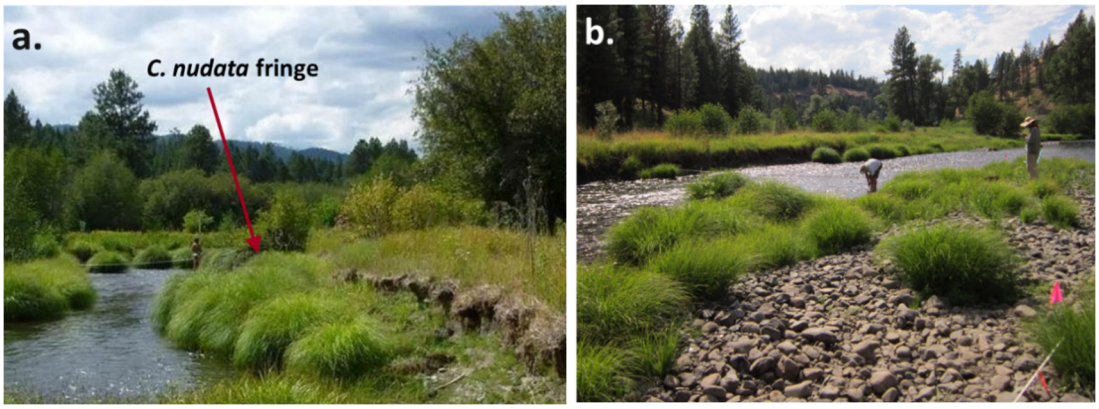

Figure 3.1. *C. nudata* established a) as a fringe in front of a cut bank and b) along the edge of a gravel bar. For reference, the bank in (a) is about 1 m in height above the water surface.

Objectives and Questions

In this study, we aimed to describe the channel morphology of river reaches with *C. nudata* and the patterns of change associated with *C. nudata*. We then propose a conceptual model of stream evolution in rivers with *C. nudata*. Observing *C. nudata* patterns of establishment, several questions emerged:

1) What morphological features distinguish channels with *C. nudata*?
2) What patterns of erosion and deposition are associated with *C. nudata* features?
3) How has planform – channel boundaries, bank tops and islands – evolved with the establishment of *C. nudata*?
4) What are the primary pathways of *C. nudata* island genesis?

We structured our investigation around two methodologies: repeated topographic surveys and historic aerial imagery analysis. We used topographic surveys of 7 sites to address the first question. We repeated these topographic surveys and used digital elevation model (DEM) differencing to address the second question, a question focused on current change, i.e. erosion and deposition. We used historic aerial imagery of these sites to address the third question, a question of historic changes in planform associated with the establishment of *C. nudata* cohorts. To address the fourth question, we tracked

the development of islands in a 10 km stretch of river through 24 years of historical aerial imagery.

Plant-River Interactions and Biogeomorphic Succession

Our investigation is motivated both by applied questions around river restoration and the theoretical context of emerging conceptions of plant-river interactions. Increasingly, vegetation is recognized as having significant effects on river morphology (Hughes 1997, Vaughan et al. 2009). Plants may affect flow, erosion and sedimentation in complex ways (Rodrigues et al. 2006, Rodrigues et al. 2007). With the intent of moving beyond simple, unidirectional conceptions of plant-river interactions, Corenblit et al. (2007) have proposed the concept of coupled biogeomorphic succession to capture the feedbacks between vegetation and physical river processes that drive the linked development of channel morphology and riparian plant communities.

The emerging field of inquiry around plant-river interactions has described a variety of changes in river pattern following the expansion of vegetation or changes in species composition. A widely described pattern is the capacity of plants to stabilize substrate, affecting the direction of channel evolution. Following reductions in flow by dams, the expansion of vegetation has led to the conversion of broad, braided channels toward narrowed single thread channels (Hicks et al. 2007). The expansion of non-native *Tamarix* spp., species with traits particularly suited for substrate stabilization, has also led to the conversion of braided channels to narrower, single thread channels (Birken and Cooper 2006). By disturbing and reducing vegetation, cattle grazing has generally led to wider stream channels (Kauffman and Krueger 1984, Trimble and Mendel 1995, Magilligan and McDowell 1997). Conversely, the removal of cattle grazing has led to shifts in plant species composition toward more hydric, deep-rooted species that can stabilize banks and potentially narrow channels (Kauffman et al. 1983b, Platts and Nelson 1989, Green and Kauffman 1995, Clary 1999, Hough-Snee et al. 2013).

Plants may facilitate the development of specific features within rivers, and alternative pathways of development may be possible depending upon variable river characteristics and modes of plant establishment. In low energy river systems in England, Gurnell et al. (2006) found that by trapping sediment, the aquatic macrophyte, *Sparganium erectum*, could induce either within-channel shelf formation or channel-edge

bench formation depending on a channel's stream power. In the high energy, braided Tagliamento River of Italy, trees including *Populus* or *Salix* spp. have been characterized as ecosystem engineers that drive island formation (Edwards et al. 1999, Gurnell and Petts 2006). Gurnell et al. (2001) describe alternative pathways of island formation with varying rates of development and persistence dependent on the initial mode of vegetation establishment.

The effects of plants within a given system may not be generalizable; different plant species and communities within a system may have differing effects. In a vegetated secondary channel of the anabranching Loire River, Rodrigues et al. (2006) demonstrated that the pattern of riparian tree species with differing forms and resistance to flow could lead to differing patterns of erosion and sedimentation. In the high energy Tech River. Corenblit et al. (2009) found differential patterns of erosion and aggradation associated with differing plant communities along an elevation gradient away from the river's edge. These differing patterns of aggradation and erosion drove both morphological and successional change within the river.

While a growing body of evidence has demonstrated the capacity of vegetation to mediate stream morphologic change, certain plant guilds (aquatic macrophytes; trees and shrubs such as *Populus*, *Salix* and *Tamarix* spp.) and river types (low energy rivers with fine sediments, high energy braided rivers) have been studied extensively while other plant types and systems have received relatively less attention. (Gurnell et al. 2010, Gurnell et al. 2012). As a tussock-forming sedge forming narrow, linear patches along the edge of the low flow channel, *C. nudata* represents a plant form and an ecological role distinct from the plant guilds that have been studied extensively. The recent expansion of *C. nudata* in the MFJDR offers the opportunity to examine a system in which the plant community and river channel may be evolving together and in which the unique characteristics of *C. nudata* may drive alternative pathways of development.

Methods

Study Area

The Middle Fork John Day is one of four branches of the John Day River, a tributary to the Columbia River and the third longest free-flowing river in the contiguous United States (Fig. 3.2). The headwaters of the MFJDR arise in the Blue Mountains of

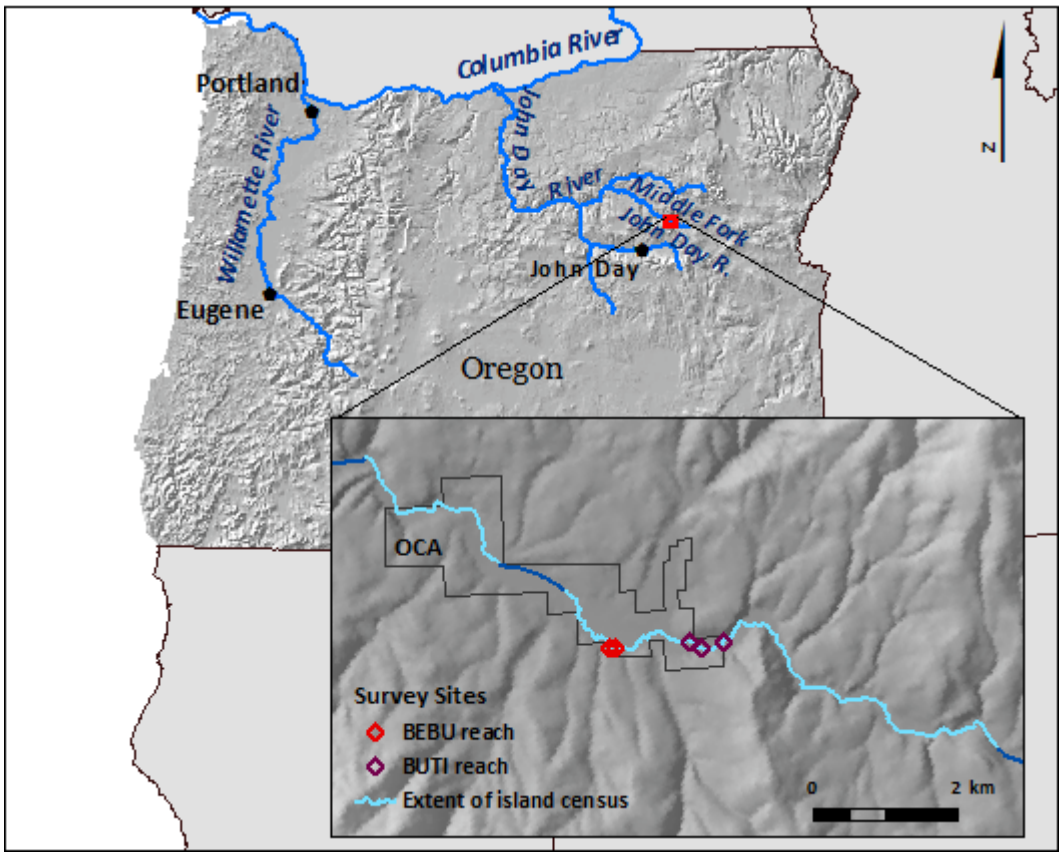

Figure 3.2. Location of Middle Fork John Day River (MFJDR). Inset focus map shows the location of the 5 full survey sites in the BEBU and BUTI reaches of the MFJDR and the extent of the 10 km river length census of C. nudata islands. Land ownership in the extent shown is U.S. Forest Service except the Oxbow Conservation Area (OCA) owned by the Confederated Tribes of the Warm Springs.

northeastern Oregon, where the climate is generally characterized by cold winters and dry, warm summers. Seventy percent of the precipitation falls between November and March, primarily as snow. Hydrology is strongly driven by snowmelt with spring peak flows with intermediate flows after fall rains, complete river ice in winter and late summer flows sustained by groundwater (OWRD 1986). Within the study area, the river is generally single-thread and sinuous and alternates between unconstrained reaches across floodplain meadows (400-500 m wide) and constrained reaches (McDowell 2001). The first part of our study, the repeated topographic surveys, was located within an unconstrained alluvial valley while the second part of our study, the extensive survey of *C. nudata* islands, included both reach types. The repeated survey sites were all located within the Oxbow Conservation Area (OCA) owned by the Confederated Tribes of Warm Springs (CTWS), whereas the extensive survey of islands crossed through both U.S.

Forest Service land and the OCA. Elevation at the OCA is around 1100 m. In the alluvial valley of the OCA, the river bed is dominated by coarse gravels and cobbles; median sediment size (D_{50}) is typically 50-80 mm (McDowell 2001). The bed in constrained canyon reaches can include a significant component of boulders. Low summer flow channel widths range from 3 to 13 m, and typical measured slopes range from .003 to .008. Pool-riffle channel reach types predominate with occasional plane-bed types. Mean annual discharge at the nearest gage (14 km downstream from surveyed sites) is 3.7 m^3/s and Q_2 flow is 21.2 m^3/s.

Repeated Topographic Surveys

We surveyed 7 sites in 2012 and 2014. We investigated changes in bed and bank morphology by constructing digital elevations models (DEMs) from these surveys and then differencing these DEMS to produce DEMs of difference (DoDs). Five of the surveyed sites were full surveys and two were partial, island-only surveys. The full surveys were placed within meander bends with a cut bank on the outside bend and gravel bar on the inside and all included either a fringe of *C. nudata* at the base of the bank (4 sites) or a cluster of islands in the outer bend near the bank (1 site). Surveys extended from beyond the bank top to beyond the exposed gravel bar usually to where woody vegetation became dominant. Sites were chosen to represent a range of *C. nudata* channel types, e.g. dense, continuous fringes vs. sparse patchy fringes. Full survey sites ranged from 24-42 m in length with an average width of 15.5 m. Partial, island-only surveys extended just beyond the water's edge on each side of the river and did not include bank tops. Partial survey average dimensions were 8 m in length and 9 m in width.

Topographic surveys were conducted with an rtk GPS (Topcon GR-3) system. Full (fringe site) surveys comprised between 1000-3900 points (2200 average). We surveyed points across a .7-1.5 m grid-based sampling scheme, capturing inflection points along grid lines and then infilling this grid with feature-based surveys of higher point density in areas of topographic complexity. For instance, we surveyed the linear features of bank tops and bank bottoms at higher density, and we conducted high density radial surveys around mature *C. nudata* tussocks.

We constructed DEMs in ESRI's ArcGIS using a two-stage process (ESRI 2016). We derived a triangular irregular network (TIN) from survey points which was then resampled into DEM with .1 m resolution. We treated linear features such as bank tops as hard breaks when creating the TIN and resampled the TIN using the natural neighbors method.

A key issue when differencing DEMs is accounting for spatially variable uncertainty such that changes in elevation are not attributed to areas where uncertainty is high nor ignored where uncertainty is minimal but change may be small (Milan et al. 2011). Uncertainty may vary as a function of slope and topographic complexity, survey point density and instrument error. To characterize uncertainty, we used a modified version of the fuzzy inference systems (FIS) of Wheaton et al. (2010) that accounts for variation in slope, point density and point quality (instrument error). We dropped point quality from our FIS, because instrument uncertainty showed little spatial variation across our sites and was generally low (average vertical RMS = .007 m). Given that we surveyed very high point densities in areas of complexity, much higher than those reported in Wheaton et al. (2010), we also modified the point density and slope membership functions and logic: we added a "very high" point density class that allowed areas of moderately high slope to be classed as "average" uncertainty rather than the "high" or "extreme" uncertainty assigned to moderate and high slopes in Wheaton et al. (2010).

Using our modified version of the Wheaton et al. (2010) FIS, we created error surfaces for the old (2012) and new (2014) DEMs for each site. For each grid cell within the DEM, propagated error can be calculated as the root mean square of the error associated with the old and new error surfaces, and a critical threshold error, U_{crit}, can be determined by:

$$U_{crit} = t(\sqrt{(\delta z_{new})^2 + (\delta z_{old})^2} \quad (1)$$

where δz_{new} and δz_{old} are the individual errors in the new and old DEMs, respectively and t is a critical student's *t*-value at a chosen confidence interval. We used a 90% confidence interval. Any changes in elevation with absolute values greater than the critical threshold error are represented as significant change in the DoD.

Aerial Imagery Analysis

In addition to the repeated topographic surveys at the 5 full sites, we also investigated historic changes in planform and vegetation at each site using historic aerial imagery. We compared sets of aerial imagery from 2013, 2006, 2001 and 1989 with resolutions of .1 m, .15 m, .48 m and .48 m, respectively (NAPP 1989, 2001, WSI 2006, Dietrich 2016). The 2013 and 2006 imagery were true color, the 2001 imagery black and white and the 1989 imagery color infrared. All imagery was taken from late July to early September during the summer low flow. To interpret planform evolution, we digitized *C. nudata* patch boundaries in the 2013 imagery and then digitized the channel boundaries and bank top lines for each year at each site, also noting when each *C. nudata* patch became established. Given the low resolution of the 1989 and 2001 imagery, we describe retreat patterns qualitatively only and do not calculate bank retreat rates.

We used this same set of imagery to assess pathways of *C. nudata* island genesis over a 10 km stretch of river that included our surveyed sites. For the 2013 imagery, we digitized all *C. nudata* islands, defined as any mature *C. nudata* individual or cluster around which water pixels were continuously visible between the tussock and bank. We then classified the status of each island in the earlier 2006, 2001 and 1989 imagery. Classes included information on the presence/absence of the *C. nudata*, the position of the *C. nudata* (midchannel vs. edge of gravel bar vs. edge of bank) and the material on which it was established (e.g. boulder, riffle, gravel bar). We deduced the origin of the islands from changes in status across time periods. The resolution of the 1989 and 2001 imagery did not allow identification of individual *C. nudata* tussocks. However, it was possible to identify midchannel bars, vegetation patches and bank lines, and thus determine whether 2013-delineated *C. nudata* locations were in midchannel or channel edge positions in 2001 and 1989.

Results

Topographic Surveys: Initial Surveys (2012)

Our initial topographic surveys (2012) revealed a compound channel morphology at three sites (BEBU_F01, BUTI_F01, BUTI_F03; Fig. 3.3a,c,e). This compound channel form has a deeper central zone (including the thalweg) inundated during low flows,

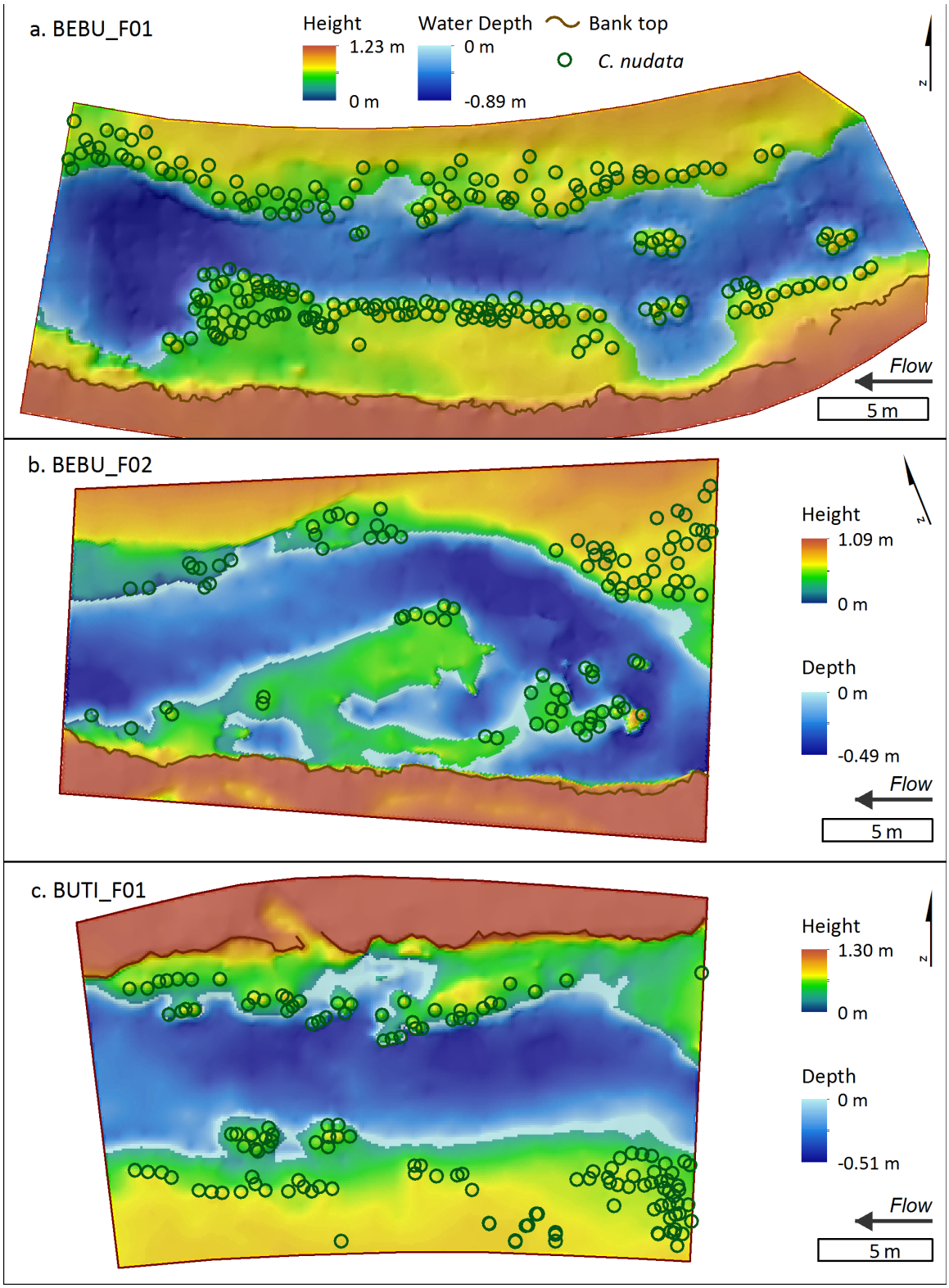

Figure 3.3. Digital elevation models (DEMs) of full survey sites, 2012. Height is relative to lowest water surface elevation. Green circles indicate *C. nudata* positions. Thick dark line represents bank top. Flow is from right to left.

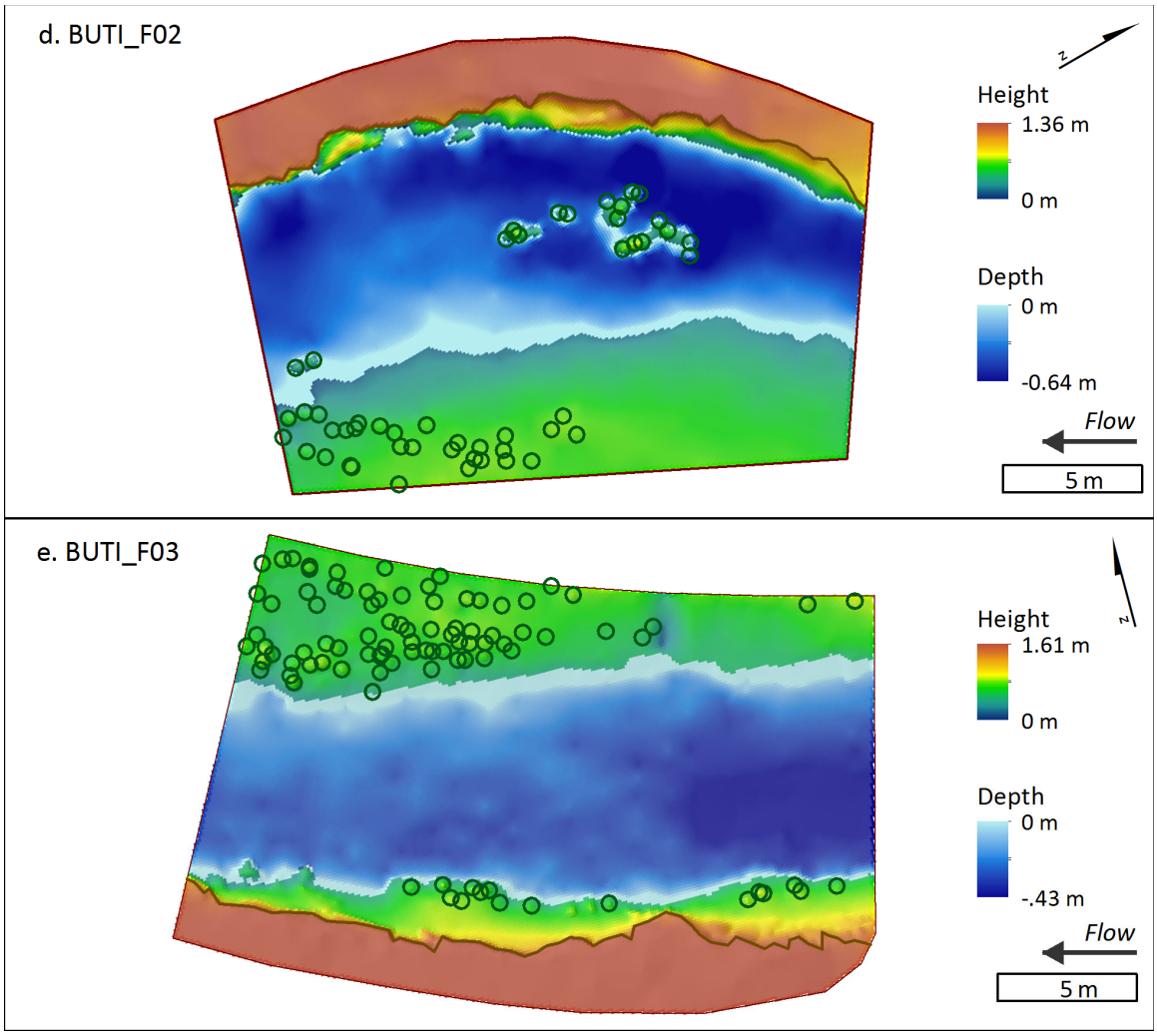

Figure 3.3 cont. Digital elevation models (DEMs) of full survey sites, 2012. Height is relative to lowest water surface elevation. Green circles indicate *C. nudata* positions. Thick dark line represents bank top. Flow is from right to left.

flanked by a shallower marginal zone that is dry during low flows but inundated during intermediate and peak flows (Fig. 3.4a,b,c,e,f,i,j). The two zones are separated by a hummocky ridge of *C. nudata*, with the marginal zone between the *C. nudata* ridge and the cut bank. One site (BUTI_F02; Fig. 3.3d; Fig. 3.4g,h) had an island morphology type in which the thalweg runs between the cut bank and the *C. nudata* islands, and the islands were inundated on both sides at all flows. Another site (BEBU_F02) had an island morphology in the upstream portion and a compound channel in the downstream portion (Fig. 3.3b; Fig. 3.4c,d). At two of the three compound channel sites (BEBU_F01, BUTI_F01), the *C. nudata* bank fringe included discontinuities that gave way to *C.*

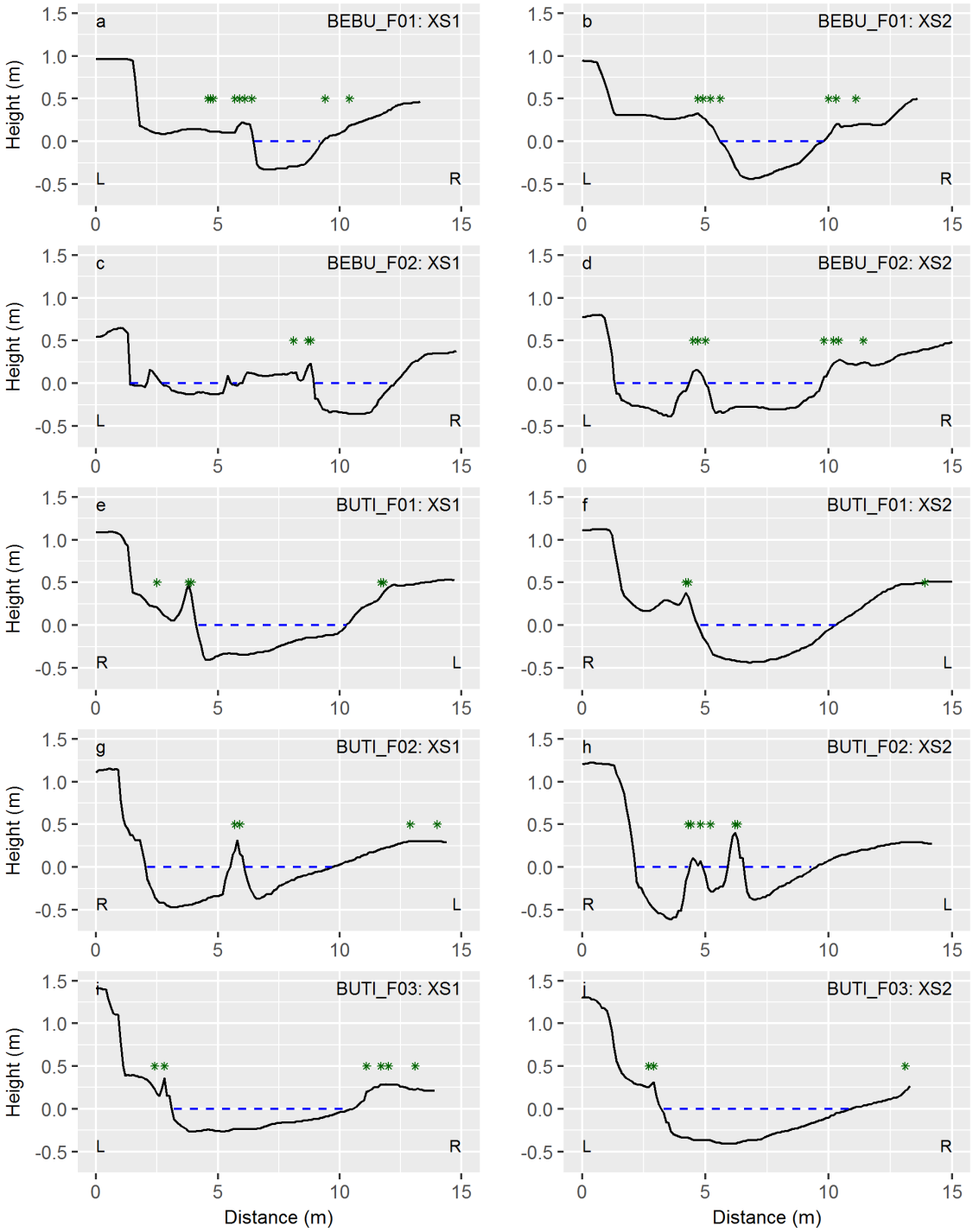

Figure 3.4. Cross sections from 2012 DEMs. Two cross sections are shown for each full survey site. Green asterisks indicate *C. nudata* locations within .5 m of cross section line.

nudata island patches, but the margin between the bank and the *C. nudata* fringe was always higher than the thalweg which remained consistently in front of the *C. nudata* fringe and small islands. A *C. nudata* fringe with elevated topography occurred on the

gravel bar edge at some sites (Fig. 3.4b,d,e,i), but on most gravel bars, *C. nudata* was dispersed and less topographically effective.

In addition to the overall channel morphology defined by *C. nudata*, microtopographic features were also evident. Deepened areas were often found along channel-facing edge of the *C. nudata* fringe and around the edges of *C. nudata* islands (Fig. 3.3, Fig. 3.5).

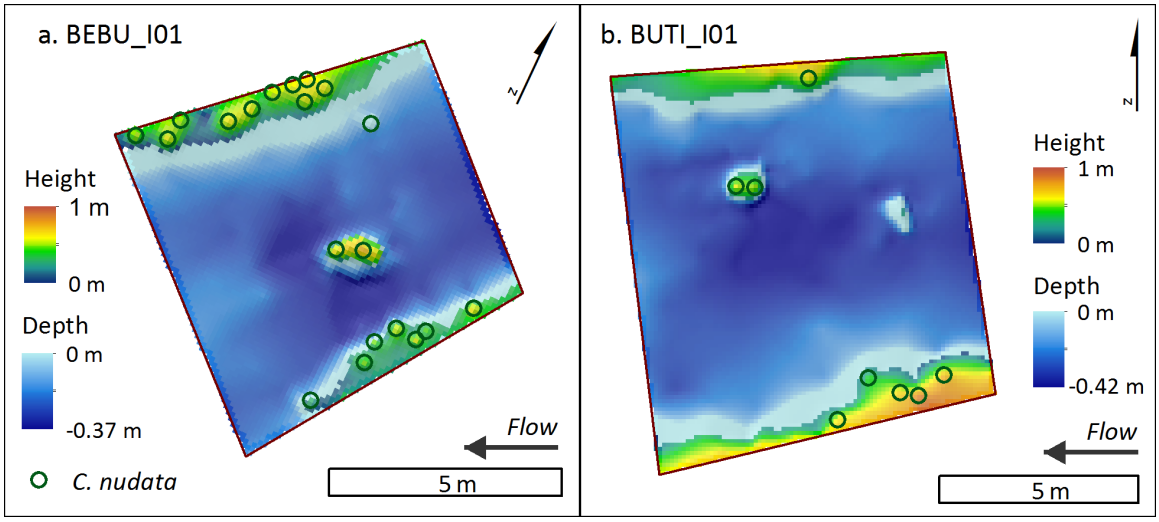

Figure 3.5. Digital elevation models (DEMs) of island-only survey sites, 2012. Height is relative to lowest water surface elevation. Green circles indicate *C. nudata* positions.

DEMS of Difference: 2012-2014

The most striking pattern of change was the significant bank erosion that occurred across all of the full survey sites. Within sites, bank erosion occurred both in areas behind *C. nudata* fringes and in areas not fronted by *C. nudata* (Fig. 3.6). Due to the large volume of bank erosion, the overall erosional volume at each site was greater than the depositional volume.

In contrast to bank erosion, streambed change across sites was varied and minimal. Changes that did occur were often in proximity to *C. nudata* features, most notably small patches of scour along the channel-facing edges of *C. nudata* fringes and along the upstream and lateral edges of islands (Fig. 3.6, 3.7). Theses scour patches did not occur consistently and were evident only at certain sites (e.g. BEBU_F01,

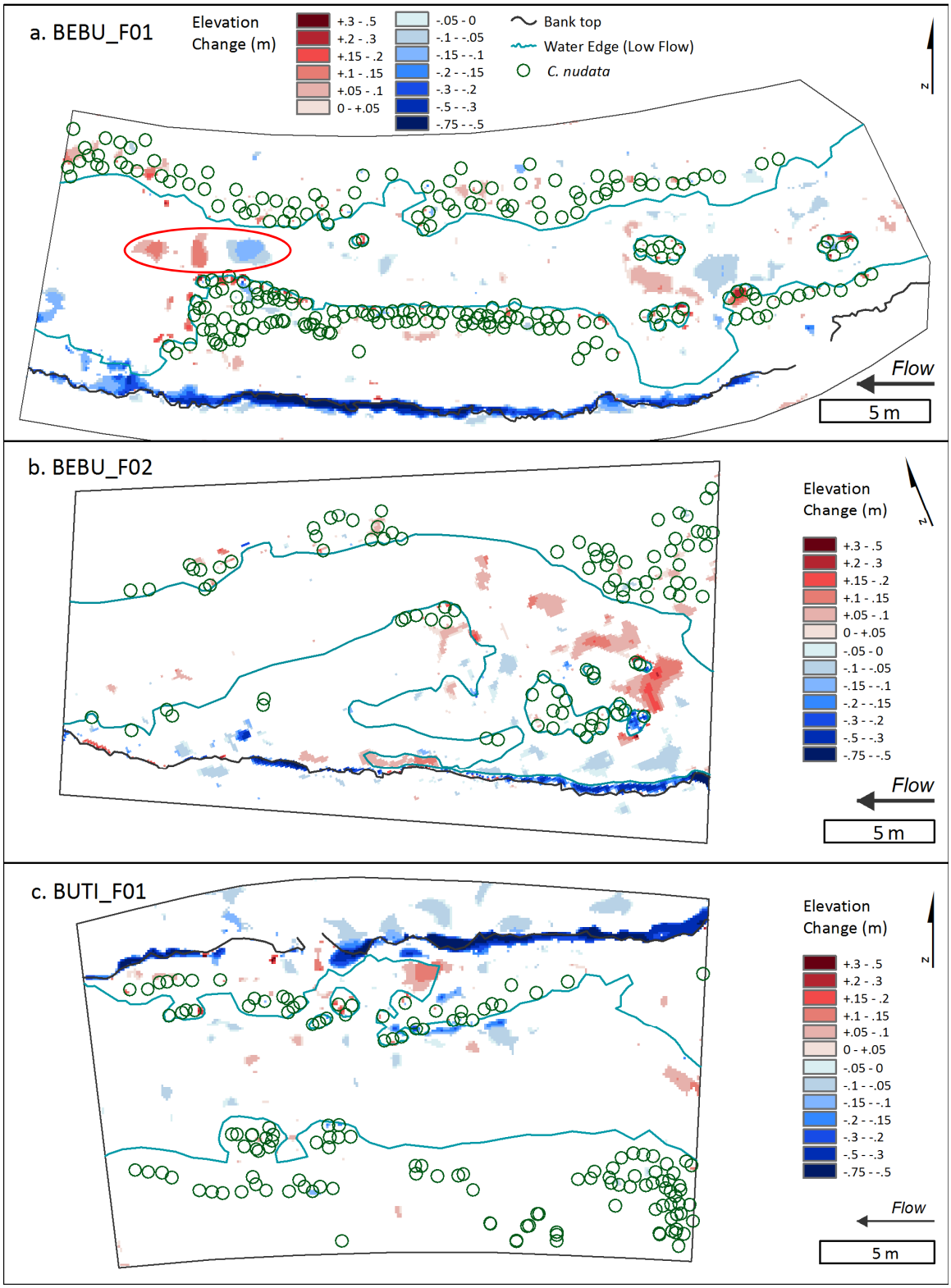

Figure 3.6. Elevation change at full survey sites, 2012-2014, after accounting for spatially variable uncertainty. In Fig 5a, red ellipse highlights paired scour and deposition from the tail of the *C. nudata*-defined chute into the pool at the downstream end of the site.

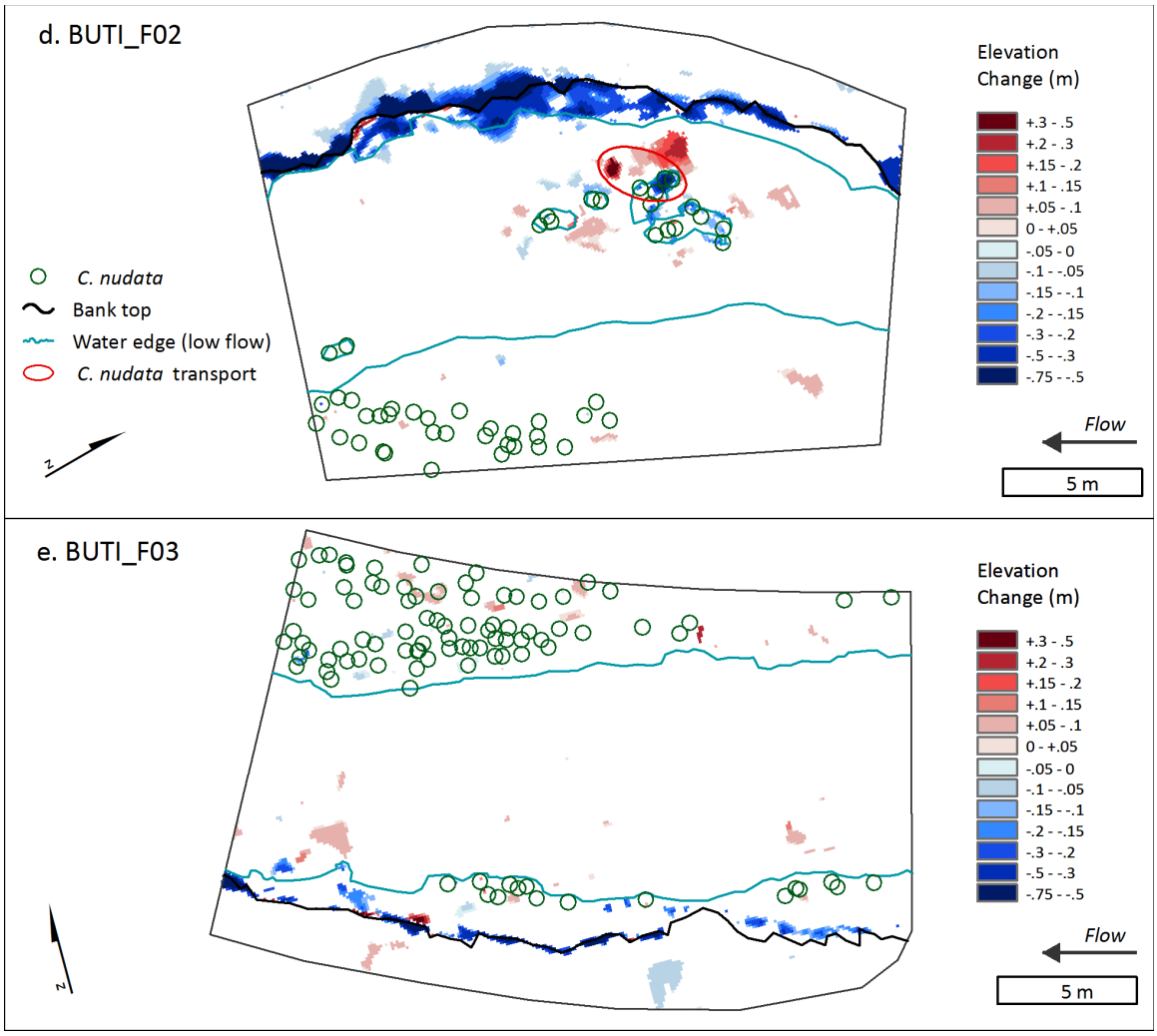

Figure 3.6 cont. Elevation change at full survey sites, 2012-2014 after accounting for spatially variable uncertainty.

BEBU_F02, BUTI_F01, BUTI_I01; Fig. 3.6a,b,c; 3.7b). In some cases, deposition occurred in spaces between islands or along the edges of islands or fringes (BEBU_F02, in particular, also BEBU_F01, BUTI_F02; Fig. 3.6a,b,d). Outside the low flow channel, elevation gains were sometimes associated with *C. nudata* tussocks within bank fringes, islands or locations on gravel bars which could be attributed to either *C. nudata* growth or deposition (e.g. BEBU_F01, BEBU_F02, BUTI_F03; Fig. 3.6a,b,e). In general, microtopographic changes that did occur, while not widespread, were often in proximity to *C. nudata* patches rather than dispersed evenly across a site.

A few in-channel changes bear specific mention. At BUTI_F02, the uprooting and transport of an entire *C. nudata* tussock left a scour hole where it was previously located

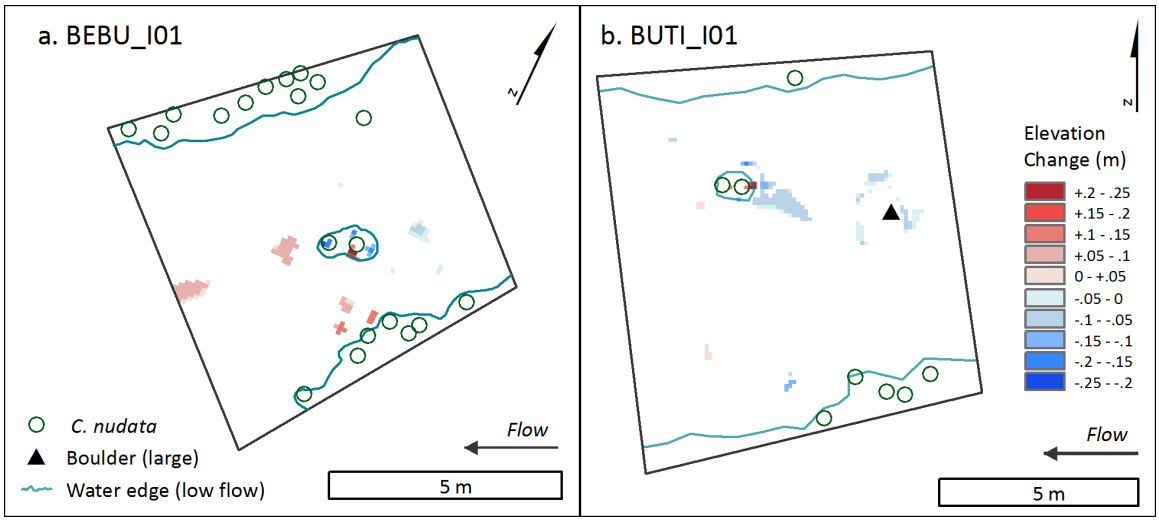

Figure 3.7. Elevation change at island-only survey sites, 2012-2014, after accounting for spatially variable uncertainty using an FIS and a 90% confidence interval.

and an elevation gain at its new location (Fig. 3.6d). At BEBU_F01, continuous *C. nudata* fringes in front of both the bank and gravel bar create a chute with a deep pool at its outlet (Fig. 3.3a). The 2012-2014 DoDs display a scour patch at the downstream tail of this chute and patches of deposition in the deep pool into which it empties (Fig. 3.6a).

Historic Change (Pre-2012) at Survey Sites

Consistent with the bank erosion revealed by our 2012-2014 DoDs, historic aerial imagery showed significant bank retreat across all sites and time intervals (1989-2001, 2001-2006, 2006-2013). The largest change occurred at the site with island type morphology, BUTI_F02. In 2006, the *C. nudata* islands in our 2012 survey were not islands, but rather were attached to the base of the bank as a *C. nudata* fringe. Therefore, between 2006-2012, the bank not only eroded behind the *C. nudata* fringe, the margin between the fringe and bank also incised, allowing the thalweg to shift to its current position between bank and *C. nudata* islands (Fig. 3.8). At another site, BUTI_F01, the one island at this site is in line with the rest of the fringe and the imagery revealed that it was also attached to the bank in 2006 (i.e. no water in between), also suggesting bed scour between the bank and the fringe in this area between 2006-2012 (Fig. 3.9). However, at BUTI_F01 the thalweg continues to run in front of the island on the opposite side from the bank. At all of the BUTI sites, all current *C. nudata* fringes and islands established post-1989 in a pattern suggesting relatively synchronous establishment

Figure 3.8. Historic imagery and island genesis from a) 2006 to b) 2013 at BUTI_F02. Black polygon outline indicates survey site boundary; red outline indicates *C. nudata* island boundary in 2013. Flow is from top to bottom of image.

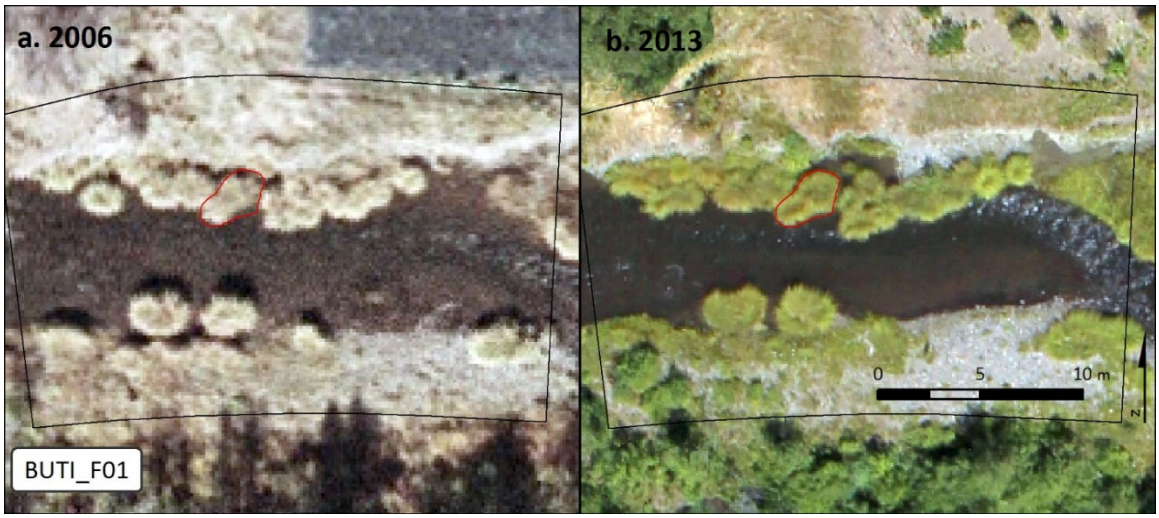

Figure 3.9. Historic imagery and island genesis from a) 2006 to b) 2013 at BUTI_F01. Black polygon outline indicates survey site boundary; red outline indicates *C. nudata* island boundary in 2013. Flow is from right to left of image.

proximate to the 2001 bank boundaries. The bank retreat and island genesis noted at BUTI_F02 between 2006-2013 may have been driven by floods in 2011 that were the largest recorded for this river.

In contrast with the BUTI sites, establishment of *C. nudata* patches in the BEBU reach started earlier and was more complex. At BEBU_F01, the large upstream midchannel island was already well-established in the 1989 imagery (Fig. 3.10). The left bank fringe and the upstream portion of the gravel bar fringe (right bank) likely established shortly before 1989 or between 1989-2001 as these patches are in line with the 1989 bank and channel boundaries and faint vegetation coloring is apparent in 1989 along the edges of both the right bank bar and the gravel margins at the base of the left bank. Bank retreat and gravel bar expansion between 1989-2001 led to the development of the pool downstream of the left bank fringe. The downstream portion of the right bank gravel bar *C. nudata* fringe and left bank pool-bounding *C. nudata* established 2001-2006 (Fig. 3.10).

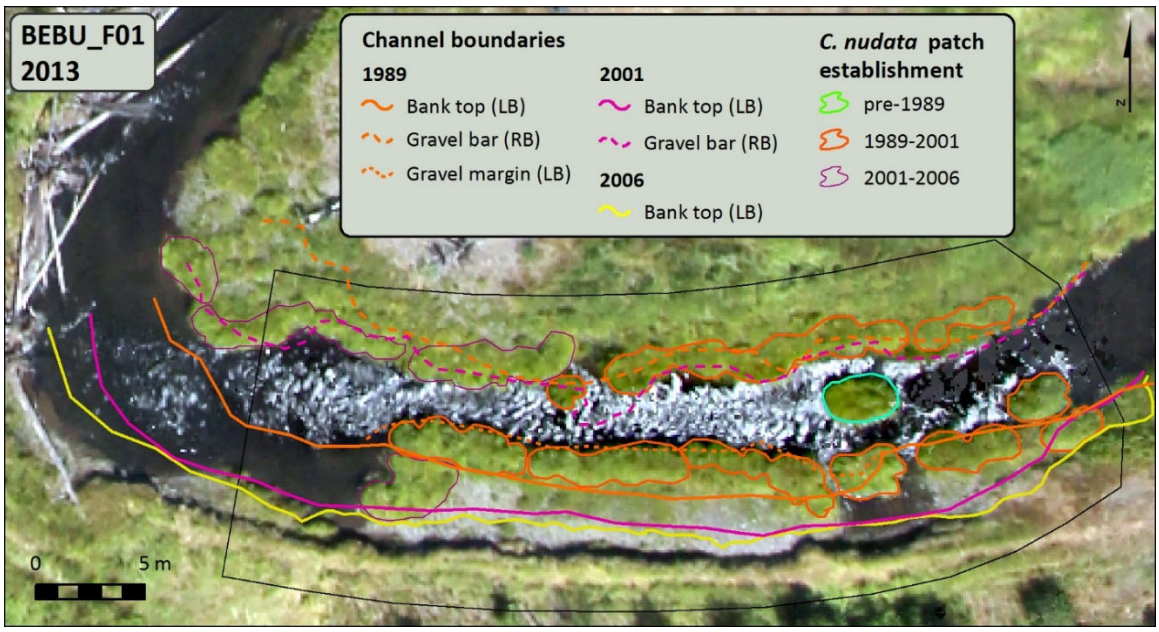

Figure 3.10. 2013 imagery for BEBU_F01 overlaid with *C. nudata* cohort boundaries, bank top lines and gravel margins from 1989, 2001 and 2006. Black polygon outline represents survey site boundary. Flow is from right to left of image. Note engineered log jam at left of image.

At BEBU_F02, the large cluster of *C. nudata* islands in the upstream portion of the site formed in three phases and revealed an additional pathway of island formation (Fig. 3.11). One row of islands evolved from *C. nudata* patches that established in front of the 1989 bank. The broad, vegetated margin in front of the bank across the middle section of

the site was also present in 1989, albeit narrower, and the apex currently occupied by a *C. nudata* patch was also apparent in 1989, but the *C. nudata* patch appeared smaller and less dense in 1989, suggesting it had just established. A second row of islands evolved from *C. nudata* patches that established as a bank fringe between 2001-2006. Finally, between 2006-2013, this island cluster grew at the upstream end with the addition of transported *C. nudata* tussocks that were uprooted from *C. nudata* bank fringes upstream of the site, possibly during the 2011 flood of record, and transported to their present location where their transport was arrested, and they re-established.

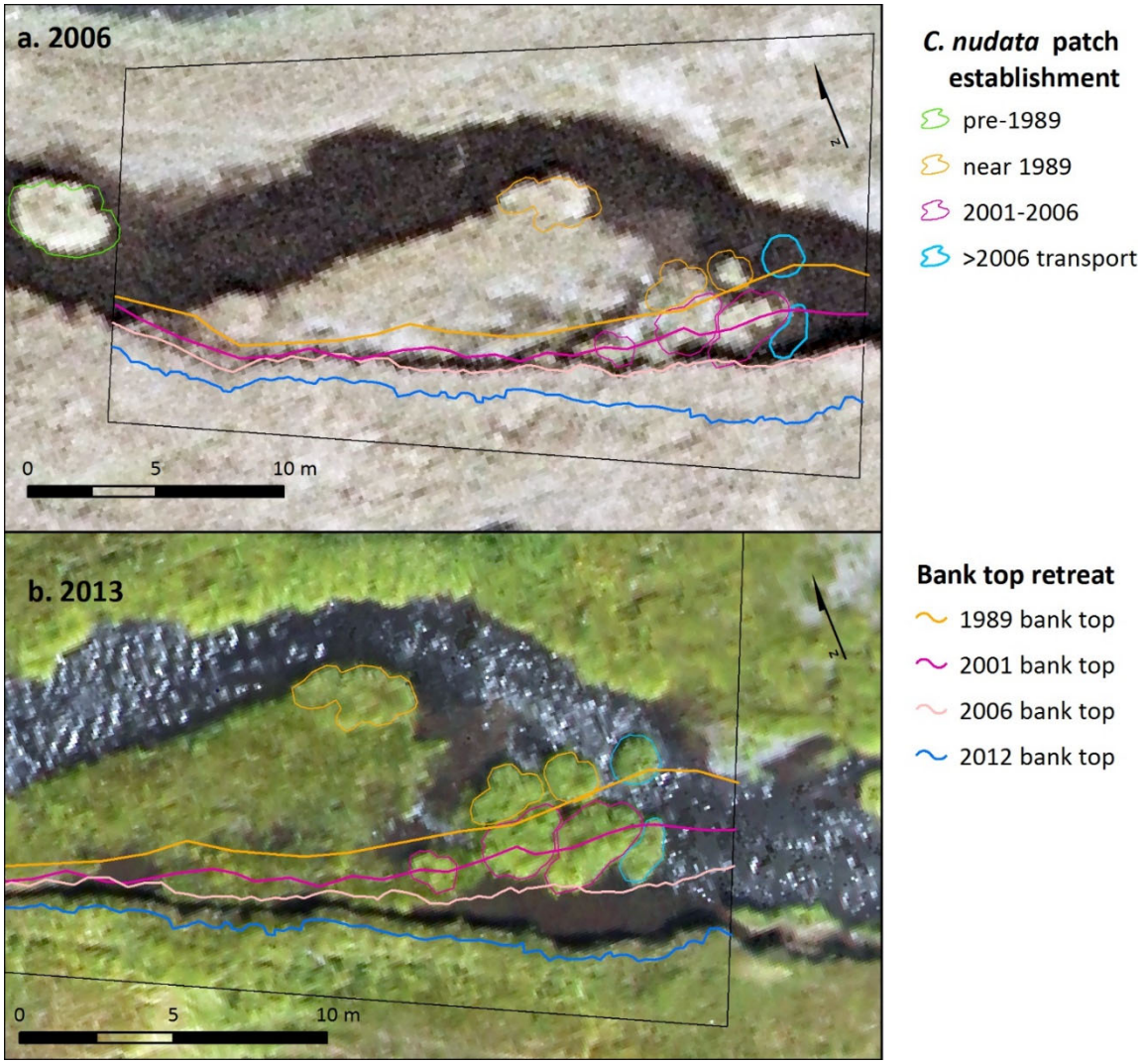

Figure 3.11. a) 2006 and b) 2013 imagery for BEBU_F02 overlaid with *C. nudata* cohort boundaries and bank top lines from 1989, 2001, 2006 and 2012. Black polygon outline represents survey site boundary. 2012 bank top line is from actual survey rather than aerial imagery interpretation. Flow is from right to left of image.

Island Genesis: Large Extent Analysis of Historic Imagery

From field observations, we had observed *C. nudata* established 1) on midchannel gravel bars, 2) on large mid-channel boulders and 3) across shallow riffles on clasts breaking the water surface (e.g. large gravels or cobbles), suggesting these establishment modes as pathways of island genesis. Our site-based historic aerial imagery suggested two additional pathways: 4) the retreat of banks leaving patches of *C. nudata* bank fringes detached from the bank and 5) the uprooting, transport and re-establishment of *C. nudata* tussocks from channel edges to midchannel positions. Through our extensive survey of islands via historic aerial imagery, we found not only further evidence for all of these pathways, but also an additional pathway: 6) detachment of gravel bar *C. nudata* fringes via erosion behind these fringes along the inner bend of the river (Fig. 3.12, 3.13).

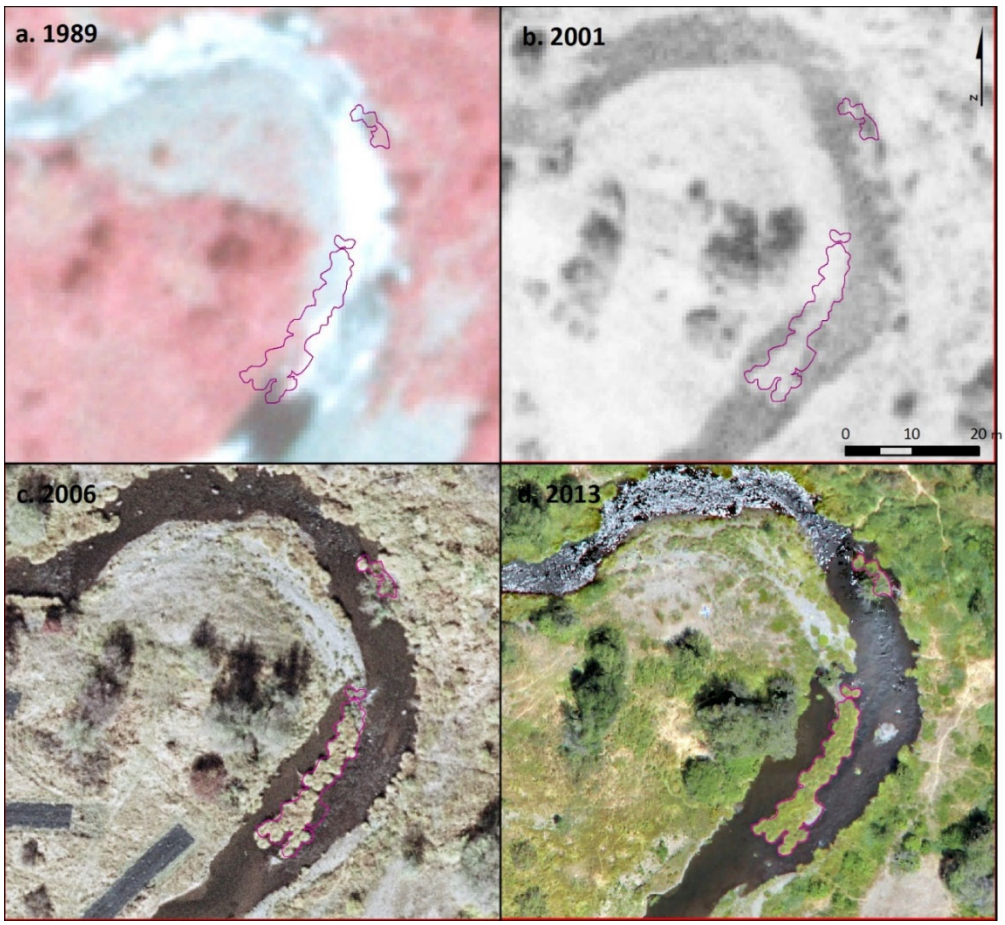

Figure 3.12. Island genesis from gravel bar fringes, example 1. Historic imagery from a) 1989 (vegetation represented as red in color infrared image), b) 2001, c) 2006 and d) 2013. Magenta polygon outline represents boundary of *C. nudata* islands in 2013. Flow is from bottom to top of images.

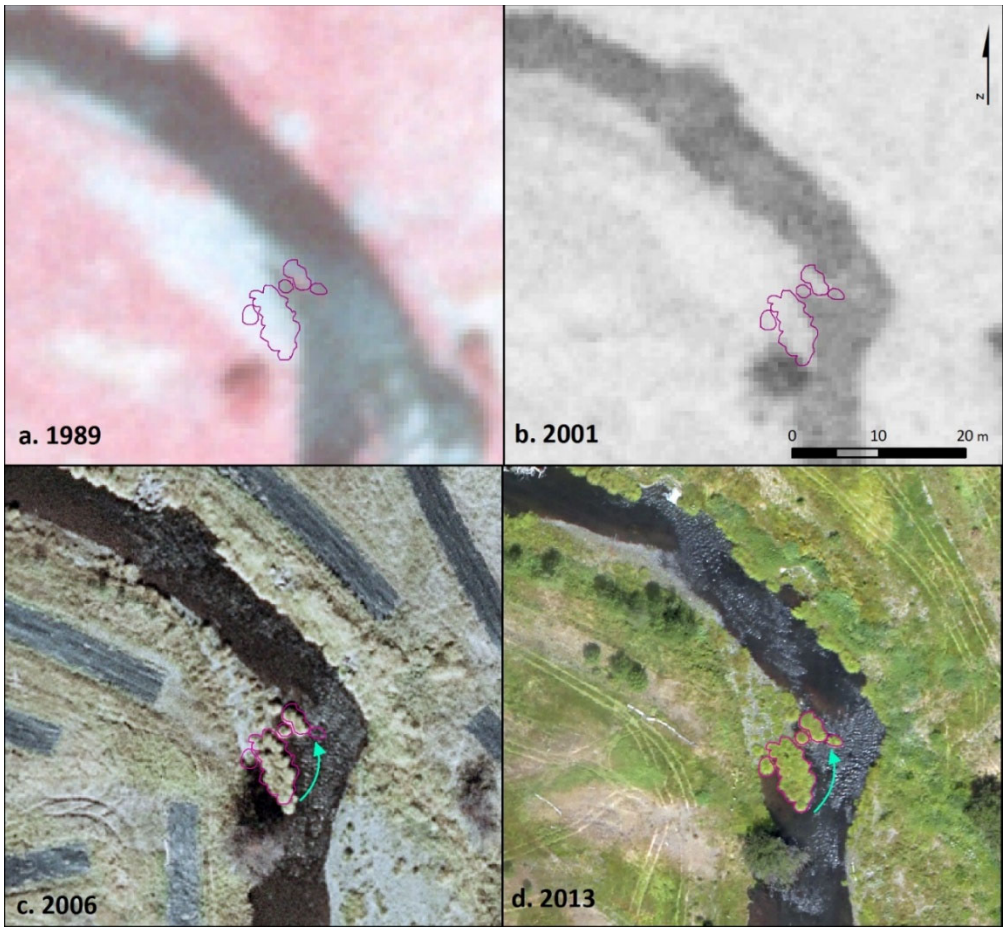

Figure 3.13. Island genesis from gravel bar fringes, example 2. Historic imagery from a) 1989 (vegetation represented as red in color infrared image), b) 2001, c) 2006 and d) 2013. Magenta polygon outline represents boundary of *C. nudata* islands in 2013. Light turquoise arrow in c) and d) represents uprooting and transport of *C.nudata* tussocks to a new position in 2013. Flow is from bottom to top of images.

Over 10 km, our census counted 440 islands of varying size consisting of 1,754 mature *C. nudata* tussocks (Table 3.1). This would suggest that on average, 4.4 islands occur every 100m. Given that these *C. nudata* islands cover 4,728 m^2 of river surface area, if we assume an average island width of 2 m, we estimate that *C. nudata* islands occupy 24 m of every 100 m of river length. Among the island census, 19% were already well-established by 1989, preventing assessment of their origin. Image quality issues (e.g. shadows in one or more photos) and other issues excluded additional island from analysis, leaving 298 islands (68%) with a clear determination of origin.

Island formation via the movement of channel boundaries away from *C. nudata* patches, either at the base of banks or along gravel bars, accounted for a plurality of

Table 3.1. Islands for which natural origin was determined relative to all islands

	N	%	Tussocks / Island (Mean)	Area (m^2) / Island (Mean)
Uncertain: pre-1989	85	*19.3*	6.0	16
Uncertain: post-1989	47	*10.7*	2.1	4.2
Artificial origin	10	*2.3*	1.7	2.5
Origin determined, natural	298	*67.7*	3.8	11
Total	**440**		**1754**	**4728**

islands (47%) and a majority by island area (51.6%) or total number of tussocks (58.2%) (Table 3.2). Bank-derived islands were greater in number (87) than gravel bar-derived islands (42) but gravel bar-derived islands were greater in area. Transported *C. nudata* blocks made up 11.1 % of all islands but were the smallest in size (1.8 m^2 average), making this class the least important by overall area (1.9%). Boulder-established *C. nudata* made up the 2nd largest class of islands by number (61 islands, 20.5%) but were also relatively small (2.4 m^2 average), such that they accounted for only 4.6% of island area. In contrast, islands originating on midchannel gravel bars were not numerous (20 islands, 6.7%), but being the largest in size, this class covered largest overall area (36.5%).

Discussion

C. nudata and Patterns of Change: Bank Retreat

Throughout this investigation, our results up-ended initial expectations. The first surprise was the continuing, significant retreat of banks behind *C. nudata* bank fringe given that vegetation has often been found to stabilize banks. Many studies have found correlations between vegetated banks and lower erosion rates during flood events (Beeson and Doyle 1995, Laubel et al. 2003, Bąk et al. 2013) and between vegetated banks and narrower channel widths (Huang and Nanson 1998, Millar 2000, Anderson et al. 2004). The expansion of vegetation following flow reductions by dams has led to channel narrowing (Hicks et al. 2007), and the introduction and expansion of non-native species, *Tamarix* spp., into an otherwise sparsely vegetated arid system, the U.S.

Table 3.2. Island genesis analysis: origin classes.

			Tussocks / Island (n)		Area / Island (m^2)	
Origin	N	%	Mean (Min-Max)	%	Mean (Min-Max)	%
Mid-channel establishment						
1. Midchannel bar	20	*6.7*	12.8 (1- 38)	*22.6*	58 (.5- 268)	*36.5*
2. Riffle	44	*14.8*	1.8 (1- 9)	*7.1*	4.0 (.3- 21)	*5.5*
3. Boulder	61	*20.5*	1.5 (1- 6)	*7.9*	2.4 (.1- 9.2)	*4.6*
Subtotal		***41.9***		***37.5***		***46.6***
Channel boundary movement						
4. Bank	87	*29.2*	3.3 (1- 22)	*25.5*	6.6 (.1- 66)	*18.1*
5. Gravel Bar	42	*14.1*	7.4 (1- 42)	*27.5*	22 (.3- 221)	*29.2*
6. Bank | Gravel Bar	11	*3.7*	5.4 (1- 15)	*5.2*	13 (2.1- 45)	*4.3*
Subtotal		***47.0***		***58.2***		***51.6***
C. nudata movement						
7. Transported	33	***11.1***	1.5 (1- 4)	***4.2***	1.8 (.3- 4.5)	***1.9***
Total	298		1132		3168	

Southwest, has led to dramatic narrowing of channel widths (Birken and Cooper 2006). Across the western U.S., studies have often found that channels where cattle grazing has been excluded or reduced are narrower and have lower width to depth ratios than intensively grazed channels (Kauffman and Krueger 1984, Magilligan and McDowell 1997, Clary 1999), differences often associated with shifts in plant species composition from ruderal grasses toward hydrophytic, densely rooted sedges (Kauffman et al. 1983b, Platts and Nelson 1989, Green and Kauffman 1995, Hough-Snee et al. 2013). Therefore, we did not expect such significant bank erosion behind *C. nudata* fringes. We should be clear, however, that our data does not establish whether bank erosion is continuing at rates similar to those prior to *C. nudata* expansion.

Nevertheless, the finding of continued bank erosion highlights the point that vegetation effects cannot be generalized. The particular form and ecology of a plant are critical to its effects on channel morphology. In the case of *C. nudata*, its reproductive strategy results in establishment in a narrow band along the edge of colonizable substrate on the stream bed. Once established, it does not expand significantly further up a bank or back on a bar. In some cases, we have observed successive vegetation colonizing behind *C. nudata*, especially on gravel bars, but the bank face and the margin between *C. nudata* and the bank typically remain sparsely vegetated and unprotected. Whether a bank continues to erode or is stabilized following *C. nudata* colonization may depend on the rate of erosion relative to the rate of colonization by additional species behind the *C. nudata* fringe. Furthermore, given the tussock form of *C. nudata,* bank fringes also typically include discontinuities and gaps that may allow further erosion.

The nature of flow patterns and associated erosion patterns around *C. nudata* warrant further investigation. For instance, a key question remains whether current erosion rates observed for banks behind *C. nudata* are similar to banks without *C. nudata* or whether stabilization of the bank toe by *C. nudata* is associated with slower rates. Understanding flow velocity patterns around *C. nudata* fringes would also permit better interpretation of bank and bed erosion patterns.

C. nudata and Patterns of Change: Bed Erosion and Deposition

In contrast to the large volume of bank erosion occurring at our sites, patches of erosion and deposition (2012-2014) across the channel bed were relatively minimal. This result was also unexpected given that our initial topographic surveys revealed much micro-topographic variation around *C. nudata* features including deepened in-channel areas in front of the steep wall of roots presented by the *C. nudata* fringe and along island edges. Continuing scour in such areas would offer further evidence of the association between *C. nudata* and this process. However, continuing scour was found in only small patches and the patterns of deposition and erosion around were not consistent. Nevertheless, the small patches of scour and deposition that were evident were typically in proximity to patches of *C. nudata* pointing to *C. nudata* as the critical organizer of morphological change in these channels.

There are several possible explanations for the minimal streambed change. During the 2012-2014 survey period, the spring 2013 peak flows were below average, and the 2014 peak flow was a 1.6-year return interval event. It may be that significant stream bed change occurs primarily during exceptional peak flows such as the 2011 flood or can only be detected over longer time periods. Our spatially variable error estimates may also be masking small changes in erosion or deposition around *C. nudata,* given that these areas had much higher error estimates and limits of detection, given the steepness around *C. nudata* features. Finally, it is also possible that the most significant changes in streambed topography occur earlier in the *C. nudata* establishment and growth life cycle. That is, our sites (as well as most of the MFJDR reaches in this area) are currently occupied by mature *C. nudata* tussocks. It is possible that most morphological adjustments occurred shortly after the *C. nudata* establishes such that a new equilibrium has now been established and many of the topographic features we observe across the streambed are products of that initial adjustment.

C. nudata Island Genesis

The next unexpected result was the revelation that *C. nudata* islands could originate from bank fringes detached from their banks via continued bank erosion and bed scour between the fringe and bank. Based on field observations in which we had observed *C. nudata* establishing in riffles, on boulders and around midchannel bars, we had assumed that *C. nudata* islands originated in mid-channel positions. The island origin census revealed another unexpected pathway, detachment of gravel bar fringes. Furthermore, the island origin census revealed that island origin via detachment from moving channel boundaries is the predominant mode for island genesis in the MFJDR.

The diversity of island genesis pathways creates a diversity of island types. Establishment of *C. nudata* on large boulders or on clasts in riffles results in small islands typically consisting of 1-2 *C. nudata* tussocks. Islands derived from the uprooting and transport of *C. nudata* are also typically small (1-2 tussocks), but in many cases, these may be deposited at the front of an existing island cluster, augmenting that cluster's size (e.g. BEBU_F02). Islands originating via detachment from channel boundaries are larger and often linear in shape. However, successive cycles of linear cohort establishment and detachment may lead to larger, wider clusters of islands (e.g. BEBU_F02). Islands

derived from midchannel gravel bars were the largest among all island types and distinct in form, less linear and broader in shape than fringe-derived islands. Analysis of historic imagery suggested that midchannel gravel bars exhibit significant growth over time. Presumably, establishment of *C. nudata* around the edges facilitates further deposition downstream and midchannel islands often exhibited additional colonization and stabilization by other plant species. *C. nudata* islands originating on midchannel bars are depositional features whereas *C. nudata* islands originating from bank fringes are essentially erosional features. While we have observed other plant species (including shrubs and trees) establishing and growing within bank-derived *C. nudata* island tussocks, overall island area expands slowly and almost exclusively through the growth of individual *C. nudata* tussocks or the addition of transported tussocks.

The evolution of *C. nudata* islands from bank detachment offers an intriguing contrast with several other studies of island evolution (Edwards et al. 1999, Gurnell and Petts 2006, Zanoni et al. 2008). In the high energy, braided Tagliamento River in Italy, Gurnell et al. (2001) describe different modes of island formation instigated by shrub and tree species (*Salix* and *Populus* spp.) including 1) stabilization of existing bars via dispersed colonization by tree seedlings; 2) enhanced deposition and subsequent colonization behind deposited dead trees; and 3) the transport, deposition and resprouting of live trees followed by enhanced deposition and colonization. In each of these cases, island formation takes place either on an existing depositional feature or via the creation of a depositional feature behind deposited vegetation (dead or alive). In the MFJDR system, while *C. nudata* may facilitate island formation via the colonization of depositional features, island formation via erosional processes around substrate stabilized by *C. nudata* appears to be the dominant mode.

Conceptual Model of River System with C. nudata

Integrating the morphological patterns described by the site surveys and temporal patterns of current and historic change, we can build a conceptual model of channel evolution with *C. nudata* in the MFJDR system. *C. nudata* is remarkably effective at stabilizing substrate and building elevated topography along the edge of the low flow channel where it initially establishes. However, it is less effective in arresting the erosion of banks such that the boundaries of the bankfull channel may continue to migrate even

though the low flow channel boundaries may be stabilized. The differing rates at which banks retreat and the differing directions of vertical change (aggradation vs erosion) in the margin between the bank and the fronting *C. nudata* fringe set up the potential for multiple alternative pathways of channel evolution (Fig. 3.14).

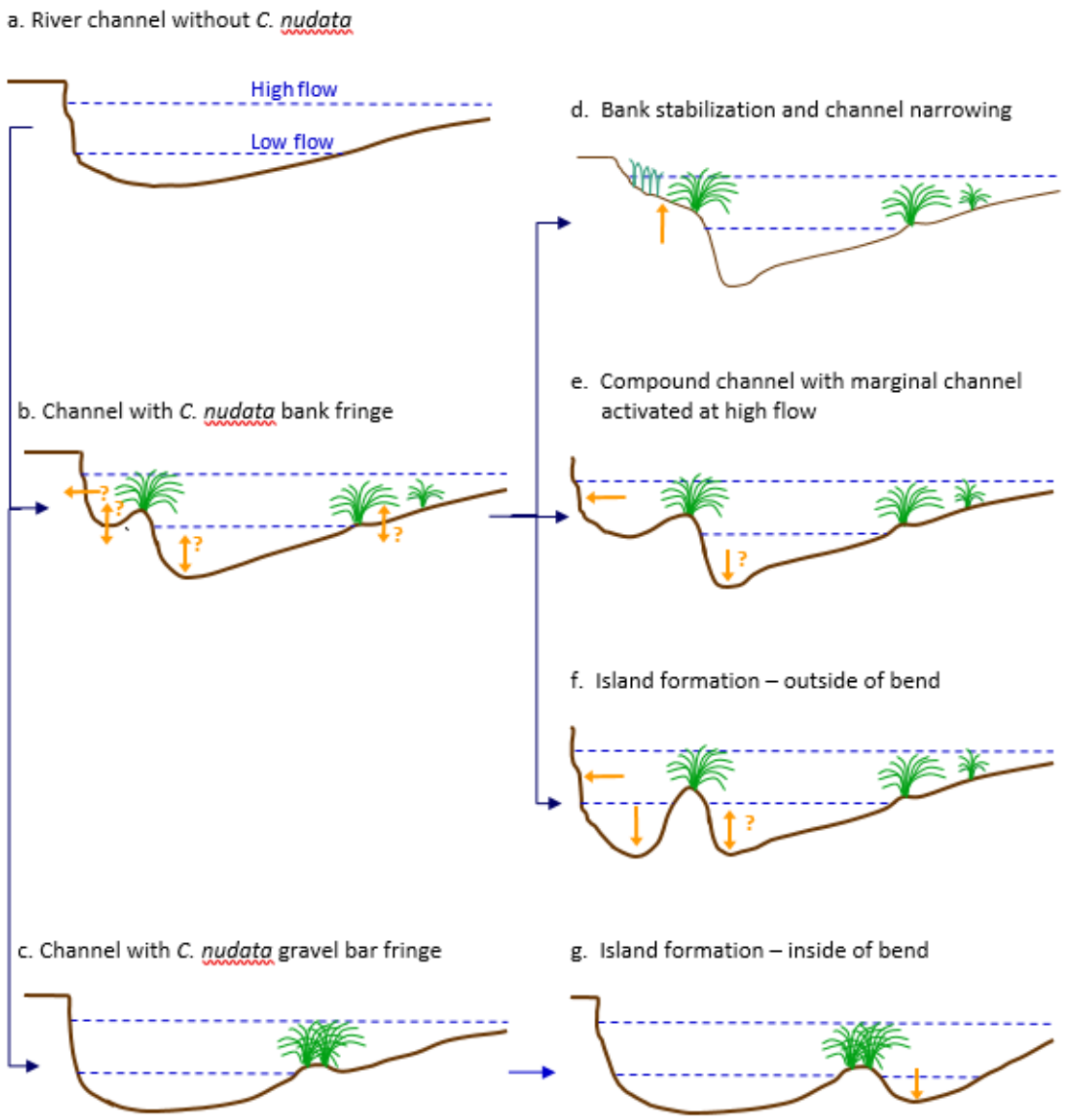

Figure 3.14. Conceptual model: alternative pathways of channel evolution in river with *C. nudata*.

After a *C. nudata* fringe establishes, if bank retreat continues without consistent net aggradation or erosion in the bank-fringe margin, a compound channel morphology develops (Fig. 3.14b,e). With the low flow channel boundaries locked in by *C. nudata*, a

compound channel would likely have narrower channel widths during low flows than channel segments without *C. nudata*. Our 2012 topographic surveys also suggested deepened areas at the face of the *C. nudata* bank fringe, but the DoDs showed inconsistent evidence for continued scour (2012-2014) at the front of the *C. nudata* fringe face.

If bank retreat continues rapidly and is coupled with erosion in the bank-fringe margin, a channel with island morphology develops (Fig. 3.14f). The thalweg may also shift into the space between the bank and fringe-derived island as was the case for BUTI_F02.

If bank retreat behind a bank fringe is sufficiently slow and the bank-fringe margin does not experience high shear stress, vegetation may colonize the bank-fringe margin, facilitating aggradation, a stabilized bank and potentially a narrower channel (Fig. 3.14d). None of the survey sites we chose provided evidence of the bank stabilization pathway, but we have observed stretches in the MFJDR in which gentle, vegetated slopes behind a *C. nudata* fringe suggest this pathway. We believe it to be the least common pathway.

The pathway along which the channel evolves may depend upon a variety of factors including the bank material, river curvature and pattern of *C. nudata* establishment. A key difference between the island-dominated BUTI_F02 site and the compound channel sites was the bank material. In general, MFJDR banks consist of cohesive upper banks with lower lens of coarse materials embedded in a cohesive matrix. In contrast with our other survey sites, the BUTI_F02 island site included a much higher percentage of coarse, non-cohesive materials that extended farther upward through much of the bank, presumably making it more erodible. Our sites were also distinguished by differences in *C. nudata* establishment pattern. The two sites with the most well-developed compound channel morphology (BEBU_F01, BUTI_F01) also had the most continuous, well-developed bank fringes, whereas BUTI_F02 had a shorter, less continuous fringe (in 2006, pre-island) which may have allowed greater erosion behind it. River curvature is also likely a critical factor in driving bank erosion rates and development pathways, but our sites were all characterized by moderate curvature and did not display significant differences among sites with one exception. In BEBU_F02,

curvature within the surveyed area was moderate, but the site is located immediately downstream of a strong bend which is migrating and resulting in more rapid bank retreat at the upstream portion of this site where island morphology developed (Fig. 3.11). Heterogeneous patterns of bank material, river curvature and *C. nudata* establishment may interact to produce an array of alternative pathways of channel evolution.

The pathways described above all depend upon the establishment of a *C. nudata* fringe in front of a bank. Another pathway is made possible by the establishment of a gravel bar fringe leading to the evolution of islands on the inside bend of the river (Fig. 3.14g). These islands were typically derived from fringes at the upstream end of a gravel bars, and the key factors in driving this pathway appeared to be river characteristics, particularly curvature, immediately upstream of the gravel bar. That is, upstream bank erosion on the same side as the gravel bar and fringe results in the migration of the channel boundary immediately upstream of the gravel bar such that the straightest flow path is directed behind the *C. nudata* fringe and erosion across the gravel bar behind the fringe leads to its detachment.

Implications for Restoration

Throughout the Pacific Northwest, enormous investments are being made in river restoration projects aimed at improving habitat for salmon populations listed as threatened or endangered under the Endangered Species Act (ESA). The Middle Fork John Day River, in particular, has been targeted as a high priority for restoration and monitoring, designated as an Intensively Monitored Watershed (IMW) (PNAMP 2021). Restoration has included such capital-intensive projects as placement of engineered log jams, often with deepened pools. Preceding these active restoration projects, however, passive restoration was initiated through reforms in cattle grazing timing and intensity or the withdrawal of cattle grazing from river banks. The results of our investigation suggest that the expansion of *C. nudata* throughout the system is resulting in systemic changes to channel morphology that are enhancing channel complexity, a key goal of restoration efforts (Beechie et al. 2008, Roni et al. 2008). In contrast to active restoration, the changes associated with *C. nudata* are less localized, but rather occur throughout the system. Furthermore, these changes in pattern have resulted from the restoration of natural processes, processes that are self-perpetuating, rather than simply the construction

of desired patterns (Kauffman et al. 1997, Palmer et al. 2005, Beechie et al. 2010). Finally, this strategy is low risk and has required relatively minimal investment apart from the reduction or withdrawal of the disturbing factor and the management required to maintain that reduction (e.g. fencing maintenance and cattle rotation).

With the expansion of *C. nudata* throughout the system, different channel segments have the potential to evolve along different channel evolution pathways. The array of alternative pathways (both with and without *C. nudata*) results in a complex mosaic of channel forms at the scale of the riverscape. The *C. nudata*-associated forms such as the compound channel and island types also exhibit complexity within the reach scale. The complex array of irregularly shaped islands and fringes with discontinuities and erosion around them may be inducing a diversity of habitat types some of which are available at low flows and others at higher flows. For instance, channel margins along the *C. nudata* fringes and islands provide deeper micro-habitats that are also shaded by overhanging *C. nudata* leaves during summer. McDowell and Goslin (2015) estimated that overhanging *C. nudata* leaves create fish cover (shade, predator protection, etc.) over 5% of river surface area in the OCA, a figure similar to the amount of fish cover produced by engineered log jams in this area. As *C. nudata* expands and shapes features throughout the river system, it induces complexity at both the large scale of the riverscape via a mosaic of different channel forms and at the scale of individual reaches via an array of micro-topographic features and associated habitats.

IV. COMPLEX BANK EROSION PROCESSES IN THE MIDDLE FORK JOHN DAY RIVER AND THE NATIVE RIPARIAN SEDGE, CAREX NUDATA

This work will be submitted for publication with Patricia McDowell as a co-author, acknowledging her contribution to conceptual and methodological development.

Introduction

Following the removal of cattle grazing from river banks in the 1990s, *Carex nudata*, a native sedge, expanded dramatically within the Middle Fork John Day River (MFJDR) in eastern Oregon. In reaches where it is now the dominant stream-side plant species, it typically forms fringes at the base of cut banks. In an earlier study investigating *C. nudata*'s effects on channel evolution, we discovered that, contrary to expectations, banks behind *C. nudata* fringes were retreating at significant rates. This raised a critical question: are the banks behind *C. nudata* fringes eroding and retreating at rates similar to or different than banks without *C. nudata*? Given that little was known about bank retreat processes in the MFJDR, we also recognized that any interpretation of comparative rates would be impossible without a comprehensive investigation of bank retreat processes in the MFJDR, processes that likely vary in importance by season. Therefore, we addressed three questions:

1) Do banks with *C. nudata* fringes erode and retreat at rates slower, faster or no different than banks without *C. nudata*?
2) What processes drive bank erosion and retreat in the MFJDR and how does the importance of these processes vary by season?
3) Apart from the *C. nudata* fringe factor, what other bank characteristics drive erosion rates?

The answers to these questions have implications for both our understanding of channel evolution in the MFJDR as well as our understanding of bank erosion processes and vegetation-river interactions more broadly.

Bank Retreat Processes

The retreat of river banks is a critical process in the development of channel morphology and planform. Bank retreat results from a complex interaction of processes

that often operate in nonlinear fashion and interact across different temporal and spatial scales. While a general conceptual framework of key processes has been established (Thorne 1982, Lawler 1992, Lawler et al. 1997), modeling these processes continues to be problematic, as so many key processes defy simple characterization (Rinaldi and Darby 2007).

Bank retreat has been conceptualized as driven by three top-level processes: weathering and weakening, fluvial erosion, and mass failure (Lawler et al. 1997). Weathering and weakening includes a variety of processes associated with freezing and thawing, wetting or desiccation. These processes have often been described as "subaerial preparation" because they reduce the cohesion of bank material, thus increasing the probability of fluvial erosion or mass failure. However, many studies have found evidence that such subaerial processes can also be dominant erosion processes, not just "preparation," particularly in the upper reaches of river basins where colder temperatures result in greater freeze/thaw action (Couper and Maddock 2001, Costard et al. 2003).

The relative importance of fluvial erosion as a driver of bank retreat increases with increasing stream power downstream, and mass failure increases in importance as floodplains become sufficiently well-developed and bank heights sufficiently tall (Lawler 1992). Fluvial erosion is a progressive, incremental process once thresholds of entrainment have been reached at high flows, whereas mass failures are discontinuous events triggered when driving forces of gravity exceed resisting forces such as bank cohesion. Banks become more susceptible to failure when high soil water content and positive pore pressure reduce cohesion. Fluvial erosion is coupled with mass failure via "basal endpoint control." That is, fluvial erosion at the bank toe makes banks susceptible to failure by steepening or undercutting the bank (Carson and Kirkby 1972, Thorne 1982, Richards and Lorriman 1987). In gravel bed rivers like the MFJDR, cantilever failure - in which upper sections of the bank fall after being undercut - are common given that such failures typically occur in composite banks in which cohesive layers overlay more erodible coarse materials (Rinaldi and Darby 2007).

Fluvial erosion is a product of multiple factors. For coarse bank material, fluvial erosion can be expected to follow principles similar to the entrainment of bed material: boundary shear stress simply needs to exceed the critical shear stress associated with

particle size. For cohesive bank materials, however, the relationship is more complex: chemical bonding associated with clays, aggregate structure, interstitial fluids and pore pressure all influence entrainment potential (Rinaldi and Darby 2007). In addition to factors associated with bank substrate, the patterns of fluid stress that drive entrainment are influenced by multi-scale factors including bank curvature, position within a bend and topographic irregularities both across the bank face and in the stream bed proximate to the bank (Konsoer et al. 2013, Konsoer et al. 2016). In addition, vegetation can influence the distribution of primary and secondary currents that occur along the outer bank, adding another dimension of complexity (Blanckaert et al. 2012, Konsoer et al. 2016).

The Middle Fork John Day River: Bank Retreat Processes and Carex nudata

In the Middle Fork John Day River, all of the top-level processes described here – subaerial weakening & erosion, fluvial entrainment, and mass failures – may be active. The study sites are located at relatively high elevation (1100 m) such that temperatures go below freezing for extended periods during winter and fluctuate around freezing in late fall and early spring. Summers are dry and hot such that desiccation and cracking is a likely subaerial weakening process. Stream power is sufficient for fluvial entrainment and bank heights are sufficiently tall for mass failures. Banks include a variety of substrate profiles ranging from entirely cohesive to entirely non-cohesive, but most are composite banks characterized by cohesive upper strata and a lower layer with coarse clasts, thus making cantilever failures likely (Fig. 4.1). Another process that may be important is the formation and break-up of river ice, an erosion process which is relatively under-studied (Uunila and Church 2015a). The MFJDR presents an ideal setting for exploring all of these processes as well as the interplay of key factors such as substrate type and curvature on fluvial erosion. In Table 4.1, we outline the processes we expected to be important by season.

C. nudata expanded dramatically within the MFJDR following the removal of cattle grazing from river banks. The MFJDR has been the focus of large investments in river restoration given its high potential for recovering threatened salmon populations. Historically degraded by intensive cattle grazing, floodplain tree removal and gold dredge mining in some reaches, river restoration efforts ramped up in the 1990s when The Nature Conservancy and the Confederated Tribes of the Warm Springs purchased

Figure 4.1. Cantilever failure block and composite bank. Note lower strata at left of photo with gravels and cobbles embedded in an eroding cohesive (sandy loam) matrix beneath upper cohesive strata.

Table 4.1. Expected bank erosion and weakening processes by season in the MFJDR.

Processes	**Summer**	**Winter**	**Spring**
Subaerial	desiccation/ cracking/ crumbling	freeze/thaw processes	freeze/thaw, early spring desiccation etc., exposed banks (S), late spring
Fluvial	none	possible modest peak flows, during short winter thaw periods river ice break-up processes, end of winter or short winter thaw periods	highest & longest peak flows w seasonal snow melt
Mass Failure	rare (after early fall rains)	common (typically cantilever)	common (typically cantilever)

Note: these seasons correspond to the seasonal periods bracketed by our erosion pin measurements: Summer: July-mid-October; Winter: mid-Oct-February; Spring: March-June. We do not include in this table processes that we did not expect and were discovered during our investigation.

ranches, establishing conservation areas where cattle were excluded from river banks, and the U.S. Forest Service initiated grazing reforms in surrounding lands. In the midst of resource-intensive active projects, the unaided explosion of *C. nudata* has been one of the most surprising developments.

A disturbance-adapted species, *C. nudata* is tussock-forming, not rhizomatous and propagates only by water-transported seeds that germinate shortly after being dispersed mid-summer along the edges of the low flow channel. The sedge derives its common name (torrent sedge) from its ability to maintain positions in the middle of fast rivers with its remarkably strong, dense root system. While *C. nudata* is particularly prominent in the John Day River basin, it occurs in varying degrees in rivers throughout the Pacific Northwest and northern California. In the MFJDR, *C. nudata* can now be found along the edges of gravel bars, at the base of cut banks and as islands in the middle of the river. At the bases of banks, *C. nudata* appears to be establishing in coarse + cohesive mixtures that often occur in the lower strata of banks. *C. nudata* forms a linear "fringe" in front of these banks with a space between the fringe and the bank, leading to a compound channel form (Figs. 2, 3). *C. nudata* defines the boundary of the low flow summer channel, the banks define the bankfull width and the space between the fringe and bank is inundated during intermediate to peak flows (Fig. 4.4).

Vegetation and Bank Retreat Processes

The question of bank retreat rates relative to *C. nudata* is not only critical to understanding stream evolution pathways within the MFJDR, it is also relevant to the broader arena of research around the role of vegetation in modifying bank retreat processes. Many studies have found correlations between vegetated banks and narrower channel widths (Huang and Nanson 1998, Millar 2000, Anderson et al. 2004) or between vegetated banks and lower erosion rates during flood events (Beeson and Doyle 1995, Laubel et al. 2003, Bąk et al. 2013). Other studies have documented channel narrowing following vegetation expansion in response to reductions in flow via dams (Hicks et al. 2007) or following vegetation expansion and/or species composition changes in response to the removal of cattle grazing (Kauffman et al. 1983a, Magilligan and McDowell 1997, Clary 1999). Such relationships point to the potential for plants to reduce erosion and stabilize banks. Nevertheless, generalizations about vegetation effects must be qualified by the wealth of observations that different kinds of vegetation may have markedly different associations with erosion rates or channel widths (Huang and Nanson 1997, Micheli and Kirchner 2002b, a, Allmendinger et al. 2005). Furthermore, in some cases vegetation may be an insignificant factor in explaining differences in channel width

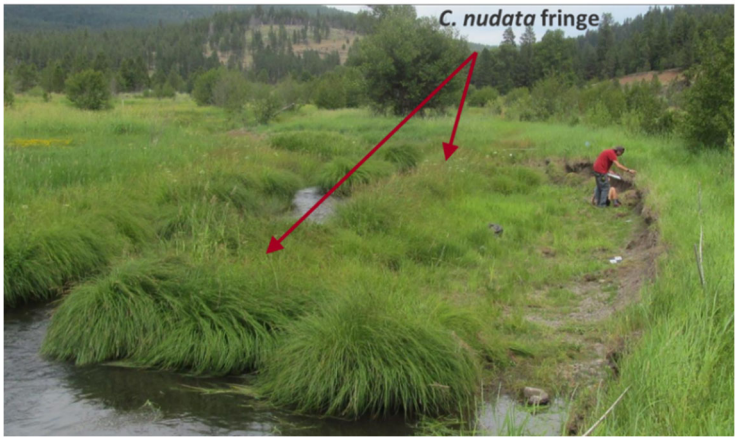

Figure 4.2. Site BEBU_F01 looking upstream, left bank at right of photo. Note the compound channel form in which the *C. nudata* fringe bounds the low flow channel, and the dry margin between the fringe and bank is inundated at intermediate and high flows.

Figure 4.3. Site BUTI_F01 looking downstream, right bank at right of photo. Note the compound channel form in which the *C. nudata* fringe bounds the low flow channel, and the dry margin between the fringe and bank is inundated at intermediate and high flows.

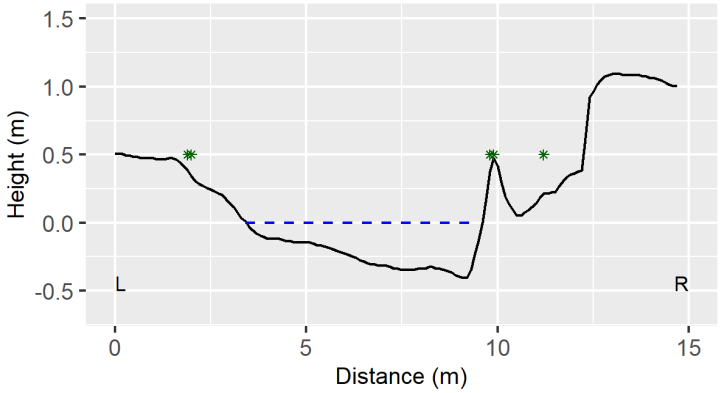

Figure 4.4. Site BUTI_F01 cross section looking downstream, right bank on right of graph. Green asterisks represent *C. nudata* locations. Dashed blue line represents summer low flow channel.

(Nanson and Hickin 1986) or may even be associated with wider channels (Anderson et al. 2004).

Vegetation can influence mass failure processes by modifying both driving and resisting forces. Plant roots enhance the mechanical cohesion of banks, but it is difficult to generalize about bank strengthening via roots given the variability among species in root depth, density, strength, longevity and position within the bank (Abernethy and Rutherfurd 2001, Wynn and Mostaghimi 2006a, Wynn and Mostaghimi 2006b, O'Hare et al. 2011). Plants can also reduce water pore pressure via evapotranspiration, and these effects may be comparable in magnitude to that of the mechanical strength imparted by roots (Simon and Collison 2002).

In addition to influences on bank strength, plants can alter hydraulic patterns. Plants rooted within the active channel may introduce roughness element that slow velocities and deflect flow away from banks, reducing shear stress at the bank toe (Konsoer 2014). The influence of plants on flow patterns varies with the diversity of plant forms, size, flexibility, branch density, presence of foliage and the position of the plants within the channel and relative to the bank (Rodrigues et al. 2007, Schnauder and Moggridge 2009, Curran and Hession 2013). Depending on the rigidity of plants and their position relative to the bank, induced turbulence and alteration of secondary currents may enhance erosive forces (Papanicolaou et al. 2007, Curran and Hession 2013, Konsoer et al. 2013).

In the case of the MFJDR, *C. nudata*'s primary effect should be the stabilization of the bank toe. *C. nudata* does not grow on the bank top or floodplain nor does it colonize the bank face behind its position at the water's edge. It is unlikely to affect bank pore pressure given that all of its roots are within the stream channel or water table. *C. nudata* also creates complex microtopography. As it accumulates sediment and grows, its tussocks form a hummocky ridge within the active channel in front of the bank. The effect of this microtopography on flow patterns is unclear. It is possible that *C. nudata* introduces significant roughness elements that slow velocity along the bank face, but it is also possible that these features create turbulence or alter secondary currents in such a way that increases erosive forces along the bank face.

The objective of our current study is not to tease apart the details of the processes by which *C. nudata* may affect bank erosion (e.g. how *C. nudata* might alter flows), but to first address the fundamental question: are banks fronted by *C. nudata* fringes eroding and retreating at a similar or different rate than banks without *C. nudata*? The second purpose of our study is to build a comprehensive understanding of bank erosion processes in the MFJDR, a framework necessary for interpreting the first question. Furthermore, no previous studies of bank erosion processes have been conducted in this basin, a basin prioritized for restoration investments and deemed critical for salmon recovery efforts. Through seasonal measurements of erosion pin arrays, annual bank retreat surveys and the characterization of key bank variables we aimed to also address questions about which seasonal processes are most important in driving bank retreat in this system and which bank characteristics influence those processes.

Methods

Study Area and Sites

The Middle Fork John Day is one of four branches of the John Day River, a tributary to the Columbia River and the third longest free-flowing river in the contiguous United States (Fig. 4.5). The headwaters of the MFJDR arise in the Blue Mountains of northeastern Oregon, where the climate is generally characterized by cold winters and dry, warm summers. Seventy percent of the precipitation falls between November and March, primarily as snow. Therefore, hydrology is strongly driven by snowmelt with spring peak flows with intermediate flows after fall rains, complete river ice in winter and late summer flows sustained by groundwater (OWRD 1986). The river is generally sinuous and alternates between constrained reaches and unconstrained reaches across floodplain meadows (400-500 m wide). Our 14 study sites were distributed across a river length of 7 km within the Oxbow Conservation Area (OCA) owned by the Confederated Tribes of Warm Springs (CTWS). Sites were located in reaches that were not directly affected by historic gold dredge mining, i.e. banks did not include tailings. Elevation at the OCA is around 1100 m. Low summer flow channel widths range from 3 to 13 m, and typical measured channel slopes range from .003 to .008. Pool-riffle channel reach types predominate with occasional plane-bed types. Mean annual discharge at the nearest gage (14 km downstream from the study sites) is 3.7 m^3/s and Q_2 flow is 21.2 m^3/s. The stream

bed is dominated by coarse gravels and cobbles; median sediment size (D_{50}) is typically 50-80 mm (McDowell 2001).

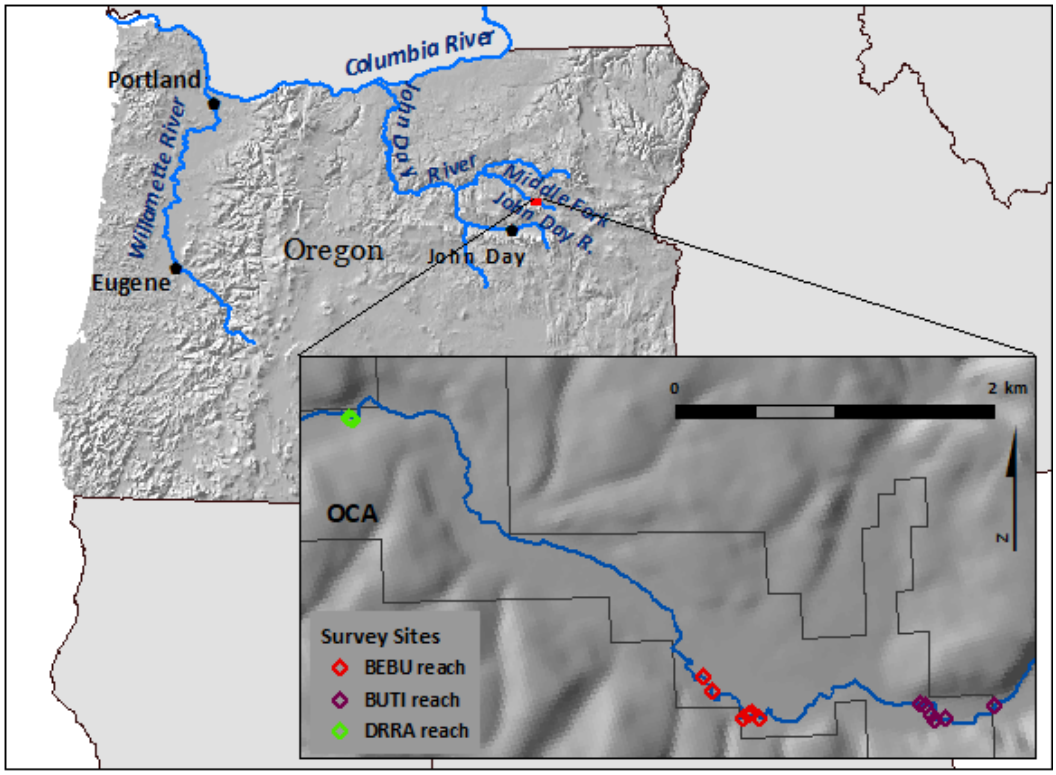

Figure 4.5. Location of study area and sites along the Middle Fork John Day River in the Oxbow Conservation Area (OCA) of the Confederated Tribes of the Warm Springs.

We selected 14 sites, 7 sites with a *C. nudata* fringe at the base of the bank ("F" sites) and 7 sites with no *C. nudata* fringe ("N" sites). We envisioned a paired site study design in which paired F and N sites represented similar bank substrate and curvature. However, as the study progressed and more detailed data was gathered on bank stratigraphy, significant heterogeneity within our paired sites became apparent. Study sites ranged from 10-43.6 m in length (Table 4.2). Bank heights ranged from .52 m to 1.41 m with an average bank height of .92 m. The uppermost soil strata in which we placed erosion pins (i.e. immediately beneath the graminoid root zone) included clay loams (most common), sandy clay loams, loams and sandy loams. Within each site, mid-to-upper strata were typically cohesive materials and relatively homogenous and consistent across each site. However, lower strata near the bank toe near or below the low water surface were highly heterogenous, ranging from clays (typically with clay hardpan

ledges below the water surface) to coarse, clast-supported materials. Among these lower strata types, cohesive matrices of varying texture with a significant component of embedded coarse clasts (fine gravels to small cobbles) were common.

At each site, we established an array of erosion pins, measured seasonally, to characterize bank face erosion patterns and rates. At these same sites, we surveyed the outer edge of the bank top annually to determine annual bank top retreat rates. While the presence or absence of *C. nudata* fringes was the focus of our analysis, we also collected ancillary data about each site, characterizing other possible explanatory variables of bank erosion and retreat including variables describing bank substrate and curvature.

Erosion Pin Arrays and Measurement

Erosion pins were arranged in columns with an average inter-column spacing across all sites of 2 m. Pins were spaced 10-30 cm apart vertically at each column. Among columns, pin location heights varied given that both bank heights and bank toe heights varied. We typically placed an uppermost pin 10 cm below the graminoid rooting zone and a pin about 10 cm above the bank toe. Intermediate pins were then spaced between these points but positions were adjusted to a) avoid bank irregularities that would make pin measurement difficult and b) avoid bank strata boundaries given that pins locations were also intended to be representative of distinct strata. Given the variation in bank height and site length, the number of pins ranged from 1-6 per column and 16-66 pins per site yielding a total of 546 pins measured across all sites in the final measurement.

For erosion pins, we used steel rods typically 61 cm in length and 4.7 mm in diameter. At initial placement, pins extended approximately 2cm beyond the bank face. At each seasonal measurement event, we measured the pin length extending beyond the bank face to the nearest 1 mm using steel rulers. Given that bank slopes were variable and bank faces irregular, for each pin we used different pin “faces” (top, bottom, right, left) for our measurement, using the face that would allow the most consistent measurement, and we then used that same face for measurements throughout the study period. During each measurement event, pins were typically measured twice, once each by two different measurers. We used the average measurements for each pin in our analyses, and differences among measurers allowed us to assess measurement error. The

Table 4.2. Site characteristics

Site	Class	Pair	Length (m)	# EP Columns	Bank Ht, Ave (m)	Aspect	Curve R (m)	Bend Location	Substrate: Upper Strata			Substrate: Bank Toe	
									Texture	% Sand	% Clay	Resistant	Erodible+
BEBU_F01	F	3	36.0	20	92.8	N	44	M	CL	22 %	29 %	40 %	21 %
BEBU_F02	F	1	30.0	15	69.4	NNE	47	H-T	CL	26 %	27 %	42 %	36 %
BEBU_F03	F	2	24.0	12	81.4	SSE	32	M	CL	42 %	29 %	19 %	78 %
BUTI_F01	F	5	41.3	28	107.5	S	73	H-T	CL	43 %	27 %	0 %	49 %
BUTI_F02	F	7	24.1	17	108.6	SE	31	M-T	CL	44 %	29 %		
BUTI_F03	F	6	41.2	19	134.0	NNE	65	M	SL	55 %	17 %	0 %	44 %
DRRA_F01	F	4	31.7	15	76.7	N	47	M	SL-SCL	59 %	20 %	8 %	19 %
BEBU_N01	N	1	43.6	16	66.7	SSW	27	H-T	CL	29 %	27 %	74 %	8 %
BEBU_N02	N	4	17.8	11	76.9	ESE	40	M-T	SC	54 %	23 %	38 %	53 %
BEBU_N03	N	3	10.0	5	81.4	SSE	32	T	CL	27 %	37 %	92 %	0 %
BUTI_N01	N	6	16.0	10	121.4	NNE	65	T	SC	57 %	23 %	0 %	100 %
BUTI_N02	N	2	29.0	11	89.4	ESE	36	M-T	L	36 %	25 %	19 %	42 %
BUTI_N03	N	7	25.2	12	98.9	NE	36	H-T	L	31 %	24 %		
DRRA_N01	N	5	10.3	8	58.4	NNE	47	T	SCL-SC	55 %	35 %	0 %	66 %

Notes. Class: F = *C. nudata* fringe, N = no fringe; EP = Erosion Pins; Curve R = thalweg radius of Curvature; Bend Location = location of site within river bend: M = Mid (middle 1/3), H = Head, T = Tail; Texture: C = Clay, S = Sand, L = Loam; Upper Strata Substrate represents texture and percent particle sizes from sample representative of relatively homogenous upper strata across the site (see Methods, Ancillary Data); Bank Toe Substrate represents percent of substrate types distributed heterogeneously across the length of the site, Erodible+ = "Highly Erodible" (see Methods, *Site Characteristic Data*). BUTI_F02 and BUTI_N03 were not used in the erosion and retreat models and therefore, do not have bank toe substrate values developed.

median standard deviation of measurements per pin across all pins and measurement events was 3.2 mm.

Deposition on pins of loose sediment derived from subaerial weakening and erosion processes above the pins was common. Because our key question centered on overall erosion rates, and most of this deposited sediment was judged to be transient, likely transported away by the next high flow, we followed a procedure in which we made two measurements. After measuring the pin "as-is" to the outer edge of the loose sediment, we used a brush to gently brush away the loose sediment until the coherent bank face was reached and then measured the pin again in order to capture any erosion of the coherent bank obscured by the loose sediment. We denote these as "pre-brush" and "post-brush" measurements.

Starting in Summer 2014 and ending in Summer 2016, we measured erosion pins three times each year – early summer (early July), fall (October), and end of winter (early March) – in order to capture erosion patterns reflecting different seasonal processes. The end of winter measurement was intended to take place immediately after the melting of the winter river ice sheet but prior the spring snowmelt peak flow.

Bank Top Surveys

We surveyed bank tops using a Topcon rtkGPS unit (.07 mm precision) with survey points placed at inflection points (in horizontal x-y dimensions) along the bank top yielding an average spacing between survey points of approximately .25 m. Banktop surveys were initiated in Fall 2013 and repeated annually through Fall 2018 with the exception of a missed annual survey in 2017, yielding a total of five surveys and four measurement periods.

Site Characteristic Data

River curvature was defined by the radius of curvature and determined by digitizing an approximate thalweg line in ArcGIS using aerial imagery and personal knowledge of each site. The river curve line extended beyond the upstream and downstream boundaries of each site to include the full curve within which each site was located.

Aspect was derived for each pin column via interpretation of high-resolution (10cm) aerial imagery (2013) in ArcGIS. Within our models, we used a "north-to-south" metric for Aspect ranging from -1 (N) to 1 (S) calculated as

$$Asp_S = -1 * \cos(\theta) \quad (1)$$

where θ is pin column aspect in radians, and the output of the cosine is multiplied by -1 simply to make southerly aspects positive. Henceforth, the variable "Aspect" in our models refers to this index, Asp_S .

For each site, we collected substrate samples for each strata from at least two different columns within the sites and used hydrometer particle-size analysis to determine the percent of sands, silts and clays for each sample (Gee and Or 2002). As an independent variable in our bank erosion/retreat models, we use percent sand from the uppermost strata for each site. The uppermost strata in which pins were located (beneath the graminoid rooting zone) was typically the most homogenous across a given site. Within this stratum, percent sand was the most variable soil texture component among sites, and the proportion of sand versus silt/clays is a key factor in both fluvial and subaerial erosion processes (Couper 2003, Clark and Wynn 2007).

The lower strata were the most heterogenous within each site and between sites, such that we chose to characterize this lower stratum in more detail for each site using hand texturing and ocular estimates. We created a hierarchical set of 14 substrate types differentiated by each type's matrix and then by the percent and size of coarse clasts within the matrix (Table 4.3). We then defined two independent variables for use in our models: 1) percent resistant substrate, the percent of bank toe length occupied by clay-dominant substrate, and 2) percent highly erodible substrate, the percent of bank toe length occupied by types with a sandy loam sand matrix or with a high percent (30-70%) of gravels within any matrix. It should also be noted that the points at which we described the bank toe vary in height relative to the water surface. That is, where *C. nudata* tussocks front the bank, the bank toe is elevated above the low water surface, whereas in locations without a *C. nudata* fronting tussock we characterized the bank toe at the low water surface.

Table 4.3. Bank toe substrate classification scheme and % occurrence of bank toe substrate types across all sites included in the erosion and retreat models.

Code	Matrix	% Clasts	Clast Size	Model Var	Occurrence
A	Clay/Sandy	<5%		Resistant	27.6 %
B	Clay/Sandy	+narrow band (1-5cm) w sand/fine			5.1 %
C	Clay loam	<5%			4.8 %
D	Sandy clay	5 - 30%	fine-med gravs		3.0 %
E1	Sandy clay	30 - 70%	fine-med gravs	Erodible+	11.3 %
E2	Sandy clay	30 - 70%	coarse gravs	Erodible+	9.8 %
E3	Sandy clay	30 - 70%	cobs + gravs		2.6 %
F	Sandy loam	5 - 30%	fine-med gravs	Erodible+	4.7 %
G1	Sandy loam	30 - 70%	fine-med gravs	Erodible+	6.7 %
G2	Sandy loam	30 - 70%	coarse gravs	Erodible+	0.0 %
G3	Sandy loam	30 - 70%	cobs + gravs	Erodible+	8.6 %
K1	Clast dominant	> 70%	fine-med gravs	Erodible+	2.0 %
K2	Clast dominant	> 70%	coarse gravs		5.3 %
K3	Clast dominant	> 70%	cobs + gravs		8.3 %

Notes: the texture of the matrix for each type can be considered a median texture. For instance, the F & G types also included loamy sands as well as some sandy clay loams near the "sandy" end of this texture class. "Clasts" include all particle sizes greater than sand. "Erodible+" types are aggregated into the "Highly Erodible" variable in the erosion and retreat models.

Weather & Hydrological Data

To provide context for interpreting seasonal patterns in erosion, we present daily temperature data during our measurement years from a weather station maintained by the CTWS at the Oxbow Conservation Area. This data can be obtained via wunderground.com (personal weather station: KOROREGO32). River discharge and river ice data were obtained from the MFJDR at Camp Creek USGS stream gage (#14043840) located 14 km downstream of our sites.

Erosion pin and banktop retreat data analysis

Changes in erosion pin length for each pin was determined by subtracting the average (among measurers) pin length (extending beyond the bank face) at each measurement event from the previous average measured pin length such that positive values (greater length) indicate erosion. While erosion pin arrays may be intended to measure rates of bank erosion, a key issue is the occurrence of negative readings, that is, a shortening of pin length. Negative pin readings may result from such processes as bank

expansion (e.g. with freezing of soil water) or deposition of sediment on the pin (Couper et al. 2002). While negative pins may initially seem to pose a problem for estimating erosion rates, the patterns of negative pin readings as well as those of positive pin readings, pins with no change and lost pins can offer key insights into bank retreat processes (Couper et al. 2002).

To better understand seasonal processes, we constructed tables presenting the percent of positive, negative, unchanged and lost pins by seasonal measurement period. In this analysis, we used the "pre-brush," "as-is" measurements for pins covered by deposited loose sediment. Pins were classified as "no change" if the absolute positive or negative change value of the pin were less than a critical threshold of error, U_{crit}

$$U_{crit} = t\sqrt{\sigma_i^2 + \sigma_j^2} \quad (2)$$

where σ_i and σ_j are the standard deviations for the pin measurements at each measurement event and t is set to 1 following a procedure used in detecting differences in surface change described by Milan et al. (2011). During pin measurements, we also made notes on bank features (e.g. sediment deposition, mass failures) and took photographs of all pin columns, such that notes and photographs were used to further classify lost and negative pin readings according to possible causal factors.

To address the fundamental question driving this study, whether banks with *C. nudata* fringes erode at a different rate than banks without *C. nudata* fringes, we used pin erosion rates. That is, a) for pins that were affected by deposition of loose sediment, we used the post-brush measurements to reflect pin length extruding from the coherent bank face and b) we set all remaining negative pin readings to zero. Alternatively, treating negative pin readings as missing values would inflate erosion rates and maintaining negative pin readings as-is would likely underestimate erosion, given that remaining negative pin readings were likely due to temporary expansion of the bank soils.

To address the question of differences in erosion rates between sites with and without *C. nudata*, we limited our sample set to 12 sites and employed linear mixed effects models. Two of the 14 sites (BUTI_F02 and BUTI_N03) were dropped from this analysis because the pattern of *C. nudata* changed at these sites during the study period

such that they did not consistently represent either an F or N class. We analyzed erosion rates by pins pooled across all sites using the linear mixed effects (lme) function in R statistics, nmle package (Pinheiro et al. 2021). We tested a set of nested random effects: site pairings, sites and columns within sites and found that despite our intended paired site design, site pairings were not a significant random effect and therefore, not included. Both sites and pin columns were significant and included as random effects (i.e. blocking units). We were also able to gain significant model improvement by using varIdent function within lme to specify different variance structures within each seasonal period. After specifying random effects & variance structures, we tested for differences among *C. nudata* fringe classes (N vs. F) and seasonal periods, both treated as factors, with additional explanatory variables and interactions tested in a full model. Additional explanatory variables included site variables (river curvature, percent sand in the upper strata, percent resistible substrate along the bank toe, percent highly erodible substrate along the bank toe), column variables (bank height and aspect) and a pin location variable (height above low water surface). We proceeded from the full model through backwards step-wise model selection process as recommended by (Zuur et al. 2009). We concluded by refitting the final model with each level of the factor (e.g. seasonal periods) used as the intercept (β_0), thus testing for differences among multiple levels.

Bank top retreat rates were analyzed using a similar approach, starting with a full linear mixed effects model, but without seasonal periods as a factor given that bank tops were surveyed annually. Also, column-based variables (aspect & bank height) were employed as site-averaged variables. Furthermore, after testing site pairings, sites and years as random effects, we found that none were significant as a random effect, such that we were able to employ a simple linear model instead.

Finally, we also used a simple linear model of annual bank top retreat by site relative to annual bank face erosion by site (seasonal erosion pin changes summed for each year) to assess how tightly these two processes are correlated annually. The relationship between these two processes was also assessed after aggregating each of these two rates by site over the entire erosion pin study period (2014-2016). In all our statistical analyses, change rates were log-transformed.

Results

Hydrological and Weather Patterns

During the study period, the reaches of the MFJDR that included our study sites experienced weather and hydrological patterns that differed for the seasonal periods among years. While there was no apparent difference between the 2014 and 2015 summers, the winter and spring seasonal periods differed dramatically between years. During the 2014-2015 winter seasonal period, multiple warming periods with temperatures above 0° C led to multiple river ice melts/breakups followed by refreezing (Fig. 4.6). Atypical of most water years, the two highest peak flows also occurred during the winter seasonal period at 16.0 m^3s on 12/22/2014 following a rain + warming event and 13.9 m^3s on 2/09/2015), both of which would have been at or above bankfull stage for 7 out of the 14 sites. For reference, bankfull flow at BEBU_F01, the site at which we've monitored flow stage most closely, is approximately 17.5 m^3s and the bank height of this site (.92 m) is just above the median bank height for our sites (.85 m). Reflecting the below average snowpacks that accumulated during the 2014-15 winter, the peak flow in spring 2015 was relatively small (6.88 m^3s) and below bankfull stage.

In contrast to the first year, the 2015-2016 winter seasonal period followed a more typical winter pattern. Temperatures only rarely and briefly went above 0° C, such that there was only one brief melting of river ice in early December followed by continuous river ice cover through mid-February (Fig. 4.7). There were no peak flows during the winter seasonal period except a brief peak flow of 12.7 m^3s on 2/18/2015 immediately following the river ice melt and just prior to our erosion pin measurements on 3/1/2016. Spring 2016 also followed a more typical hydrological pattern, with a normal winter snowpack leading to multiple, extended snowmelt-driven peak flows, the highest reaching 19.3 m^3s, a stage at or above bankfull for 10 out of 14 sites, exceeding all of our uppermost pins, but below the Q_2 flow.

Henceforth, in our reporting of erosion pin change rates, we will refer to the 2014-2015 winter simply as the 2015 winter period and the 2015-2016 winter as the 2016 winter period.

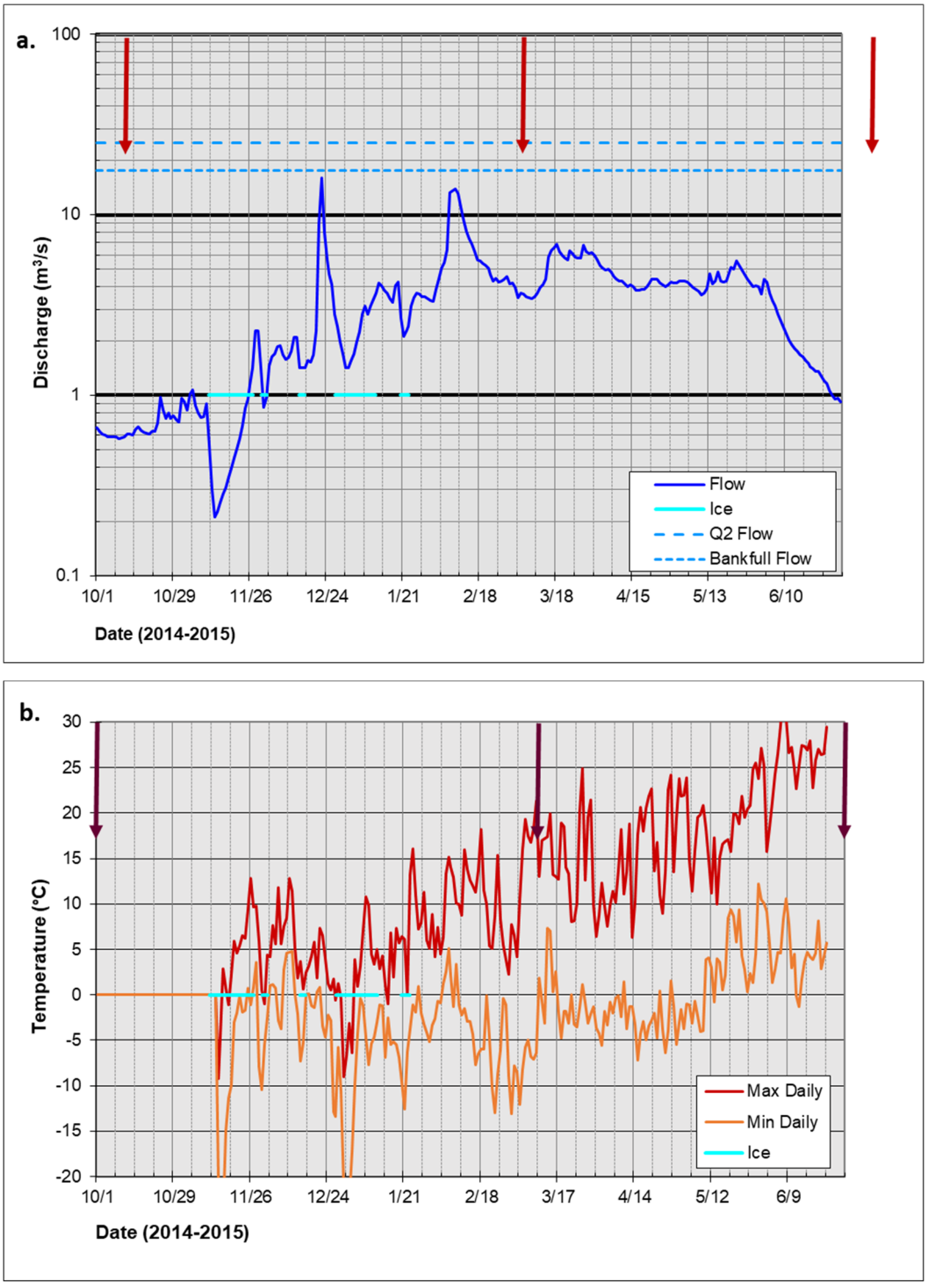

Figure 4.6. a) Daily discharge and river ice, and b) daily maximum and minimum temperatures and river ice from 10/1/2014 - 6/30/2015. Discharge and river ice data are from USGS stream gage #14043840, MFJDR at Camp Creek. Arrows indicate erosion pin measuring events. Temperature data are from the weather station at the Oxbow Conservation Area where recordings began 11/14/2014.

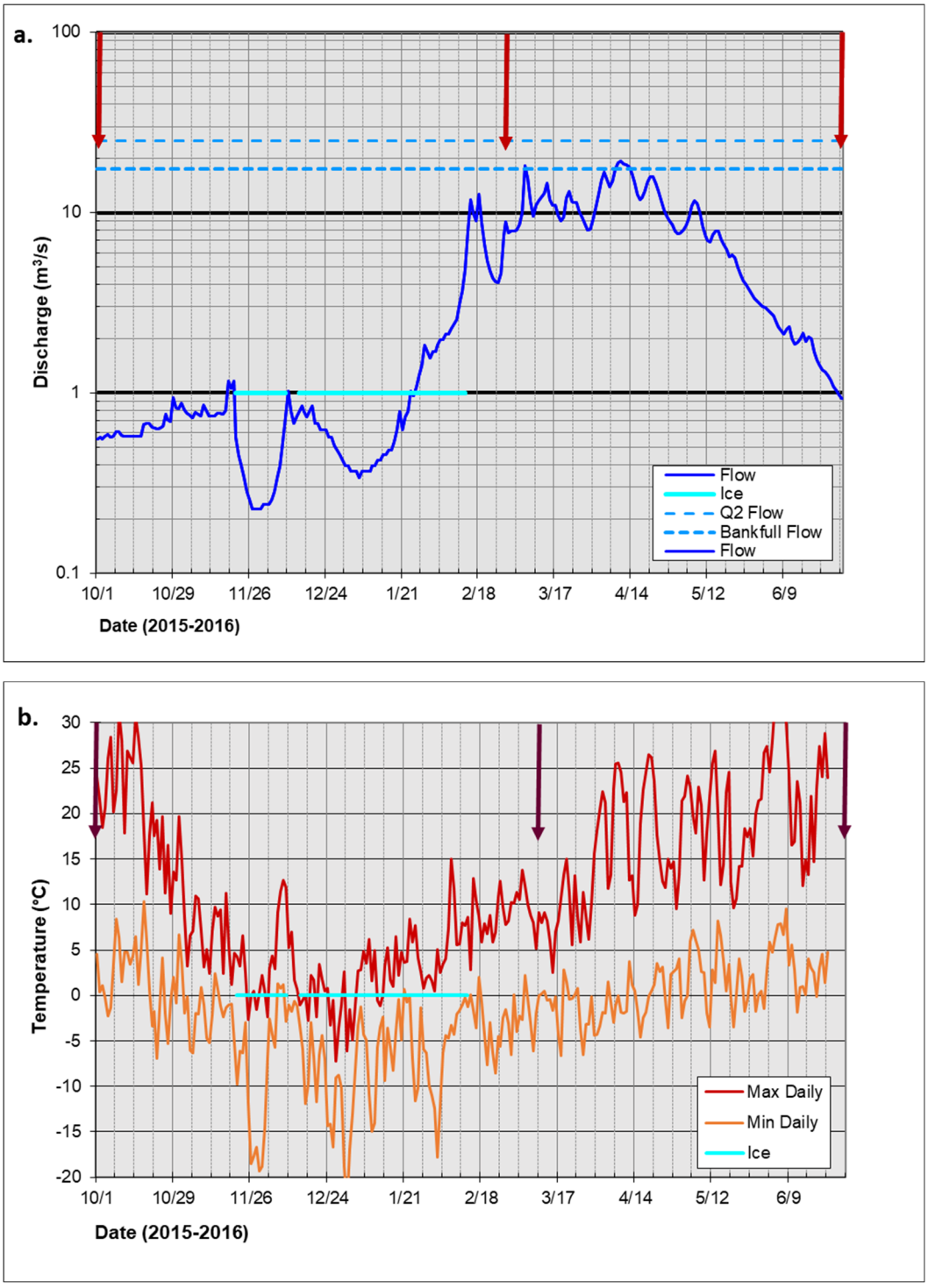

Figure 4.7. a) Daily discharge and river ice, and b) daily maximum and minimum temperature and river ice from 10/1/2015 - 6/30/2016. Discharge and river ice data are from USGS stream gage #14043840, MFJDR at Camp Creek. Arrows indicate erosion pin measuring events. Temperature data are from the weather station at the Oxbow Conservation Area.

Seasonal Patterns of Erosion Pin Change

The proportions of pins with positive (erosion), negative or no change varied across seasonal periods (Table 4.4). All of the seasonal periods with significant peak flows (Winter 2015, Winter 2016, Spring 2016) had high percentages of pins showing erosion (>70%). Most striking, the highest percentage of pins showing erosion did not occur in the seasonal period with the highest and longest peak flows (Spring 2016) but rather Winter 2015, the period that included multiple ice thawing intervals and two modest, brief peak flows following river ice thaw. Furthermore, the percent of eroding pins during Winter 2016, a period with continuous ice and one modest peak flow immediately following ice break up was similar to that of Spring 2016. Both summer periods included a plurality of pins with no change. Negative pin readings were found during all seasonal periods, and the highest percent of negative pin readings (>20%) occurred during the two summer seasons and Spring 2015, the spring that did not experience a bankfull flow. Figure 4.8 provides an example of erosion pin patterns across the first year of seasonal periods for one representative site, BEBU_F01.

Table 4.4. Erosion pin change directions by season

Pin Change	Sm 2014	W 2015	Sp 2015	Sm 2015	W 2016	Sp 2016
(+) Erosion	22.3 %	81.6 %	47.3 %	32.7 %	74.1 %	77.4 %
(0) No Change	49.2 %	5.8 %	22.7 %	43.4 %	5.5 %	8.8 %
(-)	24.5%	5.0 %	22.5 %	21.5 %	17.5 %	10.1 %
Lost	4.0 %	7.5 %	7.5 %	2.4 %	2.9 %	3.7 %

We observed several distinct depositional processes which led to negative or lost pin readings including mass failure (primarily cantilever), animal burrowing and what we describe as “non-point” deposition of loose, granular sediment, a product of subaerial weakening and erosion processes above the affected pins (Table 4.5). We classified this last process as non-point deposition to distinguish it from the “point source” process of small animal burrowing, a process distinguished by large conical mounds and small holes (5-10 cm) in the banks above the mounds (Fig. 4.9a). While the percent of pins impacted by small animal burrowing was small, it is notable that the median negative change at these pins was greater than those for non-point deposition and unknown sources. Another

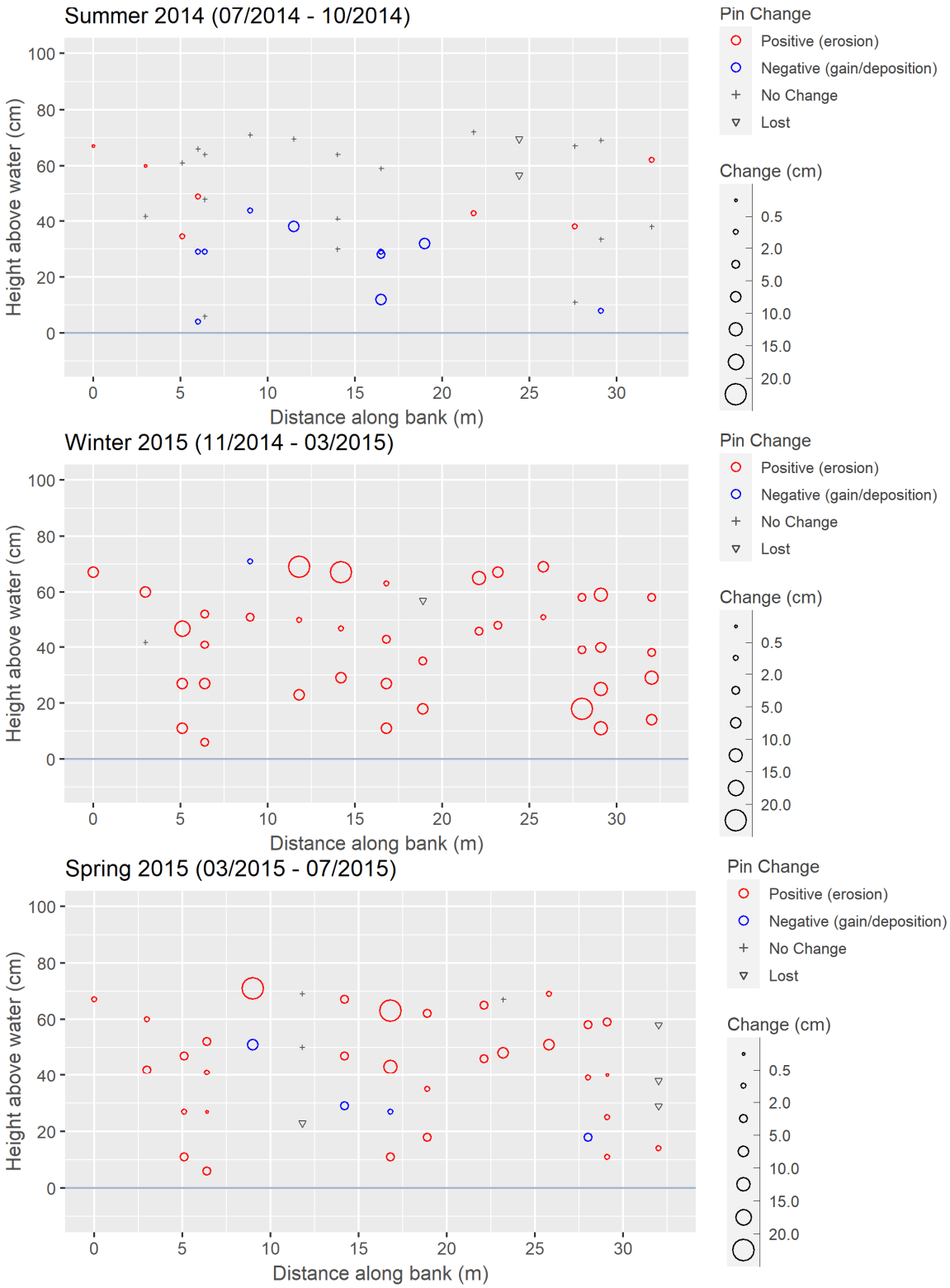

Figure 4.8. Erosion pin arrays for BEBU_F01 from Summer 2014 through Spring 2015 showing direction and magnitude of change and lost pins by seasonal period.

Table 4.5. Percent of pins with negative readings or lost classed by condition (causal factor) and the average change in pin length (cm) for pins with negative readings (not lost). The last row represents percent of pins among all pins at columns impacted by mass failure including not only lost (buried) and negative change pins, but also pins with positive or no change.

Pin Class	Condition	Sm 2014	W 2015	Sp 2015	Sm 2015	W 2016	Sp 2016
(-) & Lost	Unknown	60.0 % (-1.0)	50.0 % (-1.6)	50 % (-1.2)	55.0 % (-1.0)	69.4 % (-1.2)	37.8% (-1.5)
(-) & Lost	Deposition (Non-point)	25.8 % (-2.5)	20.0 % (-2.0)	34.7 % (-2.8)	33.0 % (-2.0)	20.7 % (-3.0)	29.7 % (-1.7)
(-) & Lost	Deposition (Animal)	8.3 % (-4.6)	0 %	.7 % (-1.9)	9.2 % (-3.4)	0 %	1.4 % (-3)
(-) & Lost	Mass Failure	5.8 % (-4.7)	30.0% (-6.2)	14.6 % (-3.4)	2.8 % (-3.4)	9.0 % (NA)	24.3 % (-3)
All	Mass Failure	1.9 %	5.9 %	6.3 %	.7 %	4.0 %	7.7 %

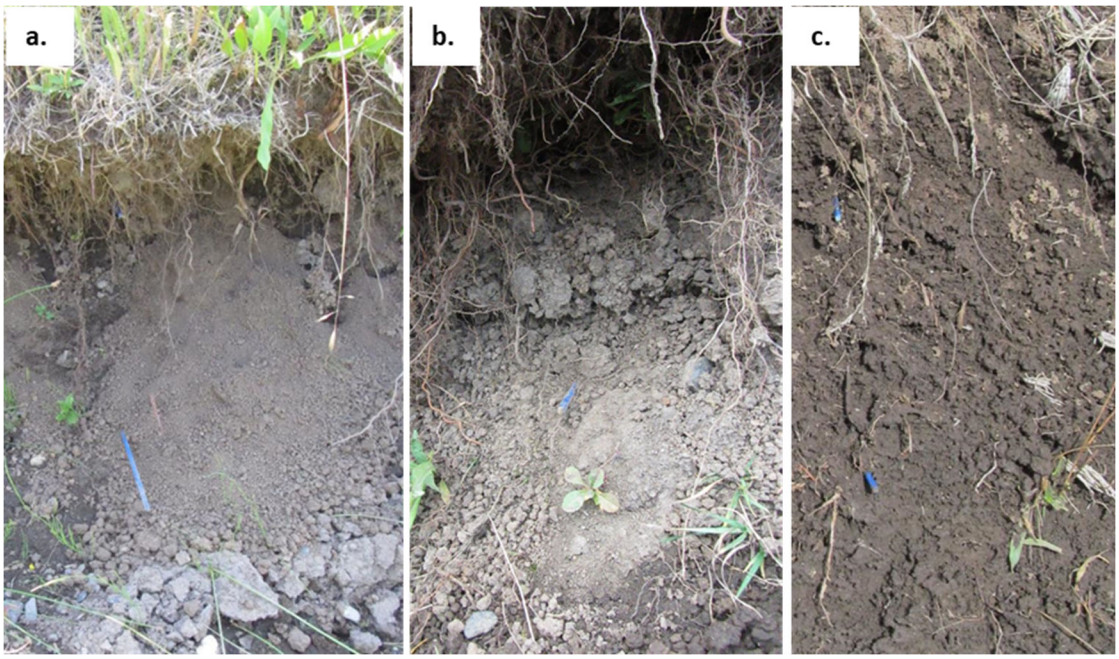

Figure 4.9. Examples of a) "point source" conical deposition mounds from small animal burrowing in early October, b) "non-point" deposition across lower portion of bank face in early October and c) saturated flow-like soil structures in early March. Blue erosion pins are visible in each picture.

key observation was that 87% of the pins impacted by animal burrowing occurred in *C. nudata* fringe sites.

Point source (animal) deposition occurred in summer and non-point deposition occurred across all seasons. Over the summer period, non-point deposition was evidenced by long "skirts" of dry, loose sediment accumulating along convex inflection points in the bank face or at the base of the bank, likely a product of soil desiccation, cracking and crumbling (Fig. 4.9b). During the winter measurements (March), we observed accumulations at similar positions of wet, granular sediment, likely a product of freeze/thaw cycles. During spring measurements, we observed accumulations of both wet and dry granular sediment.

Most of the negative/lost pin readings were not attributed to a specific cause at the time of pin measurement, but assessments of photographs and comments afterwards permit a discussion of possible causes. While this unknown category included possible fluvial deposition and disturbance by wild and domestic ungulates, both of these possible sources were miniscule (4% and 1%, respectively, of all unknown negative/lost pins). Most of the negative pin readings were likely caused either by bank expansion (i.e. due to saturation or freezing of the bank) or due to downward movement of flow-like soil structures across wetted bank face (Fig. 4.9c). We recognized this phenomenon of downward soil flow primarily via examination of photographs following field measurements making it difficult to quantify, and believe it to be a product of freeze/thaw soil loosening and saturation, perhaps similar to the "drool" described by Inamdar et al. (2018). Reflecting the subtle nature of the processes contributing to the unknown class of negative/lost pin readings, this class showed the smallest median change rate among the negative pin classes.

Mass failures occurred primarily during winter and spring periods. In the "All pins" mass failure class, we include not only pins with negative and lost pins, but also pins with positive readings and no change readings if the pin was located within a column in which a block above the pin failed and landed below it. Given that we include all pins at columns affected by new mass failures, this metric is an effective proxy for the percent of bank length failing in a seasonal period. While these percentages per season may seem small, cantilever failures are the primary mode of bank retreat, and each failure results in a significant removal of bank top material. Adding up the seasonal percentages, these results suggest that 12.4 - 14.1% of the bank top length experiences failures each year,

suggesting that the entire bank length will experience mass failures in a 7-8 year return interval.

Site Characteristics and C. nudata Fringe Classes

As described in the methods, we employed a paired site study design, pairing sites with and without *C. nudata* fringes that had similar bank curvature and substrate. However, site pairings were not significant as a random effect in the mixed effects models, indicating that variability within pairs was no less than variability among all sites. Nevertheless, the intended purpose of the design was met. That is, there were no significant differences in any of the site characterization variables between the *C. nudata* fringe and non-fringe classes (Table 4.6). While our observations suggested that non-fringe sites had a higher proportion of resistant substrate types along the bank toe whereas fringe sites had a higher proportion of large clast-dominant substrate types, between-class differences were not significant.

Table 4.6. Median values of site variables by F and N sites and p-values from non-parametric Wilcoxon test paired difference test.

Variable	**F Sites**	**N Sites**	***p***
Bank Height (m)	0.87	0.79	0.42
Aspect: -1 (N) to 1 (S)	-0.88	0.24	0.46
Curvature: Radius (m)	47	38	0.22
Sand (within upper strata sample)	43%	43%	0.87
Clay (within upper strata sample)	27%	26%	0.69
Resistant (bank toe length)	13%	28%	0.69
Erodible+ (bank toe length)	40%	47%	0.94
Clast dominant (bank toe length)	4%	0%	0.34

Bank Face Erosion Rate Models and Class Comparisons

After proceeding through the model-fitting protocol for pin erosion rates, we found no difference in erosion rates among pins with a *C. nudata* fringe and those without (Table 4.7, Fig. 4.10). Among all non-seasonal explanatory variables tested – pin distance above water surface, aspect of column, bank height of column, river curvature at site, percent sand in upper stratum of site, percent highly erodible substrate along bank toe, percent resistant substrate along bank toe – the only significant explanator of erosion rates was aspect. Erosion rates increased as aspects became more south-facing.

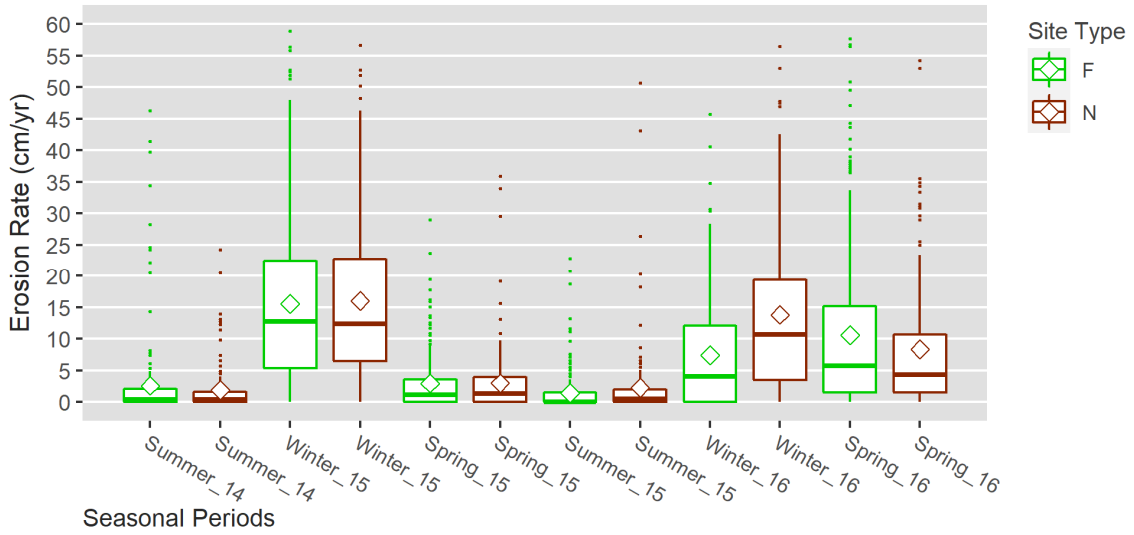

Figure 4.10. Box plots of pin erosion rates by *C. nudata* site class and seasonal period. Diamonds indicate mean values.

Table 4.7. Final LME model of bank face (pin) erosion rates including parameter values and significance of differences among seasonal periods derived from fitting the model successively with each seasonal period as the intercept. Parameter values for seasonal periods are derived from the model using Summer 2015, the seasonal period with the lowest estimated erosion rates, as the intercept.

Y = log (Erosion, cm/yr)		Significance or significance of differences among seasons					
Parameter	**Value**	**Sm 2014**	**W 2015**	**Sp 2015**	**Sm 2015**	**W 2016**	**Sp 2016**
Aspect	0.236	.035					
Su 2014	0.043						
W 2015	3.027	****					
Sp 2015	0.636	****	****				
Su 2015	-0.707	.73	****	****			
W 2016	1.934	****	****	****	****		
Sp 2016	2.081	****	****	****	****	.239	

Notes: **** $p < .0001$; AIC = 9493; DF = 2223 for intercept & seasonal periods, DF = 172 for Aspect
Sites and Columns nested in sites were included as random effects; specific variance structures were used for each seasonal period.

Erosion rates differed among the seasonal periods (Table 4.7, Fig. 4.10). The highest erosion rates occurred during Winter 2015, the winter with multiple temperature fluctuations around 0° C, multiple periods of river ice freezing & thawing and two modest peak flow events. The second highest erosion rates occurred during Winter 2016 & Spring 2016 with no significant difference between these periods. Spring 2016

included the highest and most extensive peak flows, while Winter 2016 included relatively continuous river ice and one modest peak flow immediately following river ice break up. Spring 2015, which featured relatively low peak flows also displayed lower erosion rates than any of the other winter or spring periods. Nevertheless, Spring 2015 erosion rates were greater than those of Summer 2014 and Summer 2015 with no difference between the summer seasonal periods.

Bank Top Retreat Rate Models and Class Comparisons

Visual comparisons of annual bank top survey lines at each site showed little evidence of gradual retreat but instead showed distinct segments receding in large chunks indicative of mass failures. As discussed in our erosion pin results, we had also observed mass failures burying pins. Almost all mass failures observed in the field were cantilever failures.

There was no difference in bank top retreat rates among sites with *C. nudata* fringes and those without (Table 4.8, Fig. 4.11). After testing the same set of explanatory site variables as those used in the erosion pin model-fitting process (using mean aspect & bank heights by site rather than column), none were found to be significant explanators, but mean bank height was marginally significant (p = .059) with bank top retreat increasing with mean bank height.

Table 4.8. Final linear model for annual bank retreat rates.

Y = log (Bank Retreat, cm/yr)

Parameter	Estimate	S.E.	*p*
Intercept	1.14	.456	.0157
Bank Height (m)	.975	.503	.0590

Notes: Residual S.E. = .757; DF = 46; Adj R^2 = .055

There was no difference in bank top retreat rates among years. We used a general linear model rather than a linear mixed effects model, because sites were insignificant when included as a random effect, reflecting the high amount of variation within sites among years. Essentially, the relative bank top retreat rates among sites changes each year (Fig. 4.11).

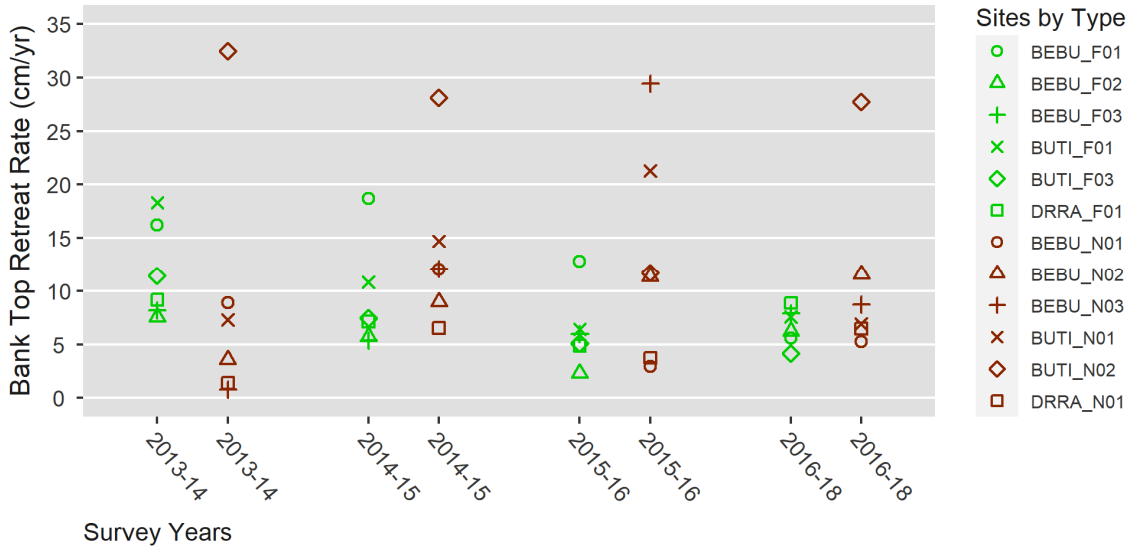

Figure 4.11. Point plot of surveyed bank top retreat rates by site, *C. nudata* site class and annual period.

Even though bank face erosion rates (pins) were a significant explanator of bank top retreat rates, the relationship between bank face erosion and bank top retreat was relatively weak (adj r^2 = .35) when pin erosion rates were aggregated by year (Fig. 4.12a). However, this relationship becomes much stronger (adj r^2 = .63) when both bank top retreat and bank face erosion rates were aggregated over the entire 2014-2016 erosion pin study period (Fig. 4.12b). Another key observation from these models is that the slope parameters are greater than one, i.e. the bank top retreat rate is slightly greater than our pin erosion rates. This is important for two reasons. First, we were concerned that the high erosion pin rates we found during the winter periods might be exaggerated, reflecting a process by which freezing/thawing pushes pins outward rather than actual erosion. The bank retreat-erosion pin relationship suggests this concern is not warranted; our high winter erosion rates do indeed reflect erosion and not pin movement. Second, it suggests that our pin erosion rates may not fully capture the processes contributing to bank retreat. It's possible that this underestimate could be attributed to pins lost to mass failures, if those pins had experienced higher than average erosion rates prior to being buried. Alternatively, it's possible this underestimate reflects the importance of bank weakening processes (freeze-thaw, desiccation, animal burrowing) that are not fully captured by pins measuring loss of bank face surface.

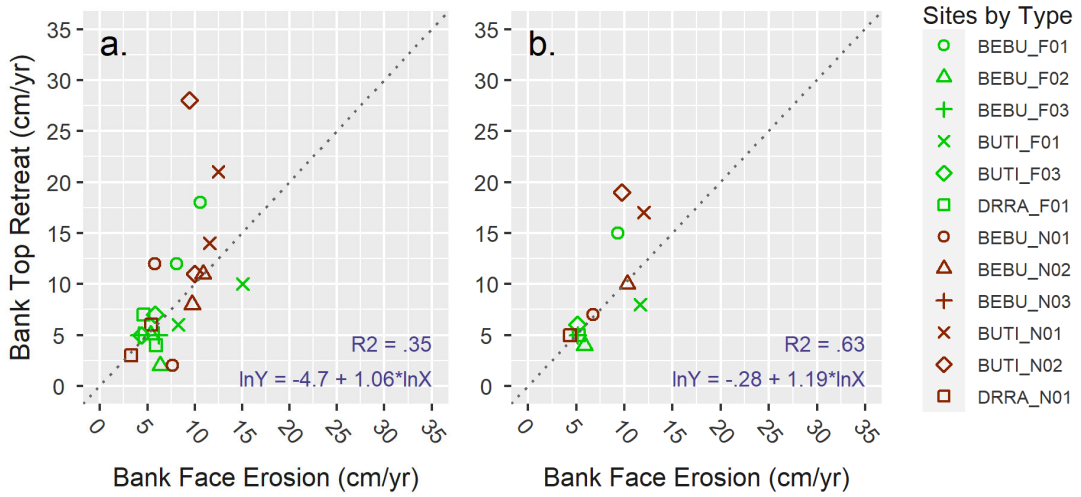

Figure 4.12. Relationship between surveyed bank top retreat and bank face (pin) erosion rates by sites when (a) represented by individual year (2014-2015, 2015-2016) vs. (b) averaged for each site across the full erosion pin study period (2014-2016).

Discussion

Seasonal Patterns and Bank Erosion Processes in the MFJDR

Although we did not find statistical relationships between bank erosion rates, *C. nudata* and key variables we expected to be driving these rates such as bank substrate and river curvature, the big picture painted by these results substantively changed our framework for understanding bank erosion processes in the MFJDR and further advanced our understanding of *C. nudata's* role in stream evolution.

Contrary to our expectations, the interaction of winter processes was equally or more important than fluvial erosion during the highest peak flows of the spring snow melt. Erosion rates during the Winter 2016 were of similar magnitude to those of Spring 2016 during which the highest and most extensive peak flows occurred. Furthermore, the greatest erosion occurred during Winter 2015 in which two modest peak flows occurred within a context of multiple cycles of river ice freezing and break up as well as additional fluctuations around freezing temperatures beyond those associated with full river icing and thawing.

There are several processes that our observations suggest may be interacting to drive high rates of winter erosion. First, freeze/thaw cycles of bank soils can break down soil structure leading to weakening or erosion. Subaerial processes such as freezing/thawing or desiccation/cracking have often been classified simply as bank

substrate weakening processes that make banks more susceptible to the forces of fluvial erosion. However, several authors have demonstrated that these processes can directly lead to bank face erosion (Lawler 1986, 1993b, Couper and Maddock 2001, Ferrick et al. 2005, Wynn and Mostaghimi 2006b, Yumoto et al. 2006, Wynn et al. 2008, Harden et al. 2009). Our findings across seasons of extensive non-fluvial deposition of both dry and wet granular sediment derived from the erosion of bank substrate above pins supports the contention that subaerial processes can drive erosion directly. In addition to "skirts" of deposited granular bank sediment, we also observed drip-like, soil structures down bank faces in winter and spring when banks were still wetted. Nevertheless, we do not discount the role of subaerial processes in weakening. It may be that the high rates of winter erosion are attributable to the coupling of freeze-thaw weakening with peak flows accompanying river thaw, essentially a "one-two punch" that amplifies the effectiveness of a peak flow (Inamdar et al. 2018). Furthermore, summer desiccation prior to winter – clearly evidenced by deposition of loose sediment deposited on pins – may cause cracking, the breaking of soil aggregates, making them more susceptible to freeze-thaw action (Gatto 1995, Gatto et al. 2001).

In addition to our observations of non-fluvial deposition across seasons, compelling support for the importance of subaerial processes was the significance of aspect as the only explanator of bank erosion rates in our model other than seasonal periods. Southerly aspects likely experience greater diurnal temperature ranges leading to greater desiccation during summer and greater freeze-thaw cycling during winter. Similarly, Ferrick et al. (2005) found greater erosion on south-facing banks of the Connecticut River attributed to greater freeze-thaw cycling. Wynn and Mostaghimi (2006b) found that subaerial erosion rates in a set of Appalachian rivers were greater in banks that were more exposed during the season in which a particular subaerial process occurred and differences in exposure were mediated by differences in vegetation type. Banks with deciduous trees and no understory vegetation experienced greater temperature ranges, freeze/thaw cycles and subaerial erosion in winter, whereas banks covered with grasses and forbs were more exposed during summer and experienced higher rates of subaerial erosion associated with desiccation and crumbling.

The other critical process during winter is that of river ice thawing and break up. In their study of the Peace River in Canada, Uunila and Church (2015b) found that river ice break-up could enhance erosion through several processes: 1) moving broken ice slabs can directly abrade bank faces, 2) toppling ice attached to soils can pull off soils if river stage recedes too quickly and 3) ice slabs can form dams at constriction points in the river that significantly elevate water stage and then fluvial erosion as the dams break up. These processes are effective predominantly during rapid ice break-up rather than gradual thawing, and ice damming accounted for the most extensive erosion. During Winter 2015, the weather data suggest that ice break ups were relatively gradual prior to peak flows and there were so many fluctuations around freezing that river ice does not appear to have formed over long period. These weather patterns suggest that the impact of freeze-thaw cycles on bank substrate may have been more important than river ice break up. During Winter 2016, however, river ice built up across the river for 61 consecutive days and broke up rapidly, with flow peaking two days after ice was last recorded at the gage station. Such a sequence would likely have led to slabs of ice forced down river, abraiding bank faces, building dams and elevating river stage in certain reaches far above that expected for an otherwise below-bankfull flow. While we did not observe this sequence in February 2016 directly, we did observe the break-up of river ice in late November 2014, river ice that had accumulated for two weeks and then broke up rapidly with a rise in temperature and a much smaller rise in flow (2.3 m^3s). Even during this much smaller ice break-up and flow rise, we observed the formation of small ice dams and elevated river stage. Consistent with the observations of Uunila and Church (2015b), these ice dams typically formed at constriction points, in our case, at tight river bends and where *C. nudata* islands presented obstacles. A critical point here is that the effects of river ice break up present an additional, difficult-to-model variable independent of the river curvature in which the site is located and independent of site substrate. A site may experience elevated river stage and heightened erosion simply as a result of a tight bend or the presence of *C. nudata* islands immediately downstream of the site and the curve in which it is located.

While we have thus far focused on subaerial and river ice erosion processes in the context of winter erosion, our results do not diminish the importance of fluvial erosion.

Comparing the two spring seasons, erosion rates in 2016 greatly exceeded those during 2015 and the primary difference was higher, extended bank-full peak flows in 2016 versus peak flows far below average in 2015.

Given the evidence that peak flows and fluvial erosion are indeed key drivers of high erosion rates, our results beg the question, why did none of the variables that would presumably interact with fluvial erosion prove significant in our model of bank erosion rates? To some extent, the lack of significant relationships with these variables is not surprising. Bank erosion is a complex process of multiple interacting factors and processes, such that many studies have found relationships between erosion rates and expected explanatory factors to be weak or insignificant (Harden et al. 2009, Veihe et al. 2011, Henshaw et al. 2013). Erosion across a bank can often be heterogenous and difficult-to-model because of the interaction between flow patterns and complex microtopography, surface topography that changes as erosion proceeds (Papanicolaou et al. 2007, Konsoer et al. 2013, Konsoer et al. 2016). In the case of the MFJDR, given our field observations, we were somewhat surprised that none of the bank toe substrate variables helped explain erosion rates. That is, the bank toe types defined as "highly erodible," those with a high percent of sand in their matrix and/or a high percent of gravels embedded in the matrix, are easily identifiable because these types can be seen to be eroding faster and undercutting the bank above. And in contrast, those types defined as "resistant" (clays) are easily identified by convex bank forms at the bank toe which extends outward into the water rather than being undercut. Nevertheless, neither of these variables, expressed as a percent of the site's bank toe in that type, helped explain erosion rates. We continue to suspect that the distribution of these types is an explanator of erosion patterns, but this result points to the heterogeneity of these lower strata and the sheer complexity of these sites. Along the bank toe, lower strata rise and fall vertically across the bank, reflecting the pattern of ancient gravel bars or clay-accumulating ponding areas, leading to a complex patchwork of alternating substrate types, patterns that could not be adequately captured by the metrics used here.

Bank Top Retreat Rates

In the MFJDR, bank top retreat occurs primarily through cantilever failures as banks are progressively undercut and overhanging banks eventually collapse from their

own weight. Bank retreat would presumably be connected to the erosion rates of the banks being progressively undercut, but on an annual basis this relationship would be expected to be weak given the stochastic nature of mass failures. Indeed, our results show a weak relationship between bank top retreat and bank face erosion rates on an annual basis, but the correlation becomes much stronger when we average bank top retreat and bank face erosion rates over the entire 2-year erosion pin study period. Over the 5-year bank retreat study span, there was no significant difference among years, sites were not significant as a random effect, and an examination of individual site bank retreat rates revealed that the relative bank retreat rates (ranks) among sites shifted each year.

All of these observations point to the stochastic nature of bank retreat driven by mass failures. Mass failures do not necessarily occur when and where bank face erosion is the greatest in a given year but at thresholds where cumulative erosion and undercutting reach a point at which a hanging bank top can no longer support itself. Furthermore, after a segment of bank top has collapsed, it may create a negative feedback, buffering from fluvial erosion the lower portions of the bank where it has fallen (Konsoer et al. 2016). This offers another contributor to the stochastic pattern of bank retreat and the shifting retreat ranks among sites: a site with particularly high bank retreat via mass failures in one year may be less likely to have similarly high rates of collapse the next year. Our observations suggest that, depending on the block's size, it may take 2-4 years for a fallen bank block to be removed by fluvial erosion.

Bank top retreat rates exceeded bank face erosion rates both years, a result that might be attributable to the lost information that often accompanies mass failures. That is, if pins are lost due to excessive erosion in a location associated with mass failure, this would lead to an underestimate of erosion rates. However, most pins associated with mass failures were buried, making it impossible to assess whether they experienced below-average erosion (leading to over-estimates) or excessive erosion (leading to under-estimates). It is also possible that other processes may be contributing to be bank retreat that are not captured by the loss of bank face material measured by the pins. Small mammal burrowing may compromise bank integrity without resulting in erosion of the bank face (deposition was observed instead), but this phenomenon was observed at a minority of sites. In some cases, site-specific stochastic processes contributed to high

bank retreat. For instance, BUTI_N02 experienced a particularly high bank retreat rate in 2015, far in excess of the pin erosion rates. This was attributable to a large area of bank collapsing that had been undermined by a large, bank-burrowing beaver hole (a different phenomenon from the small mammal burrowing described earlier). In another example, BEBU_N01 included an area with subsurface seepage from the floodplain, a weakening process not captured by erosion pins but known to facilitate bank failure (Fox et al. 2007). This area of the site experienced a rare slide collapse in 2015 which is reflected in a higher bank retreat rate relative to bank face erosion rate that year. In most cases, however, we cannot identify a specific process that led to a bank retreat rate higher than the bank face erosion rate.

C. nudata and Bank Erosion Rates

The central question that inspired this investigation was whether banks with *C. nudata* fringes eroded and retreated at a slower or faster rate than banks without *C. nudata* fringes. Given that vegetation can reduce bank erosion and retreat, it was reasonable to assume that *C. nudata* fringes fronting banks could slow erosion, but repeated topographic surveys of full sites with *C. nudata* fringes in an earlier study had revealed that banks with *C. nudata* were continuing to retreat. Our results here show no difference in erosion or retreat rates between banks with *C. nudata* fringes and those without, a counter-intuitive result. In explaining this result, it is important to first point out what this does not tell us. That is, it does not tell us whether banks with *C. nudata* fringes are continuing to erode and retreat at the same rate as they did prior to *C. nudata* establishment. We do not have before/after data. It is possible that areas where *C. nudata* established were experiencing higher erosion rates, and *C. nudata* establishment subsequently slowed these rates. It is also possible that C. nudata establishment increased rates of erosion. We cannot answer the before/after question with these data.

What we can say: banks with *C. nudata* do not currently erode and retreat at a slower rate than banks without *C. nudata*. Why not? Our results exploring seasonal rates and processes have reframed our understanding of bank erosion in the MFJDR. Our results suggest that subaerial processes such as freeze-thaw cycles may be key drivers of the high winter erosion rates, and these subaerial processes are not affected by *C. nudata* patterns. That is, *C. nudata* does not ameliorate exposure given that it is leafless during

winter and it does not offer significant shading in summer given its position and growth habit relative to the bank. Southerly aspect, the only significant variable in our erosion rate models may be a key control of both freeze/thaw cycles and desiccation, and it is also independent of *C. nudata* patterns. Finally, ice dams following rapid ice break up and leading to elevated river stage may be a key driver of high winter erosion rates and are also independent of the *C. nudata* fringe pattern, likely controlled instead by constrictions downstream of the site.

Apart from a new understanding of bank erosion processes in the MFJDR that suggests that several of the key processes driving erosion are independent of *C. nudata* fringes, it is also critical to consider the distinct morphology and ecology of *C. nudata*. Given that *C. nudata* is not rhizomatous and propagates only by water-transported seeds deposited during summer low flows, it does not establish above water's edge and does not colonize the bank face, itself. Therefore, it does not provide any root-strengthening of the bank face or water removal from the bank. Depending on the timing of peak flows, it may or may not present significant roughness elements that reduce flow velocities at the bank face. *C. nudata* leaves senesce during winter such that at peak flows in winter and early spring, these fringes present a relatively smooth ridge-like feature within the channel consisting of a mass of roots and sediment. *C. nudata* begins to leaf out in mid-spring as the initial spring freshet recedes such that a late spring peak flow would encounter more roughness from emerging leaves. The most critical function of *C. nudata* is that its remarkably strong, dense root network stabilizes the substrate where it establishes, the bank toe at the time of establishment. As retreat continues behind the *C. nudata*, a compound channel forms with *C. nudata* stabilizing the boundaries of the low-flow channel, but the bank toe of the banks associated with the bankfull flow are now behind the *C. nudata* fringe and at a higher elevation. We are currently investigating flow patterns relative to *C. nudata* fringes in more detail. The microtopographic features created by *C. nudata*, i.e. within-channel hummocky ridges, may slow velocities at the bank face or alternatively, these features may create turbulence or redirect erosive secondary currents within the space between the *C. nudata* and the bank.

Implications for Stream Evolution in the MFJDR

In a companion study, the first stage of our investigation of the impacts of *C. nudata* in the MFJDR system (Chapter 3), we proposed a conceptual model of stream evolution following the expansion of *C. nudata* in the system. Repeated topographic surveys showed continuing bank erosion behind *C. nudata* fringes, but the relative rate of this erosion was unclear. Aerial imagery chronosequences revealed that *C. nudata* islands typically originate not from midchannel establishment but rather as *C. nudata* fringes at the base of banks that become "detached" from retreating banks. These findings suggested three alternative pathways for reaches with *C. nudata* fringes at bank bases (Fig. 4.13): 1) stable bank following vegetative colonization & aggradation of the space between the *C. nudata* fringe and bank (least common types); 2) compound channel in which the *C. nudata* fringe defines the boundaries of the low flow channel, the banks define the bank full channel dimensions and the space between the *C. nudata* fringe and bank, inundated only at high flows, neither aggrades or degrades significantly (most common type); 3) island formation following high rates of bank retreat and downward erosion of the space between the *C. nudata* fringe and bank.

The results presented here elaborate further upon and deepen this conceptual model. In the present study, all six of the *C. nudata* fringe sites used in the bank erosion and retreat models represented the compound channel type. One site, BUTI_F02, represented an evolving island type and was included in the assessment of seasonal patterns of positive and negative pin readings, but not in the erosion and retreat models. The banks of these compound channel types with *C. nudata* fringe in front of the bank are eroding and retreating at rates no different than simple channels lacking *C. nudata*. This finding reinforces our model of alternative developmental pathways. Throughout the system, bankfull channel boundaries, associated with both simple and compound channel forms, are continuing to move at similar rates. Establishment of *C. nudata* is unlikely to cause channel-narrowing. Instead, the distinctive role of *C. nudata* is the instigation of complex forms via the stabilization of the substrate patches upon which it establishes while the banks behind it continue to retreat at the same rate as neighboring channel segments.

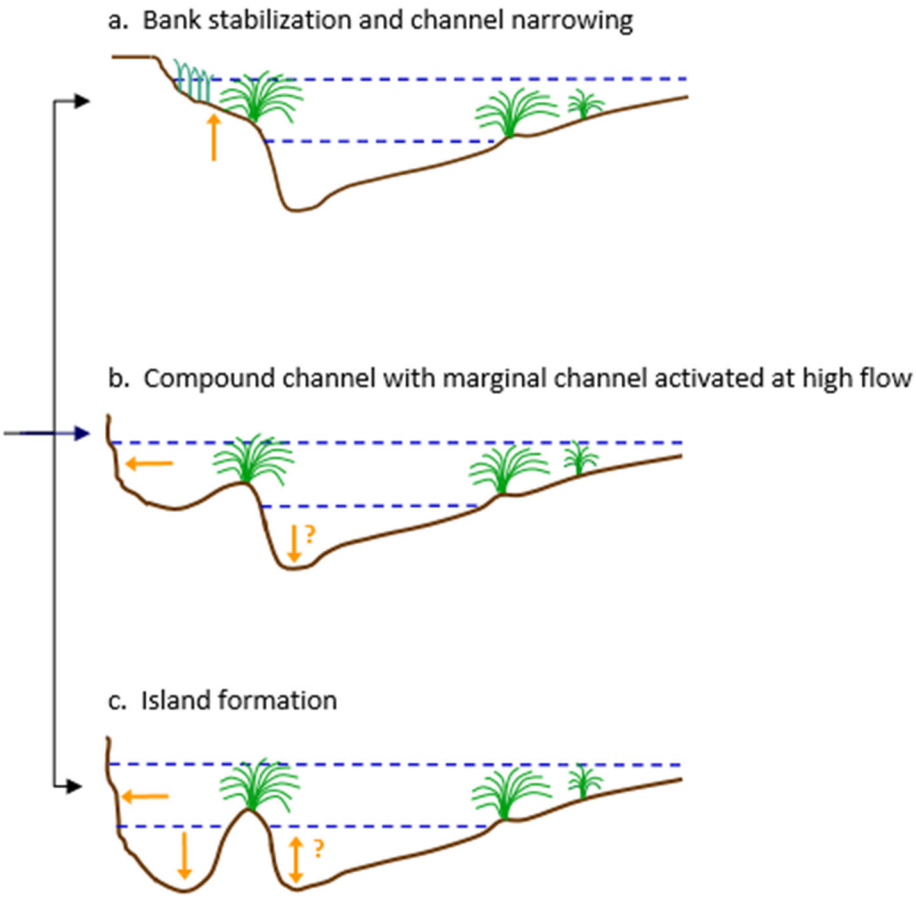

Figure 4.13. Conceptual model: alternative pathways of channel evolution for reaches with *C. nudata* fringes fronting cut banks.

The present study also provided a richer understanding of the system's bank composition and substrate types. Our delineation of bank toe substrate types revealed a diversity of substrate patterns among our sites. Furthermore, as we delineated the bank toe substrate types, it became apparent that *C. nudata* establishment rates differed among these substrate types, a key avenue for further investigation. We did not observe any *C. nudata* established on the clay bank toe types, and rarely did we find *C. nudata* established in the highly erodible types that were typically undercutting at the water surface, leaving no above-water surface for establishment. While we did not determine upon what substrate types the now-mature *C. nudata* originally established, the substrate types found behind the fringes were typically either clay loams, cohesive matrices with 30-70% coarse gravels embedded or clast dominant matrices. The key implication is that

antecedent conditions – heterogenous patterns of bank toe substrate reflecting ancient floodplain deposition patterns – may be a critical driver of *C. nudata* establishment patterns and hence the pathway of channel evolution in each segment of the river.

Conclusions

Our results join a growing set of studies that illustrates the key point that the effects of vegetation on bank erosion processes and overall stability are diverse and should not be generalized (Huang and Nanson 1997, Micheli and Kirchner 2002b, Allmendinger et al. 2005, Luppi et al. 2006, Wynn and Mostaghimi 2006a, Pollen 2007, Hopkinson and Wynn 2009). The diverse effects on vegetation reflect both the diversity of plant forms and life histories and the relative importance of diverse erosion processes in the specific river system within which given plant species occur. In the case of the MFJDR, the relative importance of winter subaerial weakening and erosion processes (and possibly river ice processes) that are not likely affected by *C. nudata* reduces the importance of any *C. nudata* influence on overall bank erosion rates. This outcome is a result of both the system specifics and the plant's traits. That is, in other systems where subaerial weakening and erosion process are important, different sets of plants have indeed been shown to have a significant impact on overall erosion rates because the suite of plants in those systems did affect subaerial processes differentially (Wynn and Mostaghimi 2006b). We also did not find a *C. nudata* effect on spring erosion rates when fluvial erosion is the most important process, a result that also reflects the specifics of *C. nudata*'s phenology and ecology. Nevertheless, given that it is likely that the microtopography created by *C. nudata* does influence flow and erosion patterns at some scale, the question of *C. nudata* microtopography effects on flow pattern remains the biggest question calling for future research. Our study also found examples of unexpected processes (small mammal burrowing, larger bank beaver burrowing) that further complexified bank retreat patterns.

The results reported here also provide support to studies asserting that subaerial processes may contribute to actual erosion in addition to bank weakening (Couper and Maddock 2001, Couper et al. 2002). Lawler (1992) has proposed a conceptual model of bank retreat process domains in which the relative dominance of top-level processes – subaerial weakening, fluvial erosion, mass failure -- changes from headwater to lower

basin reaches. The MFJDR provides a remarkable example of a system in which all top-level processes are active and important, interacting with each other in complex ways that make it difficult to assert the dominance of any one process.

V. CONCLUSION

Findings

Environmental Drivers of C. nudata Distribution

The range-wide species distribution model built on herbarium records used as a first step in this investigation revealed that hydrological variables dwarfed climate variables in their ability to explain *C. nudata* distribution. Building on predicted probabilities from the range-wide species distribution model, we used a stratified random sample design to survey *C. nudata* abundance, channel metrics and other environmental variables at 31 field sampling sites in basins representing two different climates.

Supporting the hypothesis that stream power, a measure of a river's energy and disturbance capacity, drives *C. nudata* distribution, *C. nudata* abundance displayed a threshold relationship with stream power, largely absent in reaches with low stream power and present in reaches above this threshold. Nevertheless, the most significant explanator of *C. nudata* abundance was canopy cover. Above the stream power threshold, *C. nudata* abundance was driven primarily by light availability. *C. nudata* was also associated with coarser stream bed sediment sizes, but sediment size covaried with stream power. At finer scales, our presence/absence plots within the survey sites, *C. nudata* presence was associated with colonizable space (e.g. percent substrate not occupied by competing vegetation). These findings support the conception of a *C. nudata* as a disturbance-adapted species that can tolerate the high energy environment where it establishes and needs open, colonizable substrate. Given that both stream power and light availability vary systematically within basins, *C. nudata* exhibits distinct patterning within basins along a headwater-to-mouth continuum. Furthermore, the systematic patterning of these driving variables interacts with the underlying geology and climate of each basin, leading to differing, but predictable patterning of *C. nudata* within each basin.

Geomorphic Effects and Stream Evolution with C. nudata

Initial topographic surveys of sites with *C. nudata* fringes at the base of cut banks described a compound channel form in which *C. nudata* defines the edge of the low flow channel and the space between the *C. nudata* fringe and bank are inundated at high flows. Surveys also described microtopographic features such as deepened areas in the front of

C. nudata fringes or the upstream edges of islands and an elevated, hummocky topography at channel's edge defined by mature *C. nudata* tussocks. After repeated surveys of these sites, we discovered that banks are continuing to erode behind the *C. nudata* fringes. Other patterns of sedimentation and erosion were relatively minor, but scour across small areas in front of the *C. nudata* fringes was common. We also discovered that *C. nudata* islands most often originate from the movement of channel boundaries relative to stable *C. nudata* patches rather than from initial establishment of plants in midchannel positions. For instance, *C. nudata* fringes may become "detached" from retreating banks leading to island formation. *C. nudata* appears to stabilize the edges of the low flow channel, but cut banks behind *C. nudata* fringes continue to erode and move.

Erosion pin arrays measured seasonally and bank top surveyed at sites with and without *C. nudata* fringes found no difference in bank erosion or bank retreat rates. Winter erosion rates were equal or greater than erosion during the spring seasonal period in which the annual spring snowmelt peak flows typically occur. The high winter erosion rates may be a product of a combination of freeze-thaw cycles, rapid river ice break up and modest peak flows that can, at times, exceed the erosion rates of high spring peak flows alone. The relative importance of winter erosional processes such as freeze-thaw cycles and river ice break up that may be independent of any *C. nudata* alteration of flow and therefore, fluvial erosion, may help explain why erosion rates did not differ between *C. nudata* fringe and non- *C. nudata* sites. After testing a range of variables that might explain erosion rates including river curvature and substrate types, the only significant explanatory variable was bank aspect, a variable associated with thermal subaerial processes such as freeze-thaw cycles and desiccation. Finally, the investigation of bank erosion documented a heterogenous distribution of widely variable substrate types along bank toes, substrates that may differ in erodibility as well as *C. nudata*'s ability to establish in them.

We propose a conceptual model in which alternative pathways of channel development may be possible after the establishment of *C. nudata*.

1) Bank stabilization and channel narrowing where other vegetation colonizes behind the *C. nudata* fringe and the space between the fringe and bank aggrades;
2) Formation of a compound channel in which *C. nudata* stabilizes the edges of the low flow channel, the banks continue to retreat and the space between the fringe and bank neither aggrades or erodes downward.
3) Formation of islands within the channel. This can occur when
    a) banks retreat rapidly and the space between the *C. nudata* fringe and the bank erodes downward
    b) the river cuts behind a *C. nudata* fringe along a gravel on the inside of a bend.

The potential for multiple pathways of development across different river segments makes possible a patchwork of different channel forms, enhancing complexity within a river system. The pathway along which a segment may evolves may depend upon the antecedent conditions (such as bank substrate and curvature) and stochastic factors such as the timing between *C. nudata* establishment and subsequent peak flows.

Future Research

The research presented here points to further questions in need of exploration, questions that fall into two broad categories: 1) addressing unanswered questions relevant to the *C. nudata*-MFJDR system and 2) exploring how these findings may be generalizable to other systems and plant-river interactions, in general.

Unanswered Questions within the MFJDR

Within the *C. nudata*-MFJDR system, the most critical next step is to better understand how *C. nudata* is affecting flow patterns, a question that can be addressed using an Acoustic Doppler Current Profiler (ADCP) during high flows. Understanding how flow patterns are being affected is critical to understanding the patterns of deposition and erosion around *C. nudata* and, in particular, patterns bank erosion relative to *C. nudata* fringes.

Continued long-term repeated surveys of the established sites as well as the opportunistic establishment of new sites is also critical. That is, in the two-year window

between our repeated surveys during which there were modest peak flows, we observed relatively small changes in microtopography, e.g. scouring in front of *C. nudata* fringes, and little deposition across the site relative to bank erosion. And yet, we have observed deeper portions of the stream bed in front of *C. nudata* fringes: when did this deepening occur? We also observe the levee-like features of *C. nudata* tussocks along the edge of the low-flow channel, such that we assume *C. nudata* is enhancing deposition and accumulating, but our change analysis found relatively little deposition. It is possible that some of these processes, e.g. deposition, are occurring at small change rates over broad areas below our estimated error range. It is also possible that some change occurs primarily after larger peak flows. It is also possible that much of the channel adjustment occurs in the early years of *C. nudata* establishment and growth rather than after the *C. nudata* reaches maturity. Therefore, continued surveys over a longer time frame and including higher peak flows is critical as are surveys at new sites where *C. nudata* is newly established, following channel evolution from an earlier stage.

We have postulated a conceptual model with alternative pathways development following *C. nudata* establishment, noted our perception of which pathways seem to be most common and speculated about what underlying substrate patterns or hydrological event timing might lead to one pathway or another. It would be helpful to sample or census a section of the MFJDR, classifying segments according to the pathways to assess their relative importance and attempt to ascertain the drivers of these pathways.

Our basin-wide surveys provided a model for the key drivers of *C. nudata* patterning within basins, but our understanding of *C. nudata* establishment patterns at smaller scales, i.e. within a reach are still lacking. We undertook some seed planting experiments within the MFJDR that were helpful in our understanding of *C. nudata*, but insufficient, in and of themselves, to understand within-reach patterning. We suspect that substrate, microtopography, summer flow patterns (influencing deposition of seeds) and winter/spring erosion patterns (affecting first year mortality) may be critical. Sampling germinants at the end of the summer and 1st and 2nd year seedlings in spring across substrate and geomorphological positions (including position within a bend) could help address the question of reach-level patterning.

Other key questions arise around *C. nudata*'s ecological role within the plant community. Levine (2000a) addressed specific questions regarding *C. nudata*'s role in changing the competitive balance among species and enhancing diversity. A key question that I have often been asked following presentations is whether *C. nudata* is facilitating colonization of other species behind its "leading edge" establishment or on the islands it forms. Anecdotal observations suggest that it may indeed be facilitating colonization, and given that such a positive feedback has important implications, this is also an important question.

Restoration activities in the MFJDR may also provide opportunistic avenues for research. For instance, mangers have been spreading *C. nudata* seed and establishing transplants in an upstream segment of the river where *C. nudata* currently does not occur and which is below the stream power threshold at which it is typically observed. Monitoring these activities could provide a clue as to the importance of dispersion versus limitations due to lack of colonizable space (associated with low stream power) or other limiting environmental factors (e.g. colder temperatures at higher elevations upstream).

Moving beyond the MFJDR

A key question in science is the degree to which findings are generalizable beyond the systems in which they were investigate. To some extent, the pathways of development we document in the MFJDR represent the product of *C. nudata*, a plant with a particular suite of properties, matched to a system – a sinuous, gravel bed river of modest width and energy with cohesive banks and heterogeneous lower strata of coarser material – that make possible these pathways. When sharing these results with outside investigators, a common reaction is the uniqueness of the plant and system. To some extent, a key message of our research may be the need to be careful with generalizations about vegetation and river interactions. Certain plant guilds and systems have received a great deal of attention while many other plant types and systems have not received attention and the outcomes of plant-river interactions may depend on the particularities of a plant's establishment patterns, growth, phenology and morphology. Furthermore, the effects of particular plant types may differ in different systems.

Given that *C. nudata* occurs throughout Oregon and much of California, it would be useful to assess whether other basins similar to the MFJDR exist and whether similar

pathways of development have arisen in these systems. It also seems likely that other sedge species that possess a similar suite of traits as *C. nudata* – i.e. strong-rooted, tussock-forming, non-rhizomatous sedges that establish by seed in mid-summer at the edge of the low flow channel. Do similar plant species exist elsewhere in the U.S. West that play similar geomorphic roles?

Another area of inquiry extending this research is to explore how *C. nudata* affect geomorphic processes in different systems, especially given that *C. nudata* occurs across dramatically different systems. In our basin-wide surveys (Chapter 2), we explored *C. nudata* distribution in the Santiam basin, a context in which *C. nudata* is typically found growing on bedrock and mid-channel boulder bars. *C. nudata* would appear to be a less effective geomorphic change agent in this setting but it is possible that attention to these systems and a different set of questions would reveal a different set of effects. Does *C. nudata* help stabilize mid-channel boulder bars? Does *C. nudata* help weather bedrock forms and facilitate erosion?

C. nudata is particularly abundant in southern Oregon and northern California such that these regions could offer excellent settings for exploring the applicability of our *C. nudata* conceptual models to different systems. On particularly relevant system is the Trinity River, a river where flows have been severely reduced and altered in timing by dams. The Trinity River Restoration Program is now engaged in a significant adaptive management experiment to restore more natural flow regimes (TRRP 2013). There are likely legacy effects of these extended low flows, and concern has been expressed about excessive *C. nudata* colonization, and substrate stabilization in response to this history of low flows (B. Wilson, pers. comm.). How will channel morphology interact with *C. nudata* populations in response to higher environmental flows? Our model may provide a starting point for addressing such questions.

Management Implications

Management implications from our study may fall into three broad areas, implications for passive restoration, active restoration and flow management.

The most striking aspect of this research is the dramatic changes documented in response to *C. nudata*'s expansion with the MFJDR, changes that were not envisioned in restoration planning or engineered via capital-intensive active restoration projects.

Without diminishing the importance or efficacy of active restoration projects, our research demonstrates that passive restoration – i.e. identifying and removing key anthropogenic disturbances in a system, in this case, intensive cattle grazing – can yield a remarkable return relative to a minimum investment of labor and capital. By facilitating the development of microtopography within channel segments and instigating a patchwork of multiple alternative pathways of channel evolution, *C. nudata* is enhancing morphological complexity and resultant habitat at multiple scales. Specific features may be particularly beneficial to salmonids. For instance, deepened, shaded areas at the front of *C. nudata* islands or fringes may be beneficial resting spots for juvenile salmonids in summer. The shallower spaces between the *C. nudata* fringe and bank in the compound channel types may provide slower velocity refuges during high flows. At this point, the benefits of specific features for salmonids is somewhat speculative (and another area for future research), but the development of complexity and habitat diversity, key restoration goals (Beechie and Bolton 1999, Beechie et al. 2008), is clear. While the positive effects of active restoration projects may be localized, e.g. to area immediately around an engineered log jam, the changes induced by passive restoration may be system-wide. Our research illustrates that the role of passive restoration should not be underestimated, but rather considered and assessed explicitly within restoration planning.

Our research also has implications for the implementation of active restoration projects. An emerging critique of active restoration is that such projects often try to reproduce desired patterns in a river system rather than restoring key, natural processes that might give rise to those patterns (Beechie et al. 2010). Some of the active restoration projects recently completed and in progress within the MFJDR illustrate the difference. Recently, a 2 km straightened, dredged channel lined by large clast tailings was replaced by an engineered, sinuous channel about, a needed intervention given that natural processes would be unlikely to transform the dredge channel toward a more natural meandering form. *C. nudata* was also transplanted into this project, typically placed near the edges of gravel bars or sporadically as small midchannel islands. Furthermore, large engineered log jams were placed in front of cut banks to reduce the potential for extreme erosion. Similar placement of ELJs and *C. nudata* has also occurred in other projects that did not include the entire creation of a new channel, i.e. projects that removed rip-rap,

groins etc. What is striking about this approach is the intended aim to reproduce a key *C. nudata* feature, i.e. islands, without considering the process by which these islands evolved. A more process-based approach might transplant the *C. nudata* as a fringe right at the base of a bank, forgo the ELJ and allow areas of bank erosion that could give rise to the islands and compound channel types documented here. There is often a double motivation for ELJ placement: a) enrichment of fish habitat and b) a softer (than riprap) mitigation against bank erosion. Bank erosion is often portrayed as simply a "bad thing" as floodplain land area is lost and erosional sediment input into the river (Florsheim et al. 2008). But as this study illustrates, bank retreat is a fundamental natural process that may give rise to channel forms consistent with restoration goals (Florsheim et al. 2008).

The research here also points toward the importance of environmental flow programs that seek to move dam operations toward a more natural flow regime within their regulatory constraints (Richter et al. 2006). Such programs have been promoted nationally through such initiatives as the Sustainable Rivers Partnership (SRP) between the Nature Conservancy and the Army Corps of Engineers, and several Willamette River tributaries including the Santiam Basin have been included in the SRP initiative (Konrad et al. 2012, Bach et al. 2013, Warner et al. 2014). The planning processes typically includes identifying ecological/geomorphic goals and then evaluating what timing and magnitude of flows might achieve those goals. Key species such as threatened fish (e.g. salmon) are always included in these goals, plants are less often included and those plants that are included in the goal-setting are typically large plants with well-understood hydrological niches such as *Populus* species (Gregory et al. 2007a, b). We do not have a sufficient understanding of the hydrological sequence of events conducive for *C. nudata* establishment to make detailed recommendations. Nevertheless, our research does suggest the importance of a more natural hydrological regime in sustaining *C. nudata* populations. Clearly, high peak flow events capable of creating disturbed, newly colonizable space are critical for *C. nudata* establishment, just as disturbing flows creating colonizable substrate have been shown to be critical for *Populus* and *Salix spp*. However, while *Populus* dispersal and establishment occurs in spring on the recessionary limb following peak flows, *C. nudata* establishes in summer at the lowest flows. Dam operations often maintain higher summer flows than is typical of the natural flow regime,

and our research suggests that this might be problematic for species such as *C. nudata*. While our understanding of *C. nudata*'s establishment patterns relative to hydrological regimes is limited (another avenue for future research) and this implication somewhat speculative, the clear linkages between within-basin hydrological patterns and *C. nudata* patterns do support the importance of environmental flow programs aimed at mimicking more natural flow regimes.

In summary, our findings point to the importance of natural flow regimes, passive restoration as a key strategy in achieving system-wide restoration goals and the restoration of processes in active restoration projects rather than simply reproducing patterns.

APPENDIX A: SUPPLEMENTARY MATERIAL ON CHAPTER 2 METHODS

Sampling Design: Basin-Wide Field Surveys

Selected sites were well-distributed geographically within the Santiam basin, but an examination of selected sites within the John Day basin displays a clustering in the northeast corner of the basin, the Middle and North Forks. This clustering reflects the fact that the Middle and North Forks of the John Day not only include a range of conditions and *C. nudata* predicted likelihoods, but are also the most accessible reaches in the basin, primarily in public ownership (U.S. Forest Service), whereas the upper and middle mainstem reaches of the John Day are predominantly private ranchland, heavily impacted and access-limited. The lower John Day is also primarily in public land (BLM), but much of the river is inaccessible due to extremely limited roads throughout these wild canyonlands. Nevertheless, regardless of the apparent geographic clustering, the final set of sampled sites in the John Day basin was well-representative of the range of climate and hydrological conditions throughout the basin.

In restricting potential survey sites to those without significant anthropogenic effects, I aimed, in particular, to avoid any impacts upon river boundaries (width) and sediment size by road embankments and fill. Due to access considerations, potential survey reaches were often proximate to roads (< 1 km), such that aerial imagery was then used to assess and eliminate reaches immediately bordered and impacted by roads. Nevertheless, we occasionally found evidence of anthropogenic influence while surveying sites (e.g. small patches of rip-rap or other introduced material). To disentangle such anthropogenic impacts, we distinguished naturally occurring and artificially introduced substrate when characterizing substrate.

To simplify site selection, I eliminated from consideration all first order streams. In the John Day basin, pilot surveys suggested that most first order streams are dewatered in the summer. In the Santiam basin, most first order reaches were simply problematic to access. Furthermore, most first order streams had zero predicted probability of *C. nudata.*

Field Survey Design

While the 100 m survey sites were intended to be representative of the reach within which they were located (a reach being defined as the stretch of river between two

tributaries in the NHD Plus), we also wanted to avoid any bias in our positioning of the 100 m site within the reach. To introduce an element of randomness, we aimed to position the starting point of each site as close to our initial entry point to the reach as possible. However, the starting point of each site was often adjusted upstream or downstream to avoid major discontinuities within the 100 m site length that would otherwise lead to the inclusion of distinctly different segments within a single site.

At sites where *C. nudata* was absent along both banks of the river within the100-m sampling transect, we then extended our sampling 100 m in each direction under the premise that *C. nudata* might not be absent from the reach but simply scarce, and a larger sampling distance might yield an appropriate (non-absent) percentage of occurrence representative of the reach. If *C. nudata* was not found in the first set of 100-m extensions, the sampling distance was successively extended until the entire reach had been surveyed. While we followed this protocol to ensure that any reaches with scarce *C. nudata* would not be characterized as absent simply due to the placement of the 100 m sampling site, in practice, all reaches in which *C. nudata* was absent from our initial 100-m survey were found to be lacking in *C. nudata* throughout the entire reach. Therefore, all estimates of non-zero *C. nudata* percent occurrence used in our analyses were derived from the 100-m sampling transects.

When surveying cross sections at each site, cross sections were positioned at the 10, 50 and 90 m points along the 100 m *C. nudata* survey transect that had been designated as our "reference" transect, i.e. the transect on the "shorter" bank of the river, e.g. the inner bend of a meander, and then extended perpendicular across the river. We used a "rapid survey" approach using a laser range finder (Laser Technology Inc., Impulse 200) aimed at a fixed target on a stadia rod to estimate changes in vertical and horizontal distance. Where river depths exceeded the height of the fixed target on the stadia rod (3 sites), we measured river depths manually with an extended stadia rod or with a boat-mounted depth sounder (Hummingbird 120). We made measurements at inflection points in the river bed and surveyed cross sections from bank-to-bank with at least one measurement above what we estimated to be the maximum possible bankfull height of the river. For slope measurements, we measured elevation change with an autolevel and stadia rod and horizontal distance (riffle-to-riffle) with a laser range finder.

While slope was generally estimated using field measurements, in two cases where riffle-to-riffle distances were >1 km and high resolution (1m) digital elevation models were available, I derived slope estimates instead from these high resolution, LIDAR-derived digital elevation models (DOGAMI 2017).

When using a spherical densiometer (a gridded concave mirror) to estimate percent canopy four readings are made in each of the four cardinal directions and then averaged. We tested two different canopy cover metrics: 1) an unweighted average of the four cardinal readings and 2) a weighted average in which the south-facing reading was given more weight (*1.5) and the north-facing reading was given less weight (*.5). Preliminary analyses showed a tighter relationship between *C. nudata* (both abundance and presence/absence) such that the weighted-by-aspect average was chosen as the canopy cover metric in all analyses reported here.

River aspect measured at each sample point (at WE) was the cardinal direction facing away from the bank toward and perpendicular to the water.

In our variation on Wolman (1954) gravel counts, we required a minimum of 50 particle samples along each river bank. In many cases, the standard sampling scheme (.5 m intervals along transects extending 2.5 m into and away from the river and centered at the 10, 30, 50, 70, and 90 m points) did not sample at least 50 particles. That is, sampling points hit bedrock or vegetation which cannot contribute to the total particle count used in estimating median particle size, D_{50}, or other metrics from the particle size distribution. In these cases, additional perpendicular transects were sampled to ensure at least 50 particle samples on each river bank.

In addition to focusing on the substrate potentially available for *C. nudata* colonization near WE, our sampling scheme also yielded data that was comparable across all sites given that some sites were wadeable and suitable for sampling across their entire width while others were too deep to be sampled across their entire width.

While we attempted to avoid sites that had significant anthropogenic inputs, in the few sites where some particles appeared to be anthropogenically-derived, we noted whether particles were natural or artificial in their source and differentiated these in the particle size distribution, generating a particle size distribution that reflected particles of natural origin only.

The 1 m^2 substrate plots were typically positioned along WE and extended away from the water. However, when vegetation exceeded 50% of the plot, obscuring substrate, we instead used two 1-m^2 plots in various arrangements along the WE to ensured that close to 1m^2 of substrate was sampled. In cases with a densely vegetated green line along the WE, two-plot arrangements might consist of two plots centered along the WE such that .5 m of each plot extended into the water. In cases where a single *C. nudata* tussock might centered at the WE, a two-plot arrangement might consist of both plots having an edge along the WE with one extending into the water and the other extending away, thus capturing about .5 m^2 of substrate on both the water and bank side beyond the *C. nudata* tussock edge.

Vegetation plots always had one edge along the WE and always extended away from the WE, thus overlapping the substrate plots in most, but not all, cases.

In our data analysis, we used two metrics of available colonizable space derived from the vegetation plots, **Bare** and **NoVeg**. The two metrics represent two different ways of dealing with the problem of space occupied by only *C. nudata* within a plot. Is it available colonizable space? Not currently, but prior to C. nudata establishment it might be assumed that it was if there is no other vegetation present. **Bare** might be considered a conservative estimate of colonizable space and **NoVeg** a liberal estimate. Bare channel represents the percent of open space outside any vegetation (including *C. nudata*) and is a missing value if *C. nudata* occupies the entire plot. Non-vegetated surface other than *C. nudata*, (**NoVeg**) treats area occupied only by *C. nudata* as "non-vegetated," i.e. not occupied by competing vegetation and therefore, available. Bare and **NoVeg** are identical where no *C. nudata* is present. As *C. nudata* increases, **Bare** becomes increasingly less than **NoVeg** (which remains high if no other species are present).

When a mid-channel bar was found at a site, it was treated as a distinct "bank" if it met the following criteria: > 15 m in length, > 2.5 m in average width and > 5m water between the bar and nearest bank. A *C. nudata* sampling transect was extended along its length, and *C. nudata* presence/absence points, canopy cover, substrate and vegetation plots were also measured at the 10, 50, 90 m marks on the midchannel bar if these points occurred on exposed bar material rather than under water. Given that gravel counts along the mid-channel bar were also required to meet a minimum of 50 particle samples and

given that midchannel bars were typically shorter than the full 100 m site, a denser set of the +/- 2.5 m sampling transects were arranged along mid-channel bars.

We systematically photo documented all sites with photographs taken from each of the 0, 10, 30, 50, 70, 90, 100 m points toward the opposite bank. In addition to documentation, these photographs were critical for estimating channel and vegetative roughness when conducting hydraulic analyses.

Post-Field Data Development: Discharge, Width, Stream Power and Climate

As described in the methods, peak flow estimates for ungaged river locations can be estimated by either 1) nearest-gage based equations (adjusted by catchment area) or 2) regional equations based upon multiple gages and multiple explanatory variables. The nearest-gage equations have much tighter confidence intervals such that their use is recommended when an ungaged location lies on the same river and has a catchment area +/- 50% of the catchment area of the nearest gage (Cooper 2005, Cooper 2006, OWRD 2015, USGS 2016).

While most of our sites do not experience flow alteration by dams, two sites in the lower Santiam basin are below dams that have been in place for 40-50 years. The equations for estimating peak flows from Cooper (2005) represent those for natural flows. Given the length of time these dams have been in place and our aim to model *C. nudata* distribution relative to current conditions, the natural Q_2 flow was deemed inappropriate. Since both sites below dams are proximate to USGS stream gages, we estimated dam-altered Q_2 for each gage by conducting a flood frequency analysis using only post-dam peak flow data with a Log-Pearson Type III distribution following the procedures described by OSU (2002) based upon Bedient and Huber (2002). We then adjusted these post-dam gage Q_2 estimates for each site using the area adjustment coefficients used by Cooper (2005).

River widths associated with the Q_2 flow were determined using our cross-sectional survey data and hydraulic analysis. The hydraulic analysis employed an iterative approach using the continuity equation and the Manning's equation to solve for the cross-sectional area of the Q_2 flow. The width associated with that cross-sectional area can then be derived from the cross-sectional survey data. The continuity equation is represented by

$$Q = Av \qquad \text{or} \qquad v = Q/A \tag{1}$$

where A is cross sectional area and v is velocity. Manning's equation is

$$v = R^{2/3}S^{1/2}/n \quad = \quad (A/p)^{2/3}S^{1/2}/n \tag{2}$$

where R is the stream radius, p is stream perimeter, S is slope and n is a coefficient representing roughness. The roughness coefficient is not straightforward in its determination and is influenced by channel bed substrate, shape and vegetation and the changing the depth of the river. Following the method of Arcement and Schneider (1989), I estimated total roughness additively after estimating the various contributing elements of roughness (channel substrate, shape, vegetation) using gravel count data, field notes and photos. Initial estimates of total roughness were then evaluated, and contributing elements adjusted, following the findings and advised procedures of Coon (1998). Estimated widths were evaluated for reasonableness relative to minimum and maximum possible widths suggested by bankfull indicators noted in the field. Roughness coefficients were adjusted accordingly such that final estimates fell within reasonable ranges. While some subjectivity was introduced by the estimations and adjustments of the roughness variable, all evaluation and adjustments were done systematically and consistently across sites such that final estimates of width were deemed reasonable and congruent.

Statistical Analysis

As discussed in the methods, initial data exploration highlighted several issues with the data including a large number of zeros and non-normal distribution of the response variables (*C. nudata* %), an apparent sigmoidal rather than linear relationship between *C. nudata* and key variables, and a hierarchical data structure with key variables grouped at a higher level (site) than response variables (bank, point). Generalized linear mixed effects models (GLMM) addressed the hierarchical grouping of data and with its logit link offered the potential to model the sigmoidal relationship effectively.

Examination of initial GLMM tests and their residuals suggested that there was some heteroscedasticity in the residuals, largely a reflection of the substantial number of zeros and the association of these zeros with specific ranges of explanatory variables.

Given the persistence of these issues, we experimented with alternative statistical approaches including non-parametric approaches, such as generalized additive models (Wood 2006) and non-parametric multiplicative regression (McCune and Mefford 2004) that rely on smoothing via splined regressions. In general, we found that models with default levels of smoothing did not markedly improve the residual pattern while more localized levels of smoothing yielded spurious patterns that weren't supported by any reasonable process-based explanation. We also experimented with nonlinear regression (Damgaard et al. 2002, Damgaard 2006), but the small improvements in the residual patterns did not seem to justify the additional complexity and limitations of this approach. That is, the profusion of parameters associated with each additional variable caused any models with more than two variables to be problematic. We also considered hurdle models intended for zero-inflated data (Zuur et al. 2009), but concluded that these tests were inappropriate for our data given our hypotheses assumed that the processes driving abundance patterns were the same processes driving zeroes (presence/absence), and initial tests also supported this assumption. Therefore, we deemed the GLMM approach the most satisfactory. While diagnostic tests did indicate issues with the GLMM models, these issues inherit in the data did not seem entirely solvable with any of the alternative approaches, and the GLMM models offered the most tractable solution across various goals.

A limitation of PROC GLIMMIX is that the default Pseudo-Likelihood parameter estimation method does not yield a test statistic that allows ready model comparison; the AIC (Akaike Information Criteria) and BIC (Bayesian Information Criteria) statistics produced by the Pseudo-Likelihood method are not considered valid for comparing models (SAS Institute 2013). The alternative Adaptive Quadrature method for estimating parameters has been recommended by some authors (Bolker et al. 2009), but this method was often unable to converge on a solution in our tests, whereas the Pseudo-Likelihood method was generally effective.

Stream power and all flow variables were log-transformed (base 10) as were all substrate size variables (base 2, mirroring the common phi scale for substrate size). Variables expressed as a percent were not transformed (*C. nudata* abundance, canopy cover, stable substrate).

After preliminary analysis, we removed one site from our analysis as an outlier. *C. nudata* was absent from this site, SA_07 in the Middle Santiam Wilderness, but our models placed it in the environmental space where *C. nudata* would be expected. As the nature of the model became apparent and which variables were driving C. nudata distribution, it was evident that there was likely a barrier to dispersal to this site: aerial imagery showed 11 miles of unsuitable habitat (closed canopy forest) between this site and the nearest suitable habitat for *C. nudata* predicted by our models.

APPENDIX B: SUPPLEMENTARY MATERIAL ON CHAPTER 4 METHODS

Erosion Pin arrays

While pins were arranged with an average inter-column spacing across all sites of 2m, inter-column column spacing ranged from 1.3 at one of the shortest sites to 2.7 at one of the longest sites. While rods were typically 61 cm in length, we also used a small number of 91 cm long pins at locations where we had documented particularly high erosion during the trial year. These lengths were chosen after an initial trial year in which a significant percentage of shorter pins (45 cm) were lost to erosion. Previous studies have advocated for pin lengths that are no longer than necessary given that excessively long pins may disturb bank integrity (Lawler 1993a).

We spray-painted all pins bright blue to reduce rusting, facilitate relocation and bring joy to the first author. After reading many papers in which pins have been painted white, yellow or orange and experimenting with different colors, we recommend blue, it presents a ready contrast with earth-colored banks.

During the fall and end-of-winter measurement events, we "re-set" all pins with increased lengths such that all pins would extend approximately 2 cm beyond the bank face. Re-setting pins was critical in order to mitigate against the phenomenon in which pins extending excessively beyond the bank face can vibrate and/or create turbulence during high flows, enhancing erosion (Lawler 1993a). Pins were then measured again after being re-set.

Bank Top Surveys

Bank top survey coordinates were converted into line feature classes in ArcGIS which were then used to bisect polygons that encompassed the river section in which each study site was located (ESRI 2016). Using this method, we could then calculate the area of floodplain lost after each bank top survey which was then divided by the length of a smoothed bank top line to determine a linear bank top retreat rate.

Site Characteristics

Radius of curvature was calculated using a simplified approach in which the curve is assumed to be derived from a circle using the equation

$$R = 4h^2 + l^2/4h \quad (1)$$

where R is the radius of curvature, h is the chord of the circle, i.e. the straight-line segment bisecting the circle and connecting the upstream and downstream endpoints of the, and l is the rise, i.e. the distance between the chord and the top of the curve.

Prior to surveying and classifying bank toe substrate types, we completed four detailed bank profiles using hand texturing of soils and eye-ball estimates of percentage of course materials in each stratum. Given the time-consuming nature of bank-profiling, we did not complete profiles for all 14 sites, but the profiles facilitated a better understanding of bank structure and heterogeneity among our sites. Furthermore, the profile effort coupled with lab-based hydrometer particle analysis of samples allowed us to better calibrate our hand texture characterization of soils and develop a simplified strategy for characterizing bank substrate.

Weather Data

Records at OCA weather station did not begin until 11/14/2014, somewhat later than our Fall 2014 erosion pin measurement event, but preceding the first significant stretch of below-freezing temperatures and river icing during that winter seasonal period.

Erosion Pin Data Analysis

In our analysis of erosion rates, lost pins (typically buried by mass failures) were treated as missing values unless their loss was due to excessive erosion. In the case of excessive erosion, the pin was assigned a positive change value of 3/4 of the pin length, assuming that erosion to this point would be sufficient for pins to fall out (Harden et al. 2009). Less than 5 pins were lost due to excessive erosion, accounting for <.2% of all pins over the span of the study.

For all non-negative pin readings, an annual erosion rate was determined dividing the difference in pin length by the proportion the year represented by the measurement period.

Statistically, two alternative approaches are possible: 1) pin change rates can be averaged across each site such that the sample unit is average change by site and seasonal measurement period; 2) alternatively, pin change rates can be pooled across all sites and

sites can be modeled as a random effect (i.e. a blocking unit) in a mixed effects model. The former approach has the advantage of no zero values and a normally distributed response variable when log-transformed, but is limited by the small sample size. The latter approach is challenged by the significant number of zero pin change values, but offers a much larger sample size and degrees of freedom. We experimented with both approaches and after assessments of residual plots for issues, we chose to proceed with the latter approach given our desire to test a large number of explanatory variables in addition to the *C. nudata* fringe factors.

APPENDIX C: PAT MCDOWELL AND THE MIDDLE FORK JOHN DAY RIVER

This dissertation represents the last PhD supervised by Pat McDowell, recently retired from the Department of Geography at University of Oregon (UO). It is also a dissertation that would be difficult to imagine without the particular history of experiences Pat built during her career and then contributed to the germination of this work. As such, a special recognition of Pat's work is needed.

While at UO, Pat was widely appreciated for her commitment to teaching and mentoring students. In her teaching, she never stopped trying to improve her courses, exhibiting exceptional creativity even in her later years as a teacher. In particular, her course, Watershed Science and Policy, wove together her experience not only doing research but also her experiences applying that research within collaborative groups.

She excelled at training students, using her research grants not simply as an opportunity to facilitate research but also as an opportunity to train, mentor and build friendships with innumerable students. She was tireless in the field. During long car rides across Oregon and many evenings at camp, she was a joy to talk with for all of us who worked with her. She also always included time for fun, learning field trips, giving back to those who worked for her.

She served on the scientific advisory boards of multiple local watershed councils helping bridge the gap between science and applied river restoration.

Pat began working in the Middle Fork John Day River (MFJDR) in 1996-1997 when she was invited by a group of Oregon State University investigators to join an interdisciplinary research project, "Hydrologic, Geomorphic and Ecological Connectivity in Columbia River Watersheds: Implications for Endangered Salmonids". This work led to a long-term involvement in the MFJDR that allowed her to build long-term relationships within the basin and observe the flow of changes as the basin became a focus of restoration efforts.

From 2008-2017, she returned to participate in the Intensively Monitored Watershed program, awarded annual grants, "Effectiveness monitoring for restoration projects on the Middle Fork John Day River," that allowed her to field crews of student assistants each summer. During this time (2008-2017), she also served on the

Confederated Tribes of the Warm Springs (CTWS) Middle Fork John Day Restoration Interdisciplinary Design Team. Starting in 2008 and continuing to the present, she has been a leading member of the IMW working group. With the CTWS, myself and investigators at OSU, she led an Oregon Watershed Enhancement Board (OWEB) grant, "Long-term ecological effects of passive vs. active restoration in the Middle Fork John Day River" from 2018-2020. She supervised multiple dissertations, theses and senior projects focused on the MFJDR: Steven Jett (M.S. 1998), Jeffery Bandow (M.A. 2003), Stephani Michaelson-Correa (M.S. 2011), Denise Tu (M.S. 2011), Corey Guerrant (B.S. 2014), Jenna Duffin (M.S. 2015), Daniel Baldwin (M.S. 2019). She also served on the committees of James Dietrich (PhD 2014) and Aaron Zettler-Mann (PhD 2019) that included work within the MFJDR.

Even while listing these many research projects and students mentored in the MFJDR, it is difficult to capture the enthusiasm, love and commitment to this particular place that Pat gave. It is this long-term commitment to both understand and contribute to this particular place that has been truly admirable. Furthermore, Pat's enthusiasm extended beyond the river, plants and landscape of this particular place to the people who lived there. Throughout Pat's work, she has naturally built friendships with the people that live and work in the places where she has worked. As students, we were regaled by stories, both fun and thoughtful, of the people and history of these places. In the classes she taught, Pat not only gave students a deeper understanding of river ecosystems and the need to restore these natural systems, she also shared the perspectives of the people who live and work in these landscapes from ranchers to tribal members.

Pat's enthusiasm for the rivers and landscapes where she worked and the people who live in the places she worked will continue in the many students she has mentored. Her collaboration with practitioners and managers who try to apply the lessons learned from her research will hopefully bear fruit as this river continues to evolve with the restoration of natural processes.

REFERENCES

Abernethy, B., and I. D. Rutherfurd. 2001. The distribution and strength of riparian tree roots in relation to riverbank reinforcement. Hydrological Processes **15**:63-79.

Allmendinger, N. E., J. E. Pizzuto, N. Potter, T. E. Johnson, and W. C. Hession. 2005. The influence of riparian vegetation on stream width, eastern Pennsylvania, USA. Geological Society of America Bulletin **117**:229-243.

Anderson, R. J., B. P. Bledsoe, and W. C. Hession. 2004. Width of streams and rivers in response to vegetation, bank material, and other factors. Journal of the American Water Resources Association **40**:1159-1172.

Arcement, G., and V. Schneider. 1989. Guide for selecting Manning's roughness coefficients for natural channels and flood plains. United States Geological Survey.

Auble, G. T., J. M. Friedman, and M. L. Scott. 1994. Relating riparian vegetation to present and future streamflows. Ecological Applications **4**:544-554.

Auble, G. T., M. L. Scott, and J. M. Friedman. 2005. Use of individualistic streamflow-vegetation relations along the Fremont River, Utah, USA to assess impacts of flow alteration on wetland and riparian areas. Wetlands **25**:143-154.

Bach, L., J. Nuckols, and E. Blevis. 2013. Summary report: environmental flows workshop for the Santiam River Basin, Oregon. The Nature Conservancy, Portland, OR.

Bąk, Ł., A. Michalik, and T. Tekielak. 2013. The relationship between bank erosion, local aggradation and sediment transport in a small Carpathian stream. Geomorphology **191**:51-63.

Bedient, P. B., and W. C. Huber. 2002. Hydrology and floodplain analysis. 3rd edition. Prentice-Hall, Inc.

Beechie, T., and S. Bolton. 1999. An approach to restoring salmonid habitat-forming processes in Pacific Northwest watersheds. Fisheries **24**:6-15.

Beechie, T., G. Pess, P. Roni, and G. Giannico. 2008. Setting river restoration priorities: a review of approaches and a general protocol for identifying and prioritizing actions. North American Journal of Fisheries Management **28**:891-905.

Beechie, T. J., D. A. Sear, J. D. Olden, G. R. Pess, J. M. Buffington, H. Moir, P. Roni, and M. M. Pollock. 2010. Process-based principles for restoring river ecosystems. BioScience **60**:209-222.

Beeson, C. E., and P. F. Doyle. 1995. Comparison of bank erosion at vegetated and non-vegetated channel bends. Journal of the American Water Resources Association **31**:983-990.

Bejarano, M. D., A. Sordo-Ward, M. Marchamalo, and M. González del Tánago. 2013. Geomorphological controls on vegetation responses to flow alterations in a Mediterranean stream (central-western Spain). River Research and Applications **29**:1237-1252.

Bendix, J. 1994. Among-site variation in riparian vegetation of the southern California Transverse Ranges. American Midland Naturalist **132**:136.

Bendix, J. 1997. Flood disturbance and the distribution of riparian species diversity. Geographical Review **87**:468-483.

Bendix, J. 1999. Stream power influence on southern Californian riparian vegetation. Journal of Vegetation Science **10**:243-252.

Bendix, J., and J. C. Stella. 2013. 12.5 Riparian vegetation and the fluvial environment: a biogeographic perspective.

Bennett, S. J., T. Pirim, and B. D. Barkdoll. 2002. Using simulated emergent vegetation to alter stream flow direction within a straight experimental channel. Geomorphology **44**:115-126.

Birken, A. S., and D. J. Cooper. 2006. Processes of tamarix invasion and floodplain development along the lower Green River, Utah. Ecological Applications **16**:1103-1120.

Blanckaert, K., A. Duarte, Q. Chen, and A. J. Schleiss. 2012. Flow processes near smooth and rough (concave) outer banks in curved open channels. Journal of Geophysical Research: Earth Surface (2003–2012) **117**.

Bolker, B. M., M. E. Brooks, C. J. Clark, S. W. Geange, J. R. Poulsen, M. H. H. Stevens, and J.-S. S. White. 2009. Generalized linear mixed models: a practical guide for ecology and evolution. Trends in Ecology & Evolution **24**:127-135.

Brummer, C. J., and D. R. Montgomery. 2003. Downstream coarsening in headwater channels. Water Resources Research **39**:1294.

Carson, M. A., and M. J. Kirkby. 1972. Hillslope form and process. Press, Cambridge, UK.

Clark, L. A., and T. M. Wynn. 2007. Methods for determining streambank critical shear stress and soil erodibility: Implications for erosion rate predictions. Transactions of the ASABE **50**:95-106.

Clary, W. P. 1999. Stream channel and vegetation responses to late spring cattle grazing. Journal of Range Management:218-227.

Coon, W. F. 1998. Estimation of roughness coefficients for natural stream channels with vegetated banks. 060788701X, US Geological Survey.

Cooper, R. M. 2005. Estimation of peak discharges for rural, unregulated streams in Western Oregon. US Department of the Interior, US Geological Survey, Reston, VA.

Cooper, R. M. 2006. Estimation of peak discharges for rural, unregulated streams in eastern Oregon: Oregon Water Resources Department Open-File Report SW 02-002. Salem, Oregon.

Corenblit, D., J. Steiger, E. González, A. M. Gurnell, G. Charrier, J. Darrozes, J. Dousseau, F. Julien, L. Lambs, and S. Larrue. 2014. The biogeomorphological life cycle of poplars during the fluvial biogeomorphological succession: a special focus on Populus nigra L. Earth Surface Processes and Landforms **39**:546-563.

Corenblit, D., J. Steiger, A. M. Gurnell, E. Tabacchi, and L. Roques. 2009. Control of sediment dynamics by vegetation as a key function driving biogeomorphic succession within fluvial corridors. Earth Surface Processes and Landforms **34**:1790-1810.

Corenblit, D., E. Tabacchi, J. Steiger, and A. M. Gurnell. 2007. Reciprocal interactions and adjustments between fluvial landforms and vegetation dynamics in river corridors: a review of complementary approaches. Earth-Science Reviews **84**:56-86.

Costa, J. E. 1983. Paleohydraulic reconstruction of flash-flood peaks from boulder deposits in the Colorado Front Range. Geological Society of America Bulletin **94**:986-1004.

Costard, F., L. Dupeyrat, E. Gautier, and E. Carey-Gailhardis. 2003. Fluvial thermal erosion investigations along a rapidly eroding river bank: application to the Lena River (central Siberia). Earth Surface Processes and Landforms **28**:1349-1359.

Couper, P. 2003. Effects of silt–clay content on the susceptibility of river banks to subaerial erosion. Geomorphology **56**:95-108.

Couper, P., T. I. M. Stott, and I. A. N. Maddock. 2002. Insights into river bank erosion processes derived from analysis of negative erosion-pin recordings: observations from three recent UK studies. Earth surface processes and landforms: the journal of the British Geomorphological Research Group **27**:59-79.

Couper, P. R., and I. P. Maddock. 2001. Subaerial river bank erosion processes and their interaction with other bank erosion mechanisms on the River Arrow, Warwickshire, UK. Earth Surface Processes and Landforms **26**:631-646.

Curran, J. C., and W. C. Hession. 2013. Vegetative impacts on hydraulics and sediment processes across the fluvial system. Journal of Hydrology **505**:364-376.

Damgaard, C. 2006. Modelling ecological presence–absence data along an environmental gradient: threshold levels of the environment. Environmental and Ecological Statistics **13**:229-236.

Damgaard, C., R. Hojer, M. Bayley, J. J. Scott-Fordsmand, and M. Holmstrup. 2002. Dose-response curve modeling of excess mortality caused by two forms of stress. Environmental and Ecological Statistics **9**:195-200.

DeVries, P. 2012. Salmonid influences on rivers: a geomorphic fish tail. Geomorphology **157–158**:66-74.

Dietrich, J. T. 2016. Riverscape mapping with helicopter-based Structure-from-Motion photogrammetry. Geomorphology **252**:144-157.

Dixon, M. D., M. G. Turner, and C. Jin. 2002. Riparian tree seedling distribution on Wisconsin river sandbars: controls at different spatial scales. Ecological Monographs **72**:465-485.

DOGAMI. 2017. Lidar. State of Oregon Department of Geology and Mineral Industries.

Eaton, B. C. 2013. Hydraulic geometry: empirical investigations and theoretical approaches. Pages 313-329 Treatise on Geomorphology, Fluvial Geomorphology.

Edwards, P. J., J. Kollmann, A. M. Gurnell, G. E. Petts, K. Tockner, and J. V. Ward. 1999. A conceptual model of vegetation dynamics on gravel bars of a large Alpine river. Wetlands Ecology and Management **7**:141-153.

Engelhardt, B. M., P. J. Weisberg, J. C. Chambers, and M. Huston. 2012. Influences of watershed geomorphology on extent and composition of riparian vegetation. Journal of Vegetation Science **23**:127-139.

EPA. 2010. Level III Ecoregions of North America. U. S. Environmental Protection Agency

ESRI. 2016. ArcGIS Desktop: Release 10.5. Environmental Systems Research Institute, Redlands, CA.

Evans, R., K. Gaffney, K. Gledhill, C. Dean, and G. Fisher. 2003. Riparian habitat restoration.*in* G. Flosi, S. Downie, J. Hopelain, M. Bird, R. Coey, and B. Collins, editors. California salmonid stream habitat restoration manual. California Dept. of Fish and Game, Sacramento, CA.

Fenner, P., W. W. Brady, and D. R. Patton. 1985. Effects of regulated water flows on regeneration of Fremont cottonwood. Journal of Range Management:135-138.

Ferrick, M. G., L. W. Gatto, and S. A. Grant. 2005. Soil freeze-thaw effects on bank erosion and stability: Connecticut river field site, Norfolk, Vermont. Cold Regions Research and Engineering Laboratory (US).

Fiala, A. C., S. L. Garman, and A. N. Gray. 2006. Comparison of five canopy cover estimation techniques in the western Oregon Cascades. Forest Ecology and Management **232**:188-197.

Florsheim, J. L., J. F. Mount, and A. Chin. 2008. Bank erosion as a desirable attribute of rivers. BioScience **58**:519-529.

Fonstad, M. A. 2003. Spatial variation in the power of mountain streams in the Sangre de Cristo Mountains, New Mexico. Geomorphology **55**:75-96.

Fox, G. A., G. V. Wilson, A. Simon, E. J. Langendoen, O. Akay, and J. W. Fuchs. 2007. Measuring streambank erosion due to ground water seepage: correlation to bank pore water pressure, precipitation and stream stage. Earth Surface Processes and Landforms **32**:1558-1573.

Franklin, J. 2010. Mapping species distributions: spatial inference and prediction. Cambridge University Press.

Franklin, P., M. Dunbar, and P. Whitehead. 2008. Flow controls on lowland river macrophytes: a review. Science of the Total Environment **400**:369-378.

Friedman, J. M., G. T. Auble, E. D. Andrews, G. Kittel, R. F. Madole, E. R. Griffin, and T. M. Allred. 2006. Transverse and longitudinal variation in woody riparian vegetation along a montane river. Western North American Naturalist **66**:78-91.

Gatto, L. W. 1995. Soil freeze-thaw effects on bank erodibility and stability. Cold Regions Research and Engineering Laboratory.

Gatto, L. W., J. J. Halvorson, D. K. McCool, and A. J. Palazzo. 2001. Effects of freeze-thaw cycling on soil erosion. Pages 29-55 Landscape erosion and evolution modeling. Springer.

Gee, G. W., and D. Or. 2002. 2.4 Particle-size analysis. Methods of soil analysis. Part **4**:255-293.

Goslin, M. in prep-a. Germination and survival patterns of a native riparian sedge, *Carex nudata*, relative to substrate classes and light availability.

Goslin, M. in prep-b. Range-wide species distribution model of the riparian sedge, *Carex nudata*, driven by hydrological variables.

Graf, W. L. 1983. Variability of sediment removal in a semiarid watershed. Water Resources Research **19**:643-652.

Gran, K., and C. Paola. 2001. Riparian vegetation controls on braided stream dynamics. Water Resources Research **37**:3275-3283.

Green, D. M., and J. B. Kauffman. 1995. Succession and livestock grazing in a northeastern Oregon riparian ecosystem. Journal of Range Management **48**:307.

Gregory, S. V., L. Ashkenas, and C. Nygaard. 2007a. Environmental flows workshop for the Middle Fork and Coast Fork of the Willamette River, Oregon. Technical Report, Institute for Water and Watersheds, Oregon State University.

Gregory, S. V., L. Ashkenas, and C. Nygaard. 2007b. Summary report to assist development of ecosystem flow recommendations for the Coast Fork and Middle Fork of the Willamette River. Technical Report, Institute for Water and Watersheds, Oregon State University.

Guisan, A., and N. E. Zimmermann. 2000. Predictive habitat distribution models in ecology. Ecological Modelling **135**:147-186.

Gurnell, A., D. Corenblit, D. García de Jalón, M. González del Tánago, R. Grabowski, M. O'Hare, and M. Szewczyk. 2016. A conceptual model of vegetation–hydrogeomorphology interactions within river corridors. River Research and Applications **32**:142-163.

Gurnell, A., and G. Petts. 2006. Trees as riparian engineers: the Tagliamento river, Italy. Earth Surface Processes and Landforms **31**:1558-1574.

Gurnell, A. M., W. Bertoldi, and D. Corenblit. 2012. Changing river channels: The roles of hydrological processes, plants and pioneer fluvial landforms in humid temperate, mixed load, gravel bed rivers. Earth-Science Reviews **111**:129-141.

Gurnell, A. M., J. M. O'Hare, M. T. O'Hare, M. J. Dunbar, and P. M. Scarlett. 2010. An exploration of associations between assemblages of aquatic plant morphotypes and channel geomorphological properties within British rivers. Geomorphology **116**:135-144.

Gurnell, A. M., G. E. Petts, D. M. Hannah, B. P. G. Smith, P. J. Edwards, J. Kollmann, J. V. Ward, and K. Tockner. 2001. Riparian vegetation and island formation along the gravel-bed Fiume Tagliamento, Italy. Earth Surface Processes and Landforms **26**:31-62.

Gurnell, A. M., M. P. Van Oosterhout, B. De Vlieger, and J. M. Goodson. 2006. Reach-scale interactions between aquatic plants and physical habitat: River Frome, Dorset. River Research and Applications **22**:667-680.

Gutiérrez, J. L., C. G. Jones, D. L. Strayer, and O. O. Iribarne. 2003. Mollusks as ecosystem engineers: the role of shell production in aquatic habitats. Oikos **101**:79-90.

Harden, C. P., W. Foster, C. Morris, K. J. Chartrand, and E. Henry. 2009. Rates and processes of streambank erosion in tributaries of the Little River, Tennessee. Physical Geography **30**:1-16.

Hassan, M. A., A. S. Gottesfeld, D. R. Montgomery, J. F. Tunnicliffe, G. K. C. Clarke, G. Wynn, H. Jones-Cox, R. Poirier, E. MacIsaac, H. Herunter, and S. J. Macdonald. 2008. Salmon-driven bed load transport and bed morphology in mountain streams. Geophysical Research Letters **35**:L04405.

Hassan, M. A., E. L. Petticrew, D. R. Montgomery, A. S. Gottesfeld, and J. F. Rex. 2011. Salmon as biogeomorphic agents in gravel bed rivers: the effect of fish on sediment mobility and spawning habitat. Stream Restoration in Dynamic Fluvial Systems:337-352.

Hastie, T., and W. Fithian. 2013. Inference from presence-only data; the ongoing controversy. Ecography **36**:864-867.

Henshaw, A. J., C. R. Thorne, and N. J. Clifford. 2013. Identifying causes and controls of river bank erosion in a British upland catchment. CATENA **100**:107-119.

Hicks, D. M., M. J. Duncan, S. N. Lane, M. Tal, and R. Westaway. 2007. 21 Contemporary morphological change in braided gravel-bed rivers: new developments from field and laboratory studies, with particular reference to the influence of riparian vegetation. Pages 557-584 *in* H. P. Helmut Habersack and R. Massimo, editors. Developments in Earth Surface Processes. Elsevier.

Hood, G. A., and D. G. Larson. 2015. Ecological engineering and aquatic connectivity: a new perspective from beaver-modified wetlands. Freshwater Biology **60**:198-208.

Hopkinson, L., and T. Wynn. 2009. Vegetation impacts on near bank flow. Ecohydrology **2**:404-418.

Hough-Snee, N., B. B. Roper, J. M. Wheaton, P. Budy, and R. L. Lokteff. 2013. Riparian vegetation communities change rapidly following passive restoration at a northern Utah stream. Ecological Engineering **58**:371-377.

Huang, H. Q., and G. C. Nanson. 1997. Vegetation and channel variation; a case study of four small streams in southeastern Australia. Geomorphology **18**:237-249.

Huang, H. Q., and G. C. Nanson. 1998. The influence of bank strength on channel geometry: an integrated analysis of some observations. Earth Surface Processes and Landforms: The Journal of the British Geomorphological Group **23**:865-876.

Hughes, F. M. R. 1997. Floodplain biogeomorphology. Progress in Physical Geography **21**:501-529.

Inamdar, S., E. Johnson, R. Rowland, D. Warner, R. Walter, and D. Merritts. 2018. Freeze–thaw processes and intense rainfall: the one-two punch for high sediment and nutrient loads from mid-Atlantic watersheds. Biogeochemistry **141**:333-349.

Ishikawa, Y., T. Sakamoto, and K. Mizuhara. 2003. Effect of density of riparian vegetation on effective tractive force. Journal of Forest Research **8**:235-246.

Johnson, M. F., I. Reid, S. P. Rice, and P. J. Wood. 2009. Stabilization of fine gravels by net-spinning caddisfly larvae. Earth Surface Processes and Landforms **34**:413-423.

Jones, C. G., J. H. Lawton, and M. Shachak. 1994. Organisms as ecosystem engineers. Oikos **69**:373-386.

Kamada, M. 2008. Process of willow community establishment and topographic change of riverbed in a warm-temperate region of Japan. Pages 177-190 *in* H. Sakio and T. Tamura, editors. Ecology of Riparian Forests in Japan. Springer Japan.

Kauffman, J. B., R. L. Beschta, N. Otting, and D. Lytjen. 1997. An ecological perspective of riparian and stream restoration in the western United States. Fisheries **22**:12-24.

Kauffman, J. B., W. Krueger, and M. Vavra. 1983a. Impacts of cattle on streambanks in northeastern Oregon. Journal of Range Management:683-685.

Kauffman, J. B., and W. C. Krueger. 1984. Livestock impacts on riparian ecosystems and streamside management implications: a review. Journal of Range Management **37**:430-438.

Kauffman, J. B., W. C. Krueger, and M. Vavra. 1983b. Effects of late season cattle grazing on riparian plant communities. Journal of Range Management:685-691.

Knighton, A. D. 1999. Downstream variation in stream power. Geomorphology **29**:293-306.

Konrad, C. P., A. Warner, and J. V. Higgins. 2012. Evaluating dam re-operation for freshwater conservation in the Sustainable Rivers Project. River Research and Applications **28**:777-792.

Konsoer, K. 2014. Influence of riparian vegetation on near-bank flow structure and rates of erosion on a large meandering river. University of Illinois at Urbana-Champaign.

Konsoer, K. M., B. L. Rhoads, J. Best, E. J. Langendoen, M. Ursic, J. D. Abad, and M. H. Garcia. 2013. Scales of form roughness on riverbanks with different riparian vegetation. Page 0864.

Konsoer, K. M., B. L. Rhoads, E. J. Langendoen, J. L. Best, M. E. Ursic, J. D. Abad, and M. H. Garcia. 2016. Spatial variability in bank resistance to erosion on a large meandering, mixed bedrock-alluvial river. Geomorphology **252**:80-97.

Laubel, A., B. Kronvang, A. B. Hald, and C. Jensen. 2003. Hydromorphological and biological factors influencing sediment and phosphorus loss via bank erosion in small lowland rural streams in Denmark. Hydrological Processes **17**:3443-3463.

Lawler, D. 1995. The impact of scale on the processes of channel-side sediment supply: a conceptual model. IAHS Publications-Series of Proceedings and Reports-Intern Assoc Hydrological Sciences **226**:175-186.

Lawler, D. M. 1986. River bank erosion and the influence of frost: a statistcal examination. Transactions of the Institute of British Geographers:227-242.

Lawler, D. M. 1992. Process dominance in bank erosion systems. Pages 117-143 Lowland floodplain rivers: geomorphological perspectives.

Lawler, D. M. 1993a. The measurement of river bank erosion and lateral channel change: a review. Earth Surface Processes and Landforms **18**:777-821.

Lawler, D. M. 1993b. Needle ice processes and sediment mobilization on river banks: the River Ilston, West Glamorgan, UK. Journal of Hydrology **150**:81-114.

Lawler, D. M., C. R. Thorne, and J. M. Hooke. 1997. Bank erosion and instability processes. Pages 137-172 *in* C. R. Thorne, R. D. Hey, and M. D. Newson, editors. Applied fluvial geomorphology for river engineering and management. John Wiley & Sons, Ltd.

Lecce, S. A. 2013. Stream power, channel change, and channel geometry in the Blue River, Wisconsin. Physical Geography **34**:293-314.

Levine, J. M. 1999. Indirect facilitation: evidence and predictions from a riparian community. Ecology **80**:1762-1769.

Levine, J. M. 2000a. Complex interactions in a streamside plant community. Ecology **81**:3431-3444.

Levine, J. M. 2000b. Species diversity and biological invasions: relating local process to community pattern. Science **288**:852-854.

Levine, J. M. 2001. Local interactions, dispersal, and native and exotic plant diversity along a California stream. Oikos **95**:397-408.

Levine, J. M. 2003. A patch modeling approach to the community-level consequences of directional dispersal. Ecology **84**:1215-1224.

Liffen, T., A. M. Gurnell, M. T. O'Hare, N. Pollen-Bankhead, and A. Simon. 2013. Associations between the morphology and biomechanical properties of Sparganium erectum: Implications for survival and ecosystem engineering. Aquatic Botany **105**:18-24.

Luppi, L., L. Coppi, and M. Rinaldi. 2006. River bank erosion processes interaction and effects of riparian vegetation. Page 01799.

Magilligan, F. J. 1992. Thresholds and the spatial variability of flood power during extreme floods. Geomorphology **5**:373-390.

Magilligan, F. J., and P. F. McDowell. 1997. Stream channel adjustments following elimination of cattle grazing. Journal of the American Water Resources Association **33**:867-878.

Mahoney, J. M., and S. B. Rood. 1998. Streamflow requirements for cottonwood seedling recruitment—an integrative model. Wetlands **18**:634-645.

McCune, B., and M. Mefford. 2004. Hyperniche: nonparametric multiplicative habitat modeling. MjM Software, Gleneden Beach, OR.

McDowell, P. F. 2001. Spatial variations in channel morphology at segment and reach scales, Middle Fork John Day River, Northeastern Oregon. Geomorphic processes and riverine habitat:159-172.

McDowell, P. F. 2011. Sedge (*Carex nudata*) as a mediator of river channel change in response to grazing reduction and a large flood. Pages EP31G-06 *in* AGU Fall Meeting, San Francisco, CA.

McDowell, P. F., and M. Goslin. 2015. Comparing effects of active and passive restoration on the Middle Fork John Day River, northeast Oregon. Pages EP41E-05 *in* AGU Fall Meeting, San Francisco, CA.

McKay, L., T. Bondelid, T. Dewald, J. Johnston, R. Moore, and A. Rea. 2012. NHDPlus Version 2: User Guide. U. S. Environmental Protection Agency.

Merow, C., M. J. Smith, and J. A. Silander. 2013. A practical guide to MaxEnt for modeling species' distributions: what it does, and why inputs and settings matter. Ecography **36**:1058-1069.

Merritt, D. M., M. L. Scott, N. LeRoy Poff, G. T. Auble, and D. A. Lytle. 2010. Theory, methods and tools for determining environmental flows for riparian vegetation: riparian vegetation-flow response guilds. Freshwater Biology **55**:206-225.

Merritt, D. M., and E. E. Wohl. 2002. Processes governing hydrochory along rivers: hydraulics, hydrology, and dispersal phenology. Ecological Applications **12**:1071-1087.

Micheli, E. R., and J. W. Kirchner. 2002a. Effects of wet meadow riparian vegetation on streambank erosion. 1. Remote sensing measurements of streambank migration and erodibility. Earth Surface Processes and Landforms **27**:627-639.

Micheli, E. R., and J. W. Kirchner. 2002b. Effects of wet meadow riparian vegetation on streambank erosion. 2. Measurements of vegetated bank strength and consequences for failure mechanics. Earth surface processes and landforms: the journal of the British Geomorphological Research Group **27**:687-697.

Milan, D. J., G. L. Heritage, A. R. Large, and I. C. Fuller. 2011. Filtering spatial error from DEMs: implications for morphological change estimation. Geomorphology **125**:160-171.

Millar, R. G. 2000. Influence of bank vegetation on alluvial channel patterns. Water Resources Research **36**:1109-1118.

Mosner, E., S. Schneider, B. Lehmann, and I. Leyer. 2011. Hydrological prerequisites for optimum habitats of riparian *Salix* communities–identifying suitable reforestation sites. Applied Vegetation Science **14**:367-377.

Nanson, G. C., and E. J. Hickin. 1986. A statistical analysis of bank erosion and channel migration in western Canada. Geological Society of America Bulletin **97**:497-504.

NAPP. 1989. National Aerial Photography Program.

NAPP. 2001. National Aerial Photography Program.

Neff, K. P., and A. H. Baldwin. 2005. Seed dispersal into wetlands: techniques and results for a restored tidal freshwater marsh. Wetlands **25**:392-404.

NFJDWC. 2021. North Fork John Day Watershed Council. https://www.nfjdwc.org/

Nilsson, C., R. L. Brown, R. Jansson, and D. M. Merritt. 2010. The role of hydrochory in structuring riparian and wetland vegetation. Biological Reviews **85**:837-858.

Nilsson, C., and M. Svedmark. 2002. Basic principles and ecological consequences of changing water regimes: riparian plant communities. Environmental Management **30**:468-480.

O'Hare, J. M., M. T. O'Hare, A. M. Gurnell, M. J. Dunbar, P. M. Scarlett, and C. Laizé. 2011. Physical constraints on the distribution of macrophytes linked with flow and sediment dynamics in British rivers. River Research and Applications **27**:671-683.

O'Hare, M. T., J. O. Mountford, J. Maroto, and I. D. M. Gunn. 2016. Plant traits relevant to fluvial geomorphology and hydrological interactions. River Research and Applications **32**:179-189.

Omernik, J. M., and G. E. Griffith. 2014. Ecoregions of the conterminous United States: evolution of a hierarchical spatial framework. Environmental Management **54**:1249-1266.

Osterkamp, W. R., and C. R. Hupp. 1984. Geomorphic and vegetative characteristics along three northern Virginia streams. Geological Society of America Bulletin **95**:1093-1101.

OSU. 2002. Analysis Techniques: Flood Frequency Analysis. http://streamflow.engr.oregonstate.edu/analysis/floodfreq

OWRD. 1986. John Day River Basin. Oregon Water Resources Department, Salem, OR.

OWRD. 2015. Peak discharge estimation mapping tool. http://apps.wrd.state.or.us/apps/sw/peak_discharge_map/

Palmer, M. A., E. S. Bernhardt, J. D. Allan, P. S. Lake, G. Alexander, S. Brooks, J. Carr, S. Clayton, C. N. Dahm, J. F. Shah, D. L. Galat, S. G. Loss, P. Goodwin, D. D. Hart, B. Hassett, R. Jenkinson, G. M. Kondolf, R. Lave, J. L. Meyer, T. K. O'Donnell, L. Pagano, and E. Sudduth. 2005. Standards for ecologically successful river restoration. Journal of Applied Ecology **42**:208-217.

Papanicolaou, A. N., M. Elhakeem, and R. Hilldale. 2007. Secondary current effects on cohesive river bank erosion. Water Resources Research **43**.

Peterson, T. A., M. Papeş, and M. Eaton. 2007. Transferability and model evaluation in ecological niche modeling: a comparison of GARP and Maxent. Ecography **30**:550-560.

Phillips, S. J., M. Dudík, and R. E. Schapire. 2004. A maximum entropy approach to species distribution modeling. Page 83 *in* Proceedings of the twenty-first international conference on Machine learning. ACM.

Pinheiro, J., D. Bates, D. Saikat, D. Sarkar, and R. C. Team. 2021. nlme: linear and nonlinear mixed effects models. R package version 3.1-152.

Platts, W. S., and R. L. Nelson. 1989. Characteristics of riparian plant communities and streambanks with respect to grazing in northeastern Utah. Pages 73-81 *in* Practical approaches to riparian resource management—an educational workshop. US Forest Serv. Gen. Tech. Rpt. Int-263. Billings, MT.

PNAMP. 2021. Intensively Monitored Watersheds Overview. https://www.pnamp.org/imw/overview

Pollen, N. 2007. Temporal and spatial variability in root reinforcement of streambanks: Accounting for soil shear strength and moisture. CATENA **69**:197-205.

PRISM, C. G. 2015. Spatial climate datasets for the conterminous United States. Oregon State University.

Rhoads, B. L. 1987. Stream power terminology. The Professional Geographer **39**:189-195.

Rice, S., and M. Church. 1998. Grain size along two gravel-bed rivers: statistical variation, spatial pattern and sedimentary links. Earth Surface Processes and Landforms **23**:345-363.

Richards, K. S., and N. R. Lorriman. 1987. Basal erosion and mass movement. Pages 331-357 Slope stability: geotechnical engineering and geomorphology. John Wiley and Sons New York. NY.

Richter, B. D., A. T. Warner, J. L. Meyer, and K. Lutz. 2006. A collaborative and adaptive process for developing environmental flow recommendations. River Research and Applications **22**:297-318.

Riis, T., and B. J. Biggs. 2001. Distribution of macrophytes in New Zealand streams and lakes in relation to disturbance frequency and resource supply—a synthesis and conceptual model. New Zealand Journal of Marine and Freshwater Research **35**:255-267.

Riis, T., and B. J. Biggs. 2003. Hydrologic and hydraulic control of macrophyte establishment and performance in streams. Limnology and Oceanography **48**:1488-1497.

Riis, T., A. M. Suren, B. Clausen, and K. Sand-Jensen. 2008. Vegetation and flow regime in lowland streams. Freshwater Biology **53**:1531-1543.

Rinaldi, M., and S. E. Darby. 2007. 9 Modelling river-bank-erosion processes and mass failure mechanisms: progress towards fully coupled simulations. Developments in Earth Surface Processes **11**:213-239.

Risley, J., A. Stonewall, and T. Haluska. 2008. Estimating flow-duration and low-flow frequency statistics for unregulated streams in Oregon. Geological Survey (US).

Risley, J., J. R. Wallick, J. F. Mangano, and K. F. Jones. 2012. An environmental streamflow assessment for the Santiam River basin, Oregon. Open-File Report 2012-1133, U.S. Geological Survey.

Robertson, K. M. 2006. Distributions of tree species along point bars of 10 rivers in the south-eastern US Coastal Plain. Journal of Biogeography **33**:121-132.

Rodrigues, S., J. G. Bréhéret, J. J. Macaire, S. Greulich, and M. Villar. 2007. In-channel woody vegetation controls on sedimentary processes and the sedimentary record within alluvial environments: a modern example of an anabranch of the River Loire, France. Sedimentology **54**:223-242.

Rodrigues, S., J. G. Bréhéret, J. J. Macaire, F. Moatar, D. Nistoran, and P. Jugé. 2006. Flow and sediment dynamics in the vegetated secondary channels of an anabranching river: The Loire River (France). Sedimentary Geology **186**:89-109.

Roni, P., K. Hanson, and T. Beechie. 2008. Global review of the physical and biological effectiveness of stream habitat rehabilitation techniques. North American Journal of Fisheries Management **28**:856-890.

Royle, J. A., R. B. Chandler, C. Yackulic, and J. D. Nichols. 2012. Likelihood analysis of species occurrence probability from presence-only data for modelling species distributions. Methods in Ecology and Evolution **3**:545-554.

SAS Institute, I. 2013. SAS/STAT® 12.3 User's Guide. SAS Institute Inc., Cary, NC.

Schnauder, I., and H. L. Moggridge. 2009. Vegetation and hydraulic-morphological interactions at the individual plant, patch and channel scale. Aquatic Sciences **71**:318-330.

Shafroth, P. B., G. T. Auble, J. C. Stromberg, and D. T. Patten. 1998. Establishment of woody riparian vegetation in relation to annual patterns of streamflow, Bill Williams River, Arizona. Wetlands **18**:577-590.

Shafroth, P. B., J. C. Stromberg, and D. T. Patten. 2000. Woody riparian vegetation response to different alluvial water table regimes. Western North American Naturalist **60**:66-76.

Simon, A., and A. J. C. Collison. 2002. Quantifying the mechanical and hydrologic effects of riparian vegetation on streambank stability. Earth Surface Processes and Landforms **27**:527-546.

Steinfeld, D. 2001. Experiences establishing native wetland plants in a constructed wetland. Native Plants Journal **2**:36-41.

Stromberg, J. C. 2001. Restoration of riparian vegetation in the south-western United States: importance of flow regimes and fluvial dynamism. Journal of Arid Environments **49**:17-34.

Stromberg, J. C., S. J. Lite, and M. D. Dixon. 2010. Effects of stream flow patterns on riparian vegetation of a semiarid river: Implications for a changing climate. River Research and Applications **26**:712-729.

Tal, M., and C. Paola. 2007. Dynamic single-thread channels maintained by the interaction of flow and vegetation. Geology **35**:347.

Thorne, C. R. 1982. Processes and mechanisms of river bank erosion. Gravel-bed rivers:227-259.

Trimble, S. W., and A. C. Mendel. 1995. The cow as a geomorphic agent—a critical review. Geomorphology **13**:233-253.

TRRP. 2013. Trinity River Restoration Program: Restoring the Trinity River.

Turner, M. G., S. E. Gergel, M. D. Dixon, and J. R. Miller. 2004. Distribution and abundance of trees in floodplain forests of the Wisconsin River: environmental influences at different scales. Journal of Vegetation Science **15**:729-738.

USGS. 2013. National Hydrography Geodatabase: The National Map.*in* U. S. G. Survey, editor.

USGS. 2016. StreamStats. https://water.usgs.gov/osw/streamstats/

Uunila, L., and M. Church. 2015a. Ice on Peace River: effects on bank morphology and riparian vegetation. Pages 115-140. Wiley Online Library.

Uunila, L., and M. Church. 2015b. Ice on Peace River: effects on bank morphology and riparian vegetation. Pages 115-140 The Regulation of Peace River. Wiley Online Library.

Vaughan, I. P., M. Diamond, A. M. Gurnell, K. A. Hall, A. Jenkins, N. J. Milner, L. A. Naylor, D. A. Sear, G. Woodward, and S. J. Ormerod. 2009. Integrating ecology with hydromorphology: a priority for river science and management. Aquatic Conservation: Marine and Freshwater Ecosystems **19**:113-125.

Vaughn, R. S., and L. Davis. 2015. Abiotic controls of emergent macrophyte density in a bedrock channel — The Cahaba River, AL (USA). Geomorphology **246**:146-155.

Veihe, A., N. H. Jensen, I. G. Schiøtz, and S. L. Nielsen. 2011. Magnitude and processes of bank erosion at a small stream in Denmark. Hydrological Processes **25**:1597-1613.

Warner, A. T., L. B. Bach, and J. T. Hickey. 2014. Restoring environmental flows through adaptive reservoir management: planning, science, and implementation through the Sustainable Rivers Project. Hydrological Sciences Journal **59**:770-785.

Wheaton, J. M., J. Brasington, S. E. Darby, and D. A. Sear. 2010. Accounting for uncertainty in DEMs from repeat topographic surveys: improved sediment budgets. Earth Surface Processes and Landforms **35**:136-156.

Wilson, B. L., R. E. Brainerd, D. Lytjen, B. Newhouse, and N. Otting. 2008. Field guide to the sedges of the Pacific Northwest. Oregon State University Press, Corvallis, OR.

Wolman, M. G. 1954. A method of sampling coarse river-bed material. EOS, Transactions American Geophysical Union **35**:951-956.

Wolman, M. G., and J. P. Miller. 1960. Magnitude and frequency of forces in geomorphic processes. The Journal of Geology:54-74.

Wood, S. 2006. Generalized additive models: an introduction with R. CRC press.

WSI. 2006. Middle Fork John Day River aerial photography & LIDAR project. Watershed Sciences, Inc.

Wynn, T., and S. Mostaghimi. 2006a. The effects of vegetation and soil type on streambank erosion, southwestern Virginia, USA. Journal of the American Water Resources Association **42**:69-82.

Wynn, T. M., M. B. Henderson, and D. H. Vaughan. 2008. Changes in streambank erodibility and critical shear stress due to subaerial processes along a headwater stream, southwestern Virginia, USA. Geomorphology **97**:260-273.

Wynn, T. M., and S. Mostaghimi. 2006b. Effects of riparian vegetation on stream bank subaerial processes in southwestern Virginia, USA. Earth Surface Processes and Landforms **31**:399-413.

Yumoto, M., T. Ogata, N. Matsuoka, and E. Matsumoto. 2006. Riverbank freeze-thaw erosion along a small mountain stream, Nikko volcanic area, central Japan. Permafrost and Periglacial Processes **17**:325-339.

Zanoni, L., A. Gurnell, N. Drake, and N. Surian. 2008. Island dynamics in a braided river from analysis of historical maps and air photographs. River Research and Applications **24**:1141-1159.

Zuur, A., E. Ieno, N. Walker, A. Saveliev, and G. Smith. 2009. Mixed effects models and extensions in ecology with R. Springer, New York, NY.